DEPARTMENT OF TRANSPORTATION

Evaluation of Curing Effects on Cold In-Place Recycled (CIR)

Eshan Dave, Principal Investigator
Department of Civil and Environmental Engineering
University of New Hampshire

APRIL 2022

Research Project
Final Report 2022-11

LRRB
LOCAL ROAD RESEARCH BOARD

To request this document in an alternative format, such as braille or large print, call 651-366-4718 or 1-800-657-3774 (Greater Minnesota) or email your request to ADArequest.dot@state.mn.us. Please request at least one week in advance.

Technical Report Documentation Page

1. Report No.	2.	3. Recipients Accession No.
2022-11		

4. Title and Subtitle	5. Report Date
Evaluation of Curing Effects on Cold In-Place Recycled (CIR) Materials	April 2022
	6.

7. Author(s)	8. Performing Organization Report No.
Eshan V. Dave, Jo E. Sias, Chibuike Ogbo, Eyoab Zegeye, Shongtao Dai	

9. Performing Organization Name and Address	10. Project/Task/Work Unit No.
Department of Civil and Environmental Engineering University of New Hampshire 33 Academic Way Durham, New Hampshire 03824-2619	11. Contract (C) or Grant (G) No. (c) 1035708

12. Sponsoring Organization Name and Address	13. Type of Report and Period Covered
Minnesota Department of Transportation Office of Research & Innovation 395 John Ireland Boulevard, MS 330 St. Paul, Minnesota 55155	Final Report
	14. Sponsoring Agency Code

15. Supplementary Notes

https://www.mndot.gov/research/reports/2022/202211.pdf

16. Abstract (Limit: 250 words)

Most cold In-place recycled (CIR) construction uses asphalt emulsion or foamed asphalt with or without active fillers as a stabilizing agent. To ensure the CIR layer gains appreciable stiffness and strength to support traffic, the stabilizing agents have to undergo curing (to dry additional moisture). If traffic is allowed on the CIR layer before sufficient strength and structural capacity is gained, premature damage will occur. Lack of a fast and reliable procedure to determine the extent of in-situ curing significantly increases the risk of such damage. Current construction specifications rely on empirically based time recommendations to ensure sufficient curing. Current empirical time estimates do not account for material variations, climatic inputs and construction process differences. This research uses a combination of in-situ testing of actual CIR construction projects and supplementary laboratory tests to develop a model for pavement engineers and practitioners to reliably predict the recommended time (as a function of mechanical property) for placing of overlay on CIR layers. The prediction model incorporates the critical factors that influence curing in CIR including stabilizer type and amount, presence of active filler, initial moisture content, in-situ density and curing temperature. Due to the large number of possible model variables and their interactive effects, rigorous regression analysis is conducted to determine the most significant variables. The model provides an option of defining sufficient curing based on criticality of the project. The major outcome of this research is a user-friendly spreadsheet-based tool with pre-programmed curing model predictive equations.

17. Document Analysis/Descriptors	18. Availability Statement
Cold in-place recycling, Concrete curing, Performance tests, Predictive models	No restrictions. Document available from: National Technical Information Services, Alexandria, Virginia 22312

19. Security Class (this report)	20. Security Class (this page)	21. No. of Pages	22. Price
Unclassified	Unclassified	192	

Evaluation of Curing Effects on Cold In-Place Recycled (CIR) Materials

FINAL REPORT

Prepared by:

Chibuike Ogbo (graduate researcher)
Eshan V. Dave (principal investigator)
Jo E. Sias (co-principal investigator)
Department of Civil and Environmental Engineering
University of New Hampshire

Eyoab Teshale Zegeye
(Co-principal investigator)
Shongtao Dai (co-principal investigator)
Office of Materials and Road Research
Minnesota Department of Transportation

April 2022

Published by:

Minnesota Department of Transportation
Office of Research & Innovation
395 John Ireland Boulevard, MS 330
St. Paul, Minnesota 55155-1899

ACKNOWLEDGMENTS

This research study was performed by the University of New Hampshire (UNH), with the MnDOT Office of Materials and Road Research (OMRR) serving as subcontractors. We sincerely acknowledge Eyoab Zegeye-Teshale and Shongtao Dai from OMRR for their significant efforts in coordinating the in-situ testing component of this study. We would also like to thank Eddie Johnson, Thomas Calhoon, and Anh Tran at OMRR, who played instrumental roles in the success of the in-situ testing. The field projects included in this study were realized based on the cooperation of the oversight engineers in the state department of transportation and local agencies; we sincerely appreciate their efforts. The participation of the paving contractors and quality-control personnel are also recognized and greatly appreciated. We would also like to acknowledge Project Coordinator Marcus Bekele and Technical Liaison Joel Ulring for their help in the smooth administration of this project. Special thanks also go out to the rest of the members of the Technical Advisory Panel (Timothy Andersen, Terrence Beaudry, Tim Becker, Chelsea Bennett, Chuck Grotte, Michal Hanson, Gregory Ilkka and Wayne Stevens) for their feedback throughout the course of this research.

TABLE OF CONTENTS

LIST OF FIGURES

LIST OF TABLES

LIST OF ABBREVIATIONS

CIR	–	Cold In-place Recycling/Recycled
DPS	–	Dielectric Profiling System
EE	–	Engineered Emulsion
FA	–	Foamed Asphalt
FQM	–	Full Quadratic Model
IMC	–	Initial Moisture Content
ITS	–	Indirect Tensile Strength
LDMS	–	Laboratory Dielectric Measurement System
LWD	–	Lightweight deflectometer
MC	–	Moisture Content
M_R	–	Resilient Modulus
NDMG	–	Nuclear Density and Moisture Gauge
RCCD	–	Rapid Compaction Control Device

EXECUTIVE SUMMARY

Cold in-place recycling (CIR) is one of the most cost-effective and environmentally friendly techniques for asphalt pavement rehabilitation. The benefits include in-place reuse of existing pavement materials and eliminating the need for transportation of materials. Additionally, all materials are mixed and compacted with little to no addition of heat. Most CIR construction uses asphalt emulsion or foamed asphalt with or without active fillers as a stabilizing agent. To ensure the CIR layer gains appreciable stiffness and strength to support traffic, the stabilizing agents have to undergo curing. If traffic is allowed on the CIR layer before sufficient strength and structural capacity is gained, premature damage will occur. There is a lack of a fast and reliable procedure to determine the extent of in-situ curing, which significantly increases the risk of such damage. Current construction specifications rely on empirically based time recommendations to ensure sufficient curing. These time estimates do not account for material variations, climatic inputs, and construction process differences.

The goal of this research study was to provide a reliable and practical methodology for agencies to monitor and predict the extent of curing and strength gain for CIR layers. These were met through the following study objectives:

- Recommend a reliable in-situ strength/moisture measurement method
- Propose and validate a prediction equation for required time to open CIR to traffic
- Provide guidance on adoption and implementation of this method by agencies

This research used a case study-based approach to evaluate curing. Six (6) CIR pavement projects constructed in the 2020 construction season in Minnesota were selected for in-situ testing, constituent material sampling, and collection of field data. These projects were chosen to consider different factors that may affect curing such as the mix composition and geographical location (weather variation). A test section was defined within each of the selected field projects on which in-situ tests were conducted to evaluate the curing evolution of the CIR layers. These tests included light-weight deflectometer (LWD) and rapid compaction control device (RCCD) for obtaining stiffness/strength measurements, and dielectric profiling system (DPS) and nuclear density and moisture gauge (NDMG) for measurement of moisture content. The NDMG and DPS were found to show similar trends in moisture content change as related to curing. However, the DPS also detected surface moisture resulting from rainfall events. The rainfall affected only the surface of the layer and therefore did not appear to significantly affect the curing evolution of the field projects. The LWD and RCCD were found to be effective in assessing the stiffness evolution as pertaining to curing. The RCCD had lower measurement variability than the LWD.

The reliability of any developed model can only be as good as the quantity and quality of the data employed. In-situ testing could only be conducted on 6 projects due to time and expense limitations; therefore, laboratory testing on the sampled materials was necessary to expand the dataset used for model development. The statistical analysis software JMP Pro® was used to develop a partial factorial experimental design to incorporate the variation in factors that could impact the curing process. This design resulted in at least 3 variations of the as-built materials and curing conditions of the 6 field projects. Gravimetric measurements, laboratory dielectric measurement system (LDMS), indirect tensile strength

(ITS), resilient modulus (M_R), and triaxial tests were conducted to track the evolution of moisture and mechanical properties. The LDMS showed promising results in tracking the moisture content evolution and was comparable with the gravimetric measurements. The M_R and ITS tests showed similar trends with evolution of mechanical properties. Ultimately, it was observed that there was further gain in mechanical properties after the mixtures reached an equilibrium moisture condition, which may be more significant when active filler is not included in project.

Due to the limitations in curing factors that can be simulated in a laboratory setup, a correlation between the laboratory and field measured properties was explored to translate the laboratory curing conditions to the field. The Michaelis-Menten model was found to adequately fit the measured data both in the field and the laboratory in terms of modeling the mechanical property evolution of CIR materials as pertaining to curing. Material properties were observed to evolve faster in the field as compared to the controlled laboratory curing conditions employed in this study. However, a very strong relationship was found between field and laboratory curing time.

Based on the dataset generated in the laboratory, consisting of 25 different CIR material and curing conditions, a curing prediction model was developed. The prediction model could calculate the time needed for necessary curing before allowing placement of the wear course. For this, sufficient curing was defined using three different alternatives: time it took to achieve 70%, 80% and 90% of final ITS. The factors incorporated included stabilizer type and amount, presence of active filler, initial MC, compacted density, curing temperature and RH. Multiple linear regression using a full quadratic model was explored because of its broad applicability. Stepwise regression analysis using forward selection criteria was conducted, which facilitated the identification of the most significant predictor variables that were included in the model. Among the experimental factors explored, only the curing RH did not seem to have any effect and hence did not contribute to the final model equation. Ultimately, the model consisted of 11 predictor variables (6 main effects, 5 two-way interactions and no quadratic effect). The model provided a time estimate based on laboratory conditions and could be translated to field conditions using a developed linear regression relationship.

Finally, guidelines were developed to facilitate the implementation of the curing prediction model. This included the necessary steps to gather the required information for application of the model. The limitations of the model and recommendations for future extension of this study were further discussed.

CHAPTER 1: INTRODUCTION

1.1 BACKGROUND AND MOTIVATION

Cold in-place recycling (CIR) is a viable technique for asphalt pavement rehabilitation. The benefits include in-place reuse of existing pavement materials and eliminating the need for transportation of materials. Additionally, all materials are mixed and compacted with little to no addition of heat. Generally, CIR has been identified to be a cost-effective and environmentally friendly technique (Galehouse and Chehovits, 2010). CIR mixtures are typically composed of reclaimed asphalt pavement (RAP) stabilized with asphalt emulsion or foamed asphalt. Water is essential during mixing to disperse the emulsion or foamed asphalt throughout the mixture. In addition, water enhances workability and aids in compaction (Tebaldi et al., 2014). Active fillers such as cement or hydrated lime are often added to facilitate dispersion of the asphalt binder in the cold mixture, improve adhesion of the asphalt to the RAP, accelerate the curing process, and enhance the properties of the mixture. To ensure the CIR layer gains appreciable stiffness and strength to support traffic (including that of construction vehicles used to place the wearing course on CIR), it has to cure. If traffic is allowed on the CIR layer before sufficient strength and structural capacity is gained, premature damage will occur. Curing in CIR consists of the interaction of the following mechanisms: evaporation of moisture, breaking of emulsion (when used), and hydration of active filler when added (Cardone et al., 2015; Graziani et al., 2016).

At present, there is lack of a fast and reliable procedure to determine the extent of in-situ curing, which significantly increases the risk of premature damage. Present construction specifications rely on empirically based time recommendations to ensure sufficient curing. The Asphalt Recycling and Reclaiming Association (ARRA) recommends a minimum cure time of 3 days and a maximum moisture content of 3 percent before placing a surface course. The current MnDOT 2390 special provisions for cold recycling state that the wear course on CIR should be placed no sooner than 3 calendar days and no later than 14 calendar days (regardless of location) after the CIR has been placed and compacted (MnDOT, 2020). Many other agencies express curing in their specifications as the amount of moisture in the CIR layer. This is based on the premise reported by several researchers that loss of moisture translates to increased structural capacity of the CIR layer (Kim et al., 2011; Grilli et al., 2020). Curing in CIR depends on a number of factors, which may include but are not limited to, mixture attributes, construction features, climatic factors and condition of the underlying layer. Therefore, to develop a reliable curing evolution prediction model, these factors need to be incorporated. Additionally, curing should be expressed in terms of the mechanical properties of the CIR layer and its ability to support traffic without premature damage.

Some research efforts have explored the use of in-situ testing methods to measure the degree of curing. Devices such as light weight deflectometer (LWD), falling weight deflectometer (FWD), dynamic cone penetrometer (DCP), and geogauge have been used to evaluate the structural capacity. Whereas the nuclear density and moisture gauge (NDMG), time domain reflectometer, and ground penetration radar (GPR) technology have been employed to monitor in-situ moisture content. Even though some of these in-situ tests may be reliable in monitoring the extent of curing, they are expensive to conduct on a routine

basis. Therefore, a prediction model will reduce the need for these tests. Additionally, research efforts are needed to understand how these in-situ measured properties may be linked to laboratory measured properties to facilitate modelling of the curing evolution for future purposes.

1.2 OBJECTIVES

The overall goal of this research is to provide tools and predictive capabilities for agencies and practitioners to reliably determine the extent of in-situ curing of CIR layers. The study is further divided into three (3) principal objectives, which are to:

- Recommend a reliable in-situ strength and/or moisture measurement method to monitor curing of CIR layers
- Enhance understanding of the CIR mechanical properties and moisture content evolution through monitoring of field pavement sections and controlled laboratory experiments
- Develop and validate a prediction equation/tool for required time to open CIR to traffic and/or placing of wearing course

1.3 RESEARCH METHODOLOGY

This research uses data from both field projects and laboratory testing to develop a predictive model for curing in CIR layers. The developed model uses readily available information to calculate the time needed for necessary curing before allowing placement of the wear course. The development of the predictive model integrates the various critical factors that impact curing of CIR. These factors include stabilizer type and amount, presence of active filler, initial moisture content, in-situ density and curing temperature. Due to the limited range of factors, a full quadratic model (FQM) is explored to describe the relationship between the factors and curing time. The FQM contains the main effects of the factors and all two-way interactions between the factors. Given the limited amount of experimental data, a stepwise regression approach is employed to determine the most significant variables to be included in the model, using the forward selection criteria. The identified variables are then used to develop the predictive model equations, which are programmed into a user-friendly computer tool. The project is divided into 9 tasks and a flowchart schematically shows project activities and information flow in Figure 1.1.

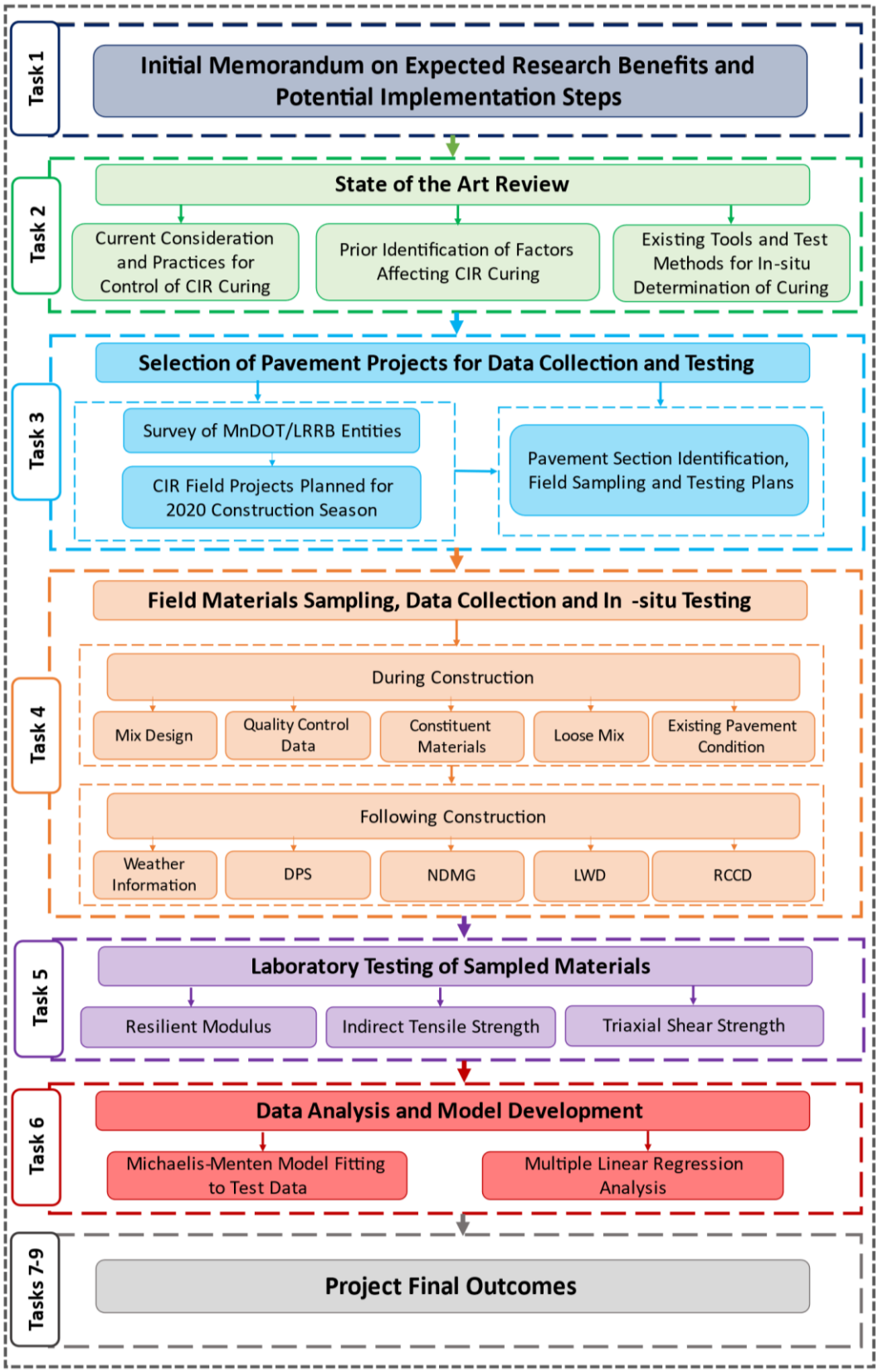

Figure 1.1 Methodology Flow Chart

1.4 ORGANIZATION OF THE REPORT

This report is organized into eight chapters with appendices. Chapter 1 covers the introduction and motivation for this research, as well as the study objectives and research approach. Chapter 2 contains the extensive literature review conducted on state of the art and practice of cold in-placing recycling, with topics relevant to curing. Chapter 3 provides information on the field study projects, materials sampled, and in-situ testing campaign. Chapter 4 presents findings of the in-situ testing conducted to evaluate curing. The result of the laboratory testing campaign is discussed in Chapter 5. Comparison between the laboratory and in-situ test results is presented in Chapter 6. Chapter 7 presents details of the prediction model development. Chapter 8 provides the key conclusions and implementation steps of the outcomes of this study. Limitations and considerations for future extension are also discussed.

CHAPTER 2: LITERATURE REVIEW

This chapter provides an overview of cold recycling techniques, existing curing prediction methods and models, and current specifications and construction methods currently used by different agencies in the United States as well as internationally. This report incorporates research that has been conducted worldwide on these topics in recent years. The existing body of knowledge and current methods and models were used as a starting point to develop an innovative prediction tool for curing of CIR mixtures that considers the range of variables that can affect this process in the field.

2.1 COLD RECYCLED MIXTURES

2.1.1 General Introduction on Cold Recycled Asphalt Mixtures

Recycled cold asphalt mixtures are typically composed of reclaimed asphalt pavement (RAP), virgin aggregates together with bituminous stabilizers (asphalt emulsion or foamed asphalt). The presence of water during mixing is essential in order to disperse the emulsion or foam asphalt throughout the mixture. In addition, water aids in compaction, enhances workability and provides a shelf-life for the asphalt mixture (Tebaldi et al., 2014). Additives such as cement and lime are often added to facilitate dispersion of the bituminous stabilizer in the cold mixture, accelerate curing, and to improve the properties of the mixture.

To provide context to the findings of the literature review presented in this report, the subsequent sub-sections provide a brief overview of the mix design processes for CIR as well as commonly encountered distresses.

2.1.2 Cold In-Place Recycled Mixtures Design

CIR mixtures need to be optimally formulated to provide reliable performance. To achieve this, a mix design procedure is required to evaluate the ingredients of the CIR mixtures, i.e., aggregate, water, bituminous stabilizer and active filler in different combinations. The process includes evaluation of the individual components as well as the blended material. The intention of mix design is to formulate a composite product with the necessary quality for a specific purpose or application. The CIR mixture constituents are:

Aggregates: Stabilization with either asphalt emulsion or foamed asphalt is suitable for treating a wide range of mineral aggregates. Aggregates of sound and marginal quality, from both virgin and recycled sources, have been successfully utilized in the process. It is important to note that cost-benefit considerations have led to selecting crushed aggregate (that is commonly used for the construction of high-density layers as opposed to natural gravel sources) and RA materials as suitable candidates for CIR mixtures (Mix Design requirements from recommendation of Asphalt Academy TG2, 2019). Only in exceptional circumstances, such as a lack of other suitable materials, can a lesser quality parent material be justified. These materials must only be used when expert knowledge on their use is available. In addition, it is vital to adhere to the boundaries of aggregate acceptability, based on gradation curve, plasticity index (PI), bearing capacity (CBR), etc. as well as recognizing the differences between CIR

mixtures prepared with foam asphalt and the ones prepared with asphalt emulsion. The aggregate properties required for successful treatment with bituminous stabilizer include durability characteristics of the natural (untreated) aggregate, as well as strength (hardness), plasticity, grading, spatial composition and the weathering characteristics.

Bituminous (Asphalt) Stabilizers: There are two forms of bituminous stabilizers that are used: foamed asphalt and asphalt emulsion, described below.

- Foamed Asphalt: cold water and air are injected simultaneously into the hot asphalt binder. It foams and is sprayed into the mixture. Foamed asphalt is a mass of bubbles, each bubble is a thin film of asphalt binder surrounding water vapor; this film is so thin that if an aggregate particle in the mixture comes in contact with the bubbles, it disintegrates into very minute splinters. The energy released from disintegration of bubbles as well as the dust particles are the carriers of asphalt. In the end, a partially bounded material is obtained with punctual mastics (asphalt + filler) randomly dispersed into the mixtures.

- Asphalt Emulsion: Asphalt binder droplets dispersed into water; in this case, the water is the carrier of the asphalt and a partially bounded mixture is obtained. While the aggregates are typically fully coated with asphalt film that is created by the curing (breaking) of the emulsion, these films are too thin to form a fully bounded material.

Fluids: The fluids in cold recycled asphalt emulsion mixes (CRAEM) are a sum of the moisture in the aggregates prior to mixing, water in the asphalt emulsion, the amount of asphalt in the emulsion or residual asphalt and any extra amount of water that may be added to the mixture. The content of fluids affects the packing of aggregate particles in the cold asphalt mixture. The optimum fluids concept is often applied to cold recycled mixtures with the aim of optimizing the packing of the solid particles. The optimum fluids content (OFC) is defined as the content of fluids at the closest packing of the aggregate particles or the maximum dry density (MDD). Since asphalt binder allows denser packing of the aggregate particles in comparison to water, the OFC of a given mixture may be lower than the optimum water content (OMC). The OFC for CRAEM is generally determined by varying the water content at a constant binder content. For cold recycled foam asphalt mixtures (CRFAM), the OFC is typically assumed to be equal to OMC (Wirtgen GmbH, 2012). It is common practice to make in-field adjustments to total fluid content of CRAEM by changing emulsion amount during construction.

Active fillers: Active Fillers such as cement, lime and fly ash are added to influence the curing, adhesion of asphalt to the aggregates and properties of the mixture such as plasticity and stiffness (Asphalt Academy, 2019; Wirtgen GmbH, 2012). The optimum active filler content (OAFC) is determined by varying the active filler content at a constant water content. The OAFC is determined by considering the active filler content at which various requirements for properties such as Marshall stability, unconfined compressive strength (UCS), indirect tensile strength (ITS) are met.

2.1.3 Distress Mechanisms of CIR Layers

Permanent deformation and moisture susceptibility are two fundamental distress mechanisms that need to be considered in CIR mix design (Asphalt Academy, 2019) as well as aspects of construction operations, such as timing to allow trafficking on CIR post construction. More recently, thermal cracking distress has also been taken into consideration during the mix design. Some researchers have also included raveling resistance as a measure of CIR durability.

Permanent Deformation: This is accumulated shear deformation caused by repeated load applications and is dependent on the shear properties of the material and densification achieved. Resistance to permanent deformation (rutting) is enhanced by:

- Improved aggregate grading (continuous), angularity, shape, hardness, and roughness
- Increased maximum particle size
- Improved compaction, i.e., higher field density during construction
- Reduced moisture content (curing)
- Limited asphalt binder application (less than 3%)
- Addition of active filler.

Moisture Susceptibility: the presence of water in CIR mixtures i.e., for compaction as well as any moisture ingress, in addition to the partially coated nature of the aggregate, makes moisture susceptibility an important consideration in the evaluation of material performance. Moisture susceptibility is a measure of the damage caused by exposure of a CIR mixture to high moisture contents and pore-pressures caused by traffic. The damage in CIR primarily occurs as loss of adhesion between the asphalt binder and aggregate leading to loss of shear strength. Moisture resistance is enhanced by:

- Increased asphalt binder addition, considering the cost implications
- Addition of active filler
- Improved compaction
- Continuous grading

Thermal Cracking: This is cracking caused by shrinkage of the CIR material due to exposure to low (cold) temperatures and is dependent on the tensile properties of the material. Resistance to thermal cracking is enhanced by:

- Improved aggregate grading (fine fraction content)
- Decreased maximum particle size
- Improved compaction
- Reduced moisture content (curing)
- Adequate asphalt binder application
- Limited active filler application (less than 1.5%)

2.2 CURRENT CONSIDERATIONS AND PRACTICES FOR CONTROL OF CIR CURING

This section summarizes review of literature on various factors that have been identified to affect curing of CIR materials in terms of strength gain and moisture loss. This section also discusses laboratory

practices that have been recently used to assess the level of curing of CIR mixtures, as well as the current practices of various states transportation agencies that routinely utilize CIR for pavement rehabilitation.

2.2.1 Factors Affecting Curing of CIR

Basing on all the findings from the literature review, the main factors that were identified as most impacting the CIR mixture curing process are: time, temperature, humidity, wind, rainfall/precipitation, component materials and construction features.

2.2.1.1 Time

Time is the most critical factor that affects the curing of CIR layers. Time is required for interaction of various mechanisms, which include (Kavussi and Modarres, 2010; Cardone et al., 2015; Graziani et al., 2016):

- Evaporation of moisture
- Emulsion curing (breaking)
- Hydration of chemical additives (and thus chemically bind moisture)

These three mechanisms contribute to improvement of mechanical properties of cold recycled materials with time. Leech (1994) reported that full curing time of cold recycled mixtures could range between 2 to 24 months depending on weather conditions. Thanaya et al. (2009) reported that even without addition of chemical additives, cold recycled mixtures could attain stiffness comparable to hot mix asphalt after full curing has been achieved.

2.2.1.2 Temperature

Researchers have shown that the effect of temperature is very significant on the curing process. It has been established that the higher the temperature, the higher the rate of moisture loss (Roberts et al., 1984; Engelbrecht et al., 1985; Cardone et al., 2015; Graziani et al., 2016; Bessa et al., 2016). Roberts et al. (1984) further observed that the higher the curing temperature, the lower the moisture susceptibility of the recycled material. Du (2018) showed that curing of mixtures with asphalt emulsion and cement is feasible even at elevated temperatures of up to 60°C without the issue of asphalt aging. On the other hand, Sefass et al. (2004) showed that at 50°C curing temperature, binder properties could change due to aging. Nassar et al. (2016) also suggested that higher temperatures may result in accelerated drying which hinders hydration of cement. Overall, it is apparent that the optimal curing temperature may be case/mixture dependent. It is also important to consider that there is a range of temperature that can be considered acceptable for a good curing process. That means that it is fundamental to define a tolerance temperature gap along with the optimal temperature for CIR curing, mainly because the conditions in field can be variable and difficult to foresee.

2.2.1.3 Humidity

Humidity generally affects the rate of moisture evaporation. It is expected that at a higher humidity, there is a reduction in the rate of evaporation. Garcia et al. (2013) established that there is a link between the environmental humidity and the rate of water loss and strength gain. The study showed that cold recycled mixtures cure faster at lower relative humidity. Nassar et al. (2016) showed that to obtain similar stiffness at a higher humidity, a longer curing period is required. Du (2018) also confirmed that humidity plays a role in strength development of cold recycled mixtures using asphalt emulsion and cement. The study recommended that faster curing evolution was obtained with lower humidity.

2.2.1.4 Wind

The rate of moisture evaporation is generally known to increase with wind speed. Wind speed typically results in a decrease in humidity. Researchers have also identified that wind speed is a factor that should be considered during the curing process as it directly impacts moisture loss (James, 2006; Woods et al., 2012; Godenzoni et al., 2016; Corvey, 2016; Baghini et al., 2017).

2.2.1.5 Rainfall/Precipitation

Precipitation generally introduces additional moisture to the CIR layer during the curing period. This has resulted in most roadway agencies restricting CIR during periods when foggy weather conditions or precipitation is expected. Whereas these weather-related restrictions may be feasible during the construction process, they may be impossible to avoid throughout the curing period. Woods et al. (2012) observed that while the amount rainfall significantly affects the in-situ moisture content of CIR layers, it did not influence the stiffness gain through the curing period.

2.2.1.6 Component Materials

It is evident that the rate of curing of CIR is greatly dependent on the range of components of the mixture. Roberts et al. (1984) reported that the initial water content significantly affected the strength of mixtures stabilized using foamed asphalt. Lee et al (2011) also confirmed that the initial water content is a significant factor in predicting the evolution of moisture loss. Graziani et al. (2018) showed that different dosages of water in cold recycled materials resulted in different rates of water loss by evaporation but there is limited impact on final mechanical performance. Ma et al. (2015) suggested that the use of slow setting asphalt emulsion gives sufficient time for cement (when used as an additive) to hydrate which is helpful for strength gain. It has been reported by various studies that the use of active fillers or chemical additives accelerate the curing process (Terrell and Wang, 1971; Oruc et al., 2007; Stimilli et al., 2013; Betti et al., 2017). Chomicz-Kowalskaa and Maciejewski (2015) suggested that the use of foamed asphalt compared to emulsion results in a shorter curing period due to a lower water content to asphalt binder ratio.

2.2.1.7 Construction Features

Past studies have suggested that construction features such as degree of compaction, layer thickness and drainage condition of the underlying layer could impact the curing of CIR layers (Kim et al., 2011; Quick and Guthrie, 2011; Godenzoni et al., 2016; Graziani et al., 2018). Fu et al. (2010) also suggested that the properties and moisture condition of the underlying layer also play a role in the curing process. In a lab setting, Serfass et al. (2004) demonstrated that the rate of moisture loss in smaller specimens is faster than in larger ones.

2.2.2 Laboratory Assessment of CIR Curing

The ability to simulate the in-situ curing of CIR mixtures in the laboratory can be used to establish the appropriate time to place the asphalt overlay on top of the new constructed recycled layer. If reliability for such laboratory simulation is high, then it can minimize or eliminate the need of in-situ tests and evaluations. Laboratory curing simulation is also very important because it can allow for testing of different types of mixtures and curing conditions prior to actual construction. For example, by comparing mechanical properties as function of curing time and conditions, material selection and design can be optimized to minimize the need to keep the new constructed layer uncovered and free from traffic. A common goal for all laboratory aging and conditioning procedures is the acceleration of the actual processes in the field (Tebaldi et al., 2014). The curing process of cold mix asphalt materials can be speeded up mainly by the following three physical parameters:

- Temperature: The higher the temperature the faster the moisture can evaporate.
- Humidity: As drying is an equilibrium process the curing in a dry climate is favorable.
- Pressure: Application of vacuum decreases the vapor pressure of water resulting in higher evaporation rate.

This subsection summarizes the review of literature on various laboratory protocols that have been used to simulate the field curing process of CIR materials.

2.2.2.1 Curing Methods

Researchers have compared various curing methods to obtain a procedure that most accurately simulates the evolution of strength gain and moisture loss during field curing of CIR. Lee and Im (2008) examined three laboratory curing procedures (illustrated in Figure 2.1):

- Uncovered specimen
- Semi-covered specimen (with impervious material)
- Covered specimen (with impervious material)

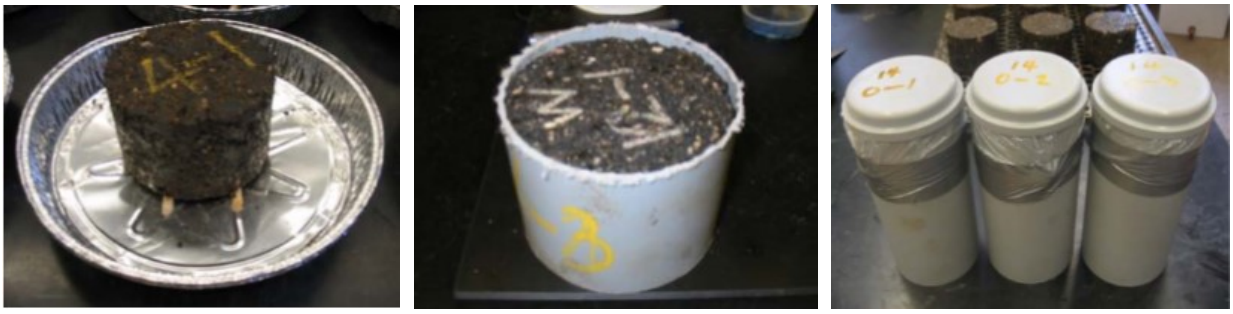

(a) (b) (c)

Figure 2.1 Curing Methods: (a) uncovered specimen (b) semi-covered specimen (c) covered specimen (Lee and Im, 2008)

For the uncovered CIR specimens; the following observations were made:

- There was a continuous gain in the indirect tensile strength for up to 28 days when cured in the oven at different temperatures (25˚C, 40˚C and 60˚C) even though the moisture content was reduced to zero after two days.
- The indirect tensile strength did not increase after 10 hours of curing in the air, but it increased when curing time increased from 10 hours to 50 hours.
- There was lack of correlation between indirect tensile strength and moisture content in the early curing stage of up to 10 hours.

For the semi-covered specimens, the following observations were made:

- The indirect tensile strength did not increase after 12 hours of curing in the air, but it increased when curing time increased from 12 hours to 14 days.
- At similar moisture content level, the indirect tensile strength of some specimens cured for 14 days were higher than those cured for 7 days.
- Given similar moisture content and curing time, semi-covered CIR-foam specimens exhibited slightly higher indirect tensile strength than semi-covered CIR-emulsion specimens.

For the covered specimens, the following observations were made:

- The indirect tensile strength of covered CIR-foam specimens increased as the curing time increased.
- For curing period of zero to 14 days, when cured in the oven at 40˚C, the indirect tensile strength increased when the initial moisture content of specimens was below 1.5%. However, the indirect tensile strength did not increase when the initial moisture content was 1.5% or higher.
- Given similar moisture content and curing time, covered CIR-foam specimens also exhibited slightly higher indirect tensile strength than covered CIR-emulsion specimens.

Fu et al. (2010) recommended that to simulate evaporation consistent with field condition, especially in first few hours after CIR construction, compacted laboratory specimens should be sealed in a plastic bag and cured for a shorter period at 20˚C. To simulate a more optimistic and longer-term curing condition of water evaporation, specimens should be cured unsealed in a forced draft oven at 40˚C for 7 days.

2.2.2.2 Environmental Curing Conditions and Duration

There has been a lack of consensus regarding laboratory environmental curing conditions that most suitably simulate the field curing process. Fu et al. (2010) identified that the laboratory curing conditions need to be relevant to the material characteristics. As a result, researchers have adopted a combination of varying time, temperatures and humidity levels to simulate field curing process. There have been detailed literature reviews that summarize a few of the existing curing conditions for CIR materials with foam and emulsion as stabilizers (for example, Kim et al., 2011 and Tebaldi et al., 2014).

The following conditions have been proposed for laboratory curing of asphalt foam stabilized CIR mixtures:

- Curing in the oven at 60°C for three days (Bowering, 1970; Bowering and Martin, 1976; Maccarrone et al., 1994; Muthen, 1998; Lane and Kazmierowski, 2003; Hodgkinson and Visser, 2004)
- Short term curing in oven at 40°C for one day and three days for long-term curing (Ruckel et al., 1982; Muthen, 1998; Marquis et al., 2003)
- Curing in the oven at 46°C for three days to simulate medium- or long-term field curing (months to years time frame). Oven curing at 40°C for one day to simulate a total of 7-14 days of field curing (Jenkens and Van de Ven, 1999)
- Ambient temperature curing for varying number of days from 1 to 28 days to simulate different stages (Ruckel et al., 1983; Saleh, 2004; Nataatmadja, 2001; Long and Theyse, 2004; Long and Ventura, 2004)

The following conditions have been employed for emulsion stabilized CIR mixtures:

- Initial curing in the mold at 25°C for 15 hours, final curing in the oven at 60°C for three days, long-term curing in the oven at 60°C for 30 days (Sebaaly et al., 2004)
- Oven curing at 60°C for 24 hours (Lee et al., 2002)
- Initial cure at ambient temperature for up to 60 min to ensure that the emulsion had broken prior to compaction. This initial curing process can however be neglected. Specimens undergo oven curing after compaction at 60°C for 48 hours (Cross, 2003)
- Oven curing at 35°C and 20% relative humidity for 14 days for smaller specimens (≈120mm diameter) and longer period for larger specimens (Serfass, 2002)

Notwithstanding the application of distinct curing conditions in past studies, Fu et al. (2010) identified that curing foamed asphalt mixes at a temperature close to ambient impairs repeatability and reproducibility of the laboratory curing process. Consequently, curing at elevated temperatures could result in significant aging. Fu et al. (2010) recommended that curing should be done at 40°C to reduce the impact of relative humidity and as well decrease the effect of aging. In addition, it has been recommended that curing temperatures above the softening point of asphalt binder be avoided as it may result in flow and dispersion within the mixture which may change mixture properties (Kuna et al., 2016). This recommendation may also be applicable to emulsion stabilized mixes (Tebaldi et al., 2014).

2.2.3 Current Practices for In-Situ Curing of CIR by State Transportation Agencies

This subsection presents results of review of state transportation agency (DOT) specifications that routinely use CIR for pavement rehabilitation. This covers a discussion of the practice and recommendations on CIR curing.

2.2.3.1 Colorado DOT

CIR operations are prohibited until the atmospheric temperature is 13°C (55°F) and rising. Operations are also required to be suspended when the temperature is 15°C (60°F) and falling. Operations are also prohibited when the weather is foggy or rainy, or when weather conditions are such that the proper mixing, spreading, compacting, and curing of the recycled material is not feasible.

Subsequently, no traffic (including Contractor's equipment) is allowed after laying the CIR material until start of initial break of the emulsion. This initial curing period is to be determined by the Engineer. However, if precipitation is imminent, it is required to proceed with compaction to seal the surface from additional moisture.

After compaction, traffic is further restricted from the CIR layer for at least two hours, unless otherwise approved by the Engineer. The CIR layer is required to cure until the free moisture (difference between moisture content of existing pavement and the CIR material) is reduced to 1% or less before any surface treatment or overlay. It is however specified that the layer be sealed with emulsion or overlaid with HMA within 10 calendar days after it is laid and compacted. The moisture conditions are expected to be met within this period.

2.2.3.2 Indiana DOT

Restrictions are placed for CIR operations when the weather is foggy or rainy. CIR operations are only permitted when pavement surface temperature is above 13°C (50°F) with overnight ambient temperatures above 2°C (35°F). There is however an exception during light precipitation if the contractor can prove that the performance of the CIR pavement will not be adversely affected. Work is also restricted when the heat index is greater than 38°C (100°F).

After compaction of the CIR, traffic (including that of the Contractor) is prohibited for at least two hours. This time can however be adjusted by the Engineer to ensure sufficient curing to prevent damage by traffic. Subsequently, prior to placing of HMA overlay, the CIR mixture is required to cure for a time period that achieves in-place moisture contents below 2.5% and on approval by the Engineer.

2.2.3.3 Iowa DOT

CIR operations are not permitted when weather conditions are such that proper mixing, placing, and compacting is not feasible. This includes when the ambient temperature is below 16°C (60°F) and when the weather is foggy or rainy.

After compaction, it is recommended that the CIR be tested to determine if it is stable enough to open to traffic. However, no particular laboratory or in-situ test is specified for this purpose. A curing time of 14 calendar days after construction of the CIR layer is specified. It is expected that within this period, the CIR layer will achieve allowable moisture content (not specified) to place the first lift of HMA overlay or specified surface treatment. Subsequent lifts of HMA overlay or surface treatment are not allowed until moisture content of the CIR layer is no more than 0.3% above the residual moisture content or 2.0%, whichever is greater. The Engineer in charge can adjust the specified curing period depending on field conditions until the specified moisture content limit is achieved.

2.2.3.4 Kansas DOT

CIR operation is only permitted when the ambient air temperature is greater than 13°C (50°F) and rising, the weather is not rainy or foggy and the weather forecast does not call for freezing temperatures within 48 hours after placement. These requirements can however be waived by the Engineer.

After compaction, traffic is allowed on the layer provided a smooth surface free of loose particles is maintained for safe movement. This is typically achieved by power brooming. Whereas there is no requirement for structural capacity of the layer to support traffic, the CIR material is required to cure until the moisture of the material is a maximum of 2.0% or otherwise approved by the Engineer. Under dry weather conditions, this moisture requirement is expected to be achieved within 48 hours. Subsequent treatment or overlay is expected to be completed within 21 calendar days.

2.2.3.5 Nevada DOT

CIR operations are subjected to weather limitations. The pavement temperature is required to be at least 16°C (60°F). The operations are also not permitted if atmospheric temperature is anticipated to drop below 2°C (35°F) within 48 hours of mixing or also during stormy weather. Additionally, if it rains during overlay paving operations, paving is to be delayed until moisture content 2.0% or less is achieved.

After compaction, the CIR layer is to be treated with an emulsified asphalt fog seal and can be open to public traffic. However, a minimum curing period of 10 days is specified prior to placing an overlay. No provision is made for evaluation of structural capacity prior to overlay.

2.2.3.6 New York State DOT

CIR operations are not permitted when the air or surface temperatures are below 7°C (45°F) or when it is expected to drop below 4°C (40°F) within 24 hours of the start of operations.

Traffic is typically not prohibited on the CIR layer after compaction; however, continuous brooming is required to remove loose materials and maintain a smooth ride. Minimum curing time of 10 days is specified when asphalt emulsion is used or 3 days when foamed asphalt is utilized. No provision is made to monitor the actual in-situ moisture content or structural capacity of the layer.

2.2.3.7 Virginia DOT

CIR operations are restricted to when both the atmospheric temperature and the material to be recycled are at least 16°C (50°F). Operations are also prohibited when freezing temperatures are expected within 48 hours after placement of CIR on any portion of the project.

Following compaction, a fog seal is required on the CIR layer after which traffic (including the contractor's equipment) is restricted until the CIR material cures to a water content of maximum of 50% of the optimum water content. This condition is to be met prior to opening to vehicular traffic or placing of overlay or any other applicable surface treatment. The curing time can however be adjusted by the Engineer to allow establishment of sufficient cure so traffic will not initiate raveling.

2.2.4 State of Practice for Control of Curing of CIR in Minnesota

A review was conducted regarding the state of art and practice of CIR curing in Minnesota. A survey was developed using UNH's Qualtrics system and distributed to all state and local road agencies in Minnesota. The primary intent of the survey was to establish the current practices at the town, county and district levels with respect to control of curing in CIR and timing for opening of traffic or application of wearing course. The survey further sought to identify common challenges and knowledge gaps in implementing CIR as a rehabilitation alternative. The survey consisted of 13 questions which are included in Appendix A. There were 18 responses that were received and included in the survey analysis, three of which are from city public works and the remaining from county public works or highway departments. Full details of the survey results are included in the Appendix A. A summary of the findings is presented in the following sub-sections.

2.2.4.1 Current practice for Control of Curing of CIR

As an initial step in establishing the state of practice of CIR in Minnesota, the survey requested information to determine whether the local road agencies within the state routinely undertake CIR projects. Only a few of the survey responders (5/18) reported that they have used CIR technology at least once in the last 10 years. Brown County stood out, indicating that they frequently undertake CIR projects with a total of 38 projects in the past ten years. Further survey analysis is based on the 5 responders that indicated CIR usage.

Specification for Quality Control and Acceptance of CIR

The survey data shows that all agencies utilize the MnDOT specification, with or without any form of modification, for quality control and acceptance of CIR projects (Figure 2.2).

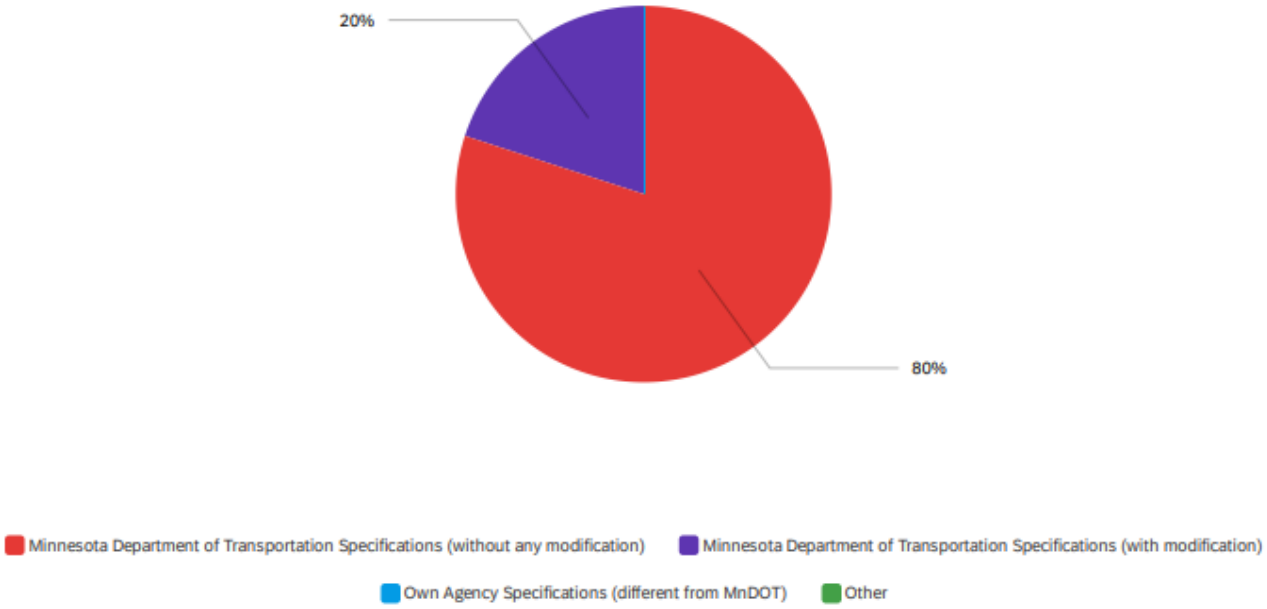

Figure 2.2 Specification for Quality Control and Acceptance of CIR as reported by Agencies

Personnel Responsible for Determination of Degree of Curing

As shown in Figure 2.3, the determination of degree of CIR curing is typically made by either an agency engineer or third-party consultant. Only in rare cases is the determination made by contractor personnel.

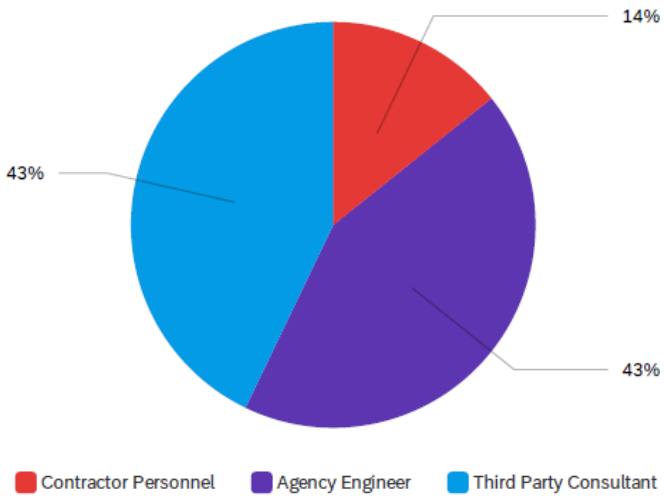

Figure 2.3 Personnel Responsible for Determination of Degree of Curing in Agencies

Method of Determination of Timing for allowing Traffic or Placing of Overlay

Figure 2.4 shows that majority of the agencies typically adopt recommendation in the specification and/or rely on in-situ measurement of material moisture content for determination of timing for allowing traffic on the CIR layer or placing of overlay. The other category involves an adjustment in timing based on weather conditions.

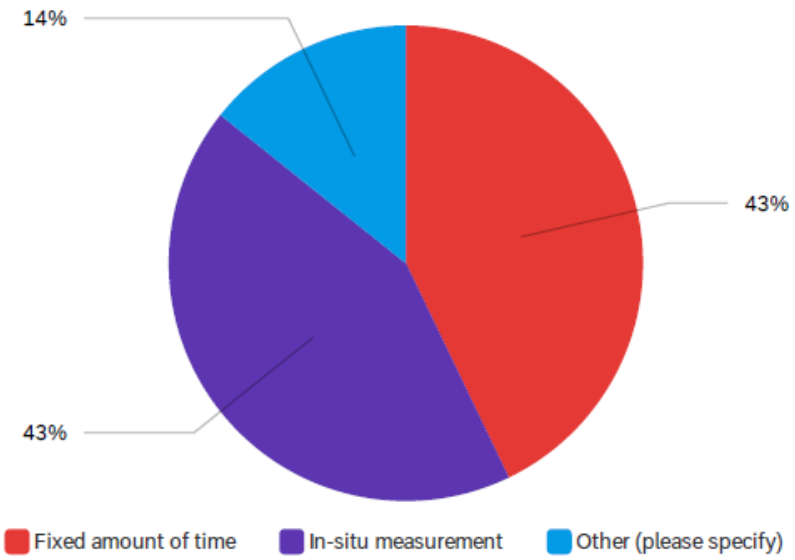

Figure 2.4 Method of Determination of Timing for allowing Traffic on the CIR Layer or Placing of Overlay as reported by Agencies

2.2.4.2 Common Challenges and Knowledge Gaps in Implementing CIR technology

Information gathered from local agencies as to why they have not considered CIR as a rehabilitation strategy points to various factors relating to:

- Lack of expertise in the CIR technology and how to identify a good candidate road for application
- Preference of full depth reclamation for better structural support.
- Preference of mill and overlay as most pavements in region are currently too thin
- Concerns relating to high void content

About 30% of the responders indicated gaps in knowledge that need to be addressed by research studies. The reported gaps include better strategy to maintain original road profile (as CIR with a higher void content typically raises profile), guidance on estimating economic benefit on a candidate road as opposed to other rehabilitation strategies, techniques for improving rutting and thermal cracking performance, methods for accelerating curing and determination of timing to allow traffic, and a more robust mix design method.

2.3 CRITICAL PERFORMANCE CHARACTERISTICS OF CIR MATERIAL

There has been a lack of consensus about the fundamental, engineering or empirical properties that are used to characterize CIR materials for pavement design and performance evaluation. This section summarizes review of literature on various characteristics that have been identified to directly affect performance of CIR materials.

2.3.1 Stiffness

Most evaluation of CIR material properties has focused on characterization of stiffness and load resistance properties to determine the structural capacity. This is most applicable during pavement design and evaluation of rutting resistance. The following tests have successfully been used to evaluate stiffness and structural contribution of CIR materials:

2.3.1.1 Resilient Modulus test

The resilient modulus has been one of the most popular tests used to evaluate the stiffness of CIR layers. Scholz et al. (1991) developed a laboratory sample preparation procedure for fabrication of CIR specimens. The study utilized the resilient modulus to show that it is possible to attain a comparable stiffness between field and laboratory compacted CIR material. Sultan et al. (2016) has shown that the resilient modulus test is adaptable at different temperatures and loading to evaluate stiffness of CIR layers. The results of the study showed the applicability of the resilient modulus test in characterizing CIR materials stabilized using different bituminous stabilizers with chemical additive and fillers. Other researchers have also employed the resilient modulus in evaluating the stiffness of CIR materials (Cross, 1999; Fu et al., 2009; Apeagyei et al., 2013)

2.3.1.2 Dynamic Modulus

Dynamic modulus test has been employed by Kim et al. (2009) to characterize stiffness of CIR materials stabilized using foamed asphalt. Results of the study showed that the test is sensitive to RAP source and foamed asphalt content. Kim et al. (2012) also showed the applicability of the dynamic modulus test in characterizing the stiffness properties of CIR materials stabilized with emulsion. The emulsion type and residual asphalt stiffness of RAP materials were found to influence the test results. Schwartz et al. (2017) measured dynamic modulus and repeated load permanent deformation properties for cold-recycled materials using different recycling/stabilizing agents and chemical additives. The study resulted in a catalog of typical values that could be used in mechanistic-empirical pavement design and analysis. Islam et al. (2018) also investigated the use of the dynamic modulus test to characterize the stiffness of CIR materials for use in Pavement Mechanistic-Empirical Design. Their study produced results that demonstrated reliable predictions of rutting distresses and IRI.

2.3.2 Strength

The strength of the CIR materials at different levels of curing has widely been used as a parameter to define the evolution of mechanical performance with time. Some of the existing curing prediction models and curing evaluation techniques are entirely and exclusively based on strength gain of the material.

2.3.2.1 Indirect Tensile Strength (ITS)

The indirect tensile strength (ITS) test has typically been used for mechanical evaluation of CIR materials. It provides an index to evaluate engineering properties and is also used to evaluate moisture susceptibility of the layer using the tensile strength ratio parameter. Consequently, several researchers have adopted the indirect tensile strength test to measure performance characteristics of CIR materials (Cross, 1999; Yan et al., 2010; Diefenderfer et al., 2012; Iwanski et al., 2013; Arimilli et al., 2016; Sangiorgi et al., 2017). Kim et al. (2011) used the ITS as a performance test to investigate the impacts of curing time on CIR mixtures. In their study, there was no observable increase in the indirect tensile strength of CIR specimens during the early stages of curing, but the strength values tended to increase at the later stages. Graziani et al. (2016) also used the ITS to evaluate effect of laboratory curing on cold recycled mixtures at two different curing temperatures.

2.3.2.2 Shear Strength

During the early stages immediately following construction, CIR is expected to be more similar to traditional unbound granular materials (i.e. non-cohesive) that are used for subbase and subgrade. As a result, it may be applicable to evaluate shear strength properties as opposed to tensile strength during this period. Santagata et al. (2010) performed triaxial tests to evaluate shear strength parameters of CIR materials at different temperatures. Their study also utilized this test to evaluate three different laboratory curing conditions. Cizkova et al. (2016) suggested that the triaxial test has a great potential for cold recycled materials, which may be most applicable with materials with low binder contents whose material behavior may better be described by the cohesion and shear parameters. In addition to shear properties, Dal Ben and Jenkin (2014) also recommended that the triaxial test could be utilized in determining resilient modulus and permanent deformation behavior of the recycled materials using foamed asphalt. Several other researchers have identified the suitability of the triaxial test in characterizing shear and resilient modulus properties for typical CIR materials (Fu et al., 2009; Gonzalez et al., 2009; Jenkins et al., 2007; Jenkins et al., 2012; Guatimosim et al., 2018).

2.3.3 Stability

A major concern in the use of CIR technology is the stability of the materials and susceptibility to rutting, especially during the early life. Researchers have used the following tests to characterize the rutting performance of CIR materials:

2.3.3.1 Flow Number and Flow Time Test

Kim et al. (2009) showed that the flow number test is applicable in characterizing the rutting potential of CIR materials stabilized using foam asphalt. The study found that the RAP source and foamed asphalt content play a role in the results of the flow number test. In another study by Kim et al. (2012), it was

found that the flow number and flow time test could also be used to characterize the permanent deformation properties of CIR materials stabilized with emulsion.

2.3.3.2 Marshall and Hveem Stability Test

Niazi and Jalili (2008) explored the use of Marshall stability in evaluating resistance to permanent deformation of CIR materials. The study showed that Marshall stability could be improved using lime and cement. Modarres and Ayar (2014) employed the Marshall stability test to assess the potential of improving the rutting resistance of CIR materials using pozzolanic additives, especially during early stages of curing. Researchers have also utilized these tests to evaluate impact of various factors on rutting potential of CIR materials with different constituents (Tia and Wood, 1983; Roberts et al., 1984; Cohen et al., 1989; Babagoli et al., 2016; Omrani and Modarres, 2018).

2.3.4 Moisture Content

The CIR process introduces a considerable amount of moisture into the recycled materials. Typically, most specifications for CIR materials tend to limit the amount of moisture that could be present prior to overlay or any form of surface treatment. Moisture content has been identified to provide lubrication to significantly improve the compaction characteristics of CIR layers (Gao et al., 2014; Grilli et al., 2016). However, there are concerns that high retained moisture contents could increase the potential of asphalt stripping in the HMA overlay or could slow the rate of strength development of the layer (Asphalt Institute, 1998). Various studies have identified that the moisture content has a significant effect on the mechanical properties of CIR materials (Jenkins et al., 2007; Kim et al., 2011; Ojum et al., 2014; Li et al., 2016)

2.3.5 Durability

Moisture susceptibility of CIR materials has raised concerns in the past as it can result in significant reduction in pavement structural capacity and could also result in premature raveling on the surface prior to wear course application. The inherent presence of moisture in these materials for better compactability and workability makes this even more critical. Most previous studies have utilized the tensile strength ratio test to evaluate these damaging effects of moisture on CIR mixtures (He and Wong, 2008; Du, 2015; Xiao and Yu, 2011; Iwanski et al., 2013; Modarres and Ayar, 2016; Kim and Lee, 2016; Arimilli et al, 2016).

2.4 TOOLS FOR DETERMINATION AND PREDICTION OF IN SITU LEVEL OF CURING

This section summarizes review of literature on in-situ testing methods as well as models that have been used to measure the degree of curing of CIR materials. Techniques used for both determination of structural capacity and moisture content are included.

2.4.1 Determination of In-Situ Level of Curing

2.4.1.1 Light Weight Deflectometer (LWD) and Falling Weight Deflectometer (FWD)

The most commonly used devices to evaluate in-situ curing of CIR are the Light Weight Deflectometer (LWD) and Falling Weight Deflectometer (FWD). Betti et al. (2017) conducted a study to analyze curing

process of mixtures with different active fillers (cement and lime) which was based on the elastic modulus evaluated at different times after construction. All the tests were carried out using the FWD, except for tests immediately after compaction; those were performed with the LWD. LWD and FWD tests were performed after 4 and 24 hours, 28 days, 9 months. To compare moduli obtained from tests conducted at different temperatures the moduli values were adjusted to a 20°C reference temperature. It was observed that the rate of stiffness growth was substantially higher during the first 14 days and a stable growth rate occurred thereafter.

Lee et al. (2011) conducted a study on in-situ curing of CIR using FWD and Geo-Gauges, along with temperature and moisture sensors installed in the newly constructed pavement layer. The study showed how the curing process in field correlated with precipitation, humidity and wind speed. The elastic moduli value measured after rainfall events were clearly lower than the values obtained before precipitation, showing how difficult it can be to have an exact determination of the right time to place wearing surface on top of CIR.

In a study by Guatimosim et al. (2018), structural evaluation of a trial section of CIR with foamed asphalt was conducted using FWD. The tests were performed one day after construction and subsequently 3, 13, 22 and 33 months later. Back calculation of the FWD measurements were done to assess the evolution of the resilient modulus of the layers and different deflection basin parameters were compared to evaluate the structural performance of the pavement. Temperature corrections were applied to the FWD measurements. It was observed that the resilient modulus increased considerably with the curing period resulting in drastic decrease of pavement deflections. This further reinforces the applicability of the FWD in monitoring the extent of in-situ curing.

2.4.1.2 Dielectric Profiling System (DPS)

The dielectric profiling system (DPS), previously known as the rolling density meter (RDM), is a device that utilizes ground penetration radar (GPR) to determine dielectric constants of typical pavement materials. It has the capacity to capture the in-place density, material uniformity and moisture in pavement layers. Whereas traditional GPR devices have the ability to capture the layer thickness, the DPS in its current version is not equipped for this purpose. While the DPS is a newer device, various studies have employed the use of GPR in evaluating in-situ properties of cold recycled material. The output of the GPR measurement is the dielectric constant of the material. In evaluating CIR materials, this property is believed to be sensitive to mix composition, curing stage, age, water content and temperature (Papavasiliou et el., 2010). It is however noteworthy that in past studies to evaluate stiffness, GPR has been used in conjunction with FWD. While the FWD provides deflection measurements, GPR is used to estimate the layer thickness for backcalculation of modulus vales (Loizos and Plati, 2007; Plati et al., 2010; Isola et al., 2013; Modarres et al., 2014; Mehranfar and Modarres, 2020). Loizos and Plati (2007) showed how change in dielectric constants measured in-situ using GPR could help explain early stages of curing in foamed asphalt stabilized material. These changes in dielectric value were observed as a result of the moisture content difference in the materials.

2.4.1.3 Dynamic Cone Penetrometer (DCP)

Quirk and Guthrie (2011) monitored a field project with emulsion treated base using portable falling weight deflectometer (PFWD) and the dynamic cone penetrometer (DCP). Field measurements were taken within 30 minutes of the final compaction of the recycled layer. Subsequent measurements were taken at 2, 3, 7, and 14 days, 4 months, and 1 year. The DCP tests were performed to a depth that allowed average penetration rates for both the cold recycled base and the subgrade layers to be determined. The study demonstrated that DCP penetration rates were able to capture the extent of curing with time. Other studies have also verified the feasibility of using the DCP in evaluating in-situ the gain in stiffness of stabilized layers with time through the curing process (Mohammad et al., 2003; Budge and Wilde, 2007).

2.4.1.4 Geogauge

The geogauge is a portable device that can directly be used to measure stiffness of the pavement structure. Woods et al. (2012) conducted a study to determine timing of overlay of five CIR projects (one project with asphalt emulsion and four with foamed asphalt). In their study, the stiffness of the layers was monitored for 36 days after construction using the geogauge. It was observed that the device accurately captured the increase in stiffness through the curing period. This led to the recommendation that the geogauge may be used to determine timing of an HMA overlay. Lee et al. (2009) observed that the stiffness measured using the geogauge is comparable to that backcalculated using FWD deflection measurements. The geogauge has been successfully implemented by several other studies to evaluate the stiffness of CIR layers over the curing period (Mohammad et al., 2003; Khosravifar et al., 2013; Lin et al., 2015)

2.4.1.5 Nuclear Gauge and Time Domain Reflectometer

The nuclear gauge device uses electromagnetic emissions to measure field density during paving. Several studies have used the device for the purpose of evaluating in-place density of CIR layers (Lee et al., 2016; Cox et al., 2016; Sebaaly et al., 2019). The nuclear gauge has also been employed to determine in-situ moisture content. The time domain reflectometer (TDR) device also uses the propagation of electromagnetic waves to detect presence of moisture. Woods (2011), in evaluating curing criteria for CIR, employed the nuclear gauge and TDR for monitoring in-situ moisture content. The study compared the moisture content evaluated using both devices and observed variations between the estimated moisture contents from each. It was suggested that neither device may be accurate in monitoring moisture loss in CIR layers. Thomas and Kadrmas (2002) also observed that the use of nuclear gauge to obtain measurements in materials with moisture is only applicable to show trends and not true density or moisture content values.

2.4.2 Prediction Tools for Level of Curing

2.4.2.1 Moisture Loss

Woods et al. (2012) monitored five CIR projects in Iowa to determine the timing for overlay placement. Capacitance moisture and temperature sensors were used to track the moisture content and pavement

temperature in the CIR layer through the curing period. A geogauge was also employed to measure the stiffness gain. Using a multiple regression approach, the data collected from the field was used to develop a moisture content prediction model (equation 1), which is a function of the initial moisture content, CIR layer temperature, wind speed, and humidity.

$$\Delta MC/h = a_1 + a_2 \cdot IMC + a_3 \cdot temp + a_4 \cdot hum + a_5 \cdot wind \quad (1)$$

where:

ΔMC/h	=	moisture change per hour during curing time
IMC	=	initial moisture content of CIR layer right after construction
temp	=	average CIR layer temperature during curing time (°F)
hum	=	average humidity during curing time (%)
wind	=	average wind speed (mph) during curing time
a_1, a_2, a_3, a_4, a_5	=	multiple linear regression coefficients

The regression coefficients were site specific and were combined to develop a generalized regression formula for the moisture loss index (equation 2). The model accuracy was estimated at an R^2 value of 70%.

$$\Delta MC/h = -0.21785 + 28.769 \cdot IMC + 1.483 \cdot temp + 0.562 \cdot hum + 12.455 \cdot wind \quad (2)$$

2.4.2.2 Stiffness Gain

Kuna et al. (2016) evaluated the applicability of the maturity method (typically used for evaluating concrete curing) to assess the in-situ characteristics of foamed asphalt layers in the pavement. The method was used to develop maturity-stiffness relationships (equations 3-5) relevant to the evolving properties of the foamed asphalt mixtures during the curing process. This tool was developed using laboratory measured indirect tension stiffness modulus (ITSM) on cured specimens at different temperatures.

$$E = E_u \frac{\sqrt{kM}}{1+\sqrt{kM}} \quad (3)$$

where:

E	=	Stiffness at a certain age
E_u	=	Limiting stiffness (which is linearly dependent on curing temperature)
k	=	Rate of stiffness gain at a constant temperature
M	=	Maturity term

The equation coefficients (E_u and *k*) were obtained using the least squares curve fitting technique. Both coefficients are material specific. The maturity term, M is given as:

$$M = t_e \cdot T = e^{B(T-T_r)} \cdot t \cdot T \quad (4)$$

$$M = \sum_0^t \Delta t_e \cdot T \text{ (when different curing temperatures are employed)} \quad (5)$$

where:

t = duration of curing at a given temperature
t_e = equivalent duration of curing at the reference temperature, T_r
B = temperature sensitivity factor (1/°C) (which is material specific)
T = actual curing temperature
T_r = reference curing temperature

This model was developed and validated based only on the combined effect of time and temperature. However, it is evident that all the other factors that affect curing identified in previous sections need to be taken into consideration for a more accurate prediction of in-situ curing.

2.4.2.3 Michaelis-Menten model

Graziani et al. (2016) analyzed different mixtures: CBTM (Cement Bitumen Treated Material) and CTM (Cement Treated Material), comparing results from specimens directly produced at the jobsite and sampled during the construction operations and mixtures produced in the laboratory. Specimens were cured in a climatic chamber at 20 ± 2 C, with a constant relative humidity of 50 ± 5%. Moisture loss by evaporation (DW), indirect tensile stiffness modulus (ITSM) and indirect tensile strength (ITS) were determined to evaluate the curing process. The measured data were analyzed using the nonlinear Michaelis–Menten (MM) model with the aim of characterizing the rate at which the mixture properties evolve over time and their values at the long-term cured state. The results showed that the adopted curing variables (DW, ITSM and ITS) gave a comparable description of the curing process when evaporation was allowed, and that the MM model gave an appropriate description of the evolutive behavior of CBTMs and CTMs.

The MM model is a nonlinear model that describes an asymptotic evolution of the measured response as a function of time (predictor variable), through the evaluation of two parameters:

$$f\left(t,(y_A,K_c)\right)=\frac{y_A\cdot t}{K_c+t} \quad (6)$$

where $y_A > 0$ is the asymptotic value of the response (when $t \rightarrow \infty$, i.e. long-term condition) and $Kc > 0$, also known as the Michaelis constant, represents the curing time when the response is equal to $y_A/2$. It is emphasized that, because of their physical meaning, both y_A and K_c are restricted to positive values and thus the equation defines a concave rectangular hyperbola through the origin. At the beginning of curing (t = 0), the MM model predicts a zero value for the considered curing variables DW, ITSM and ITS. As curing time increases, the response asymptotically approaches the long-term value y_A. The Michaelis constant Kc is used as a measure of the initial curing rate: a lower Kc value means a faster increase in DW, ITSM and ITS. The CTM results highlighted that initial moisture loss by evaporation for mixtures produced on site was more than 2 times slower with respect to that registered for mixtures produced in the laboratory.

Graziani et al. (2018) applied the same quantitative characterization method for the curing process to CIR mixtures prepared with different RAP sources (different binder contents and different age) and different initial moisture contents. This was an inter-laboratory study between Italy and Canada, and it showed

how different dosages of water resulted in different rates of water loss by evaporation, but this factor did not penalize the development of ITS. In all cases, the MM model was able to accurately match the data obtained in the laboratory, showing that it has ability to predict evolution of material properties with time independent of initial condition.

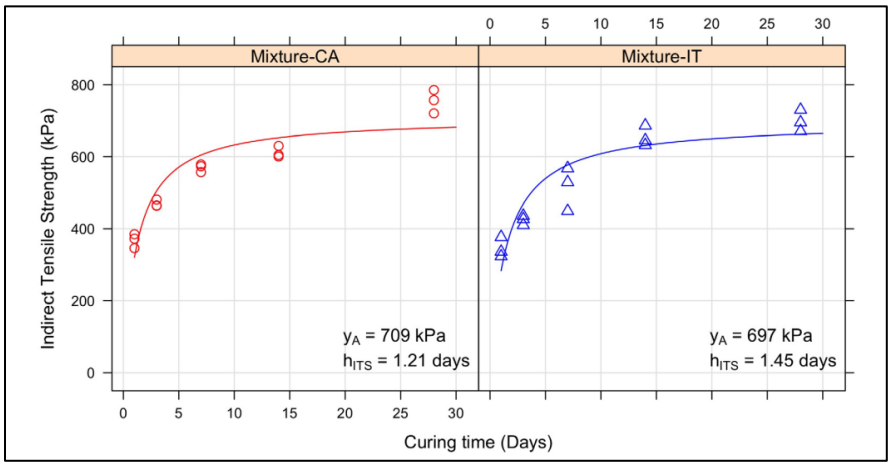

Figure 2.5 M-M model for curing prediction, fitting of ITS data at different curing levels for two CIR mixtures prepared with different RAP sources (Canada and Italy) (reproduced from Graziani et al. 2018).

2.5 SUMMARY OF FINDINGS FROM LITERATURE

An extensive literature review of the state of art and practice of CIR curing was conducted. The summary of findings is presented in this section, organized in tables by the various topics covered. The major outcomes and conclusions of the review that are most important to the current study are discussed.

2.5.1 Summary of Literature Review Findings

Tables 2.1 – 2.5 summarize findings on the consideration and practices for control of curing including various factors that have been identified to significantly affect curing of CIR, various laboratory curing methods and conditions, and current practices for control of curing and/or allowing traffic in states that routinely use CIR.

Table 2.1 Summary of Factors Affecting Curing of CIR

Factors	References
Time	Scholz et al. (1991); Sultan et al. (2016); Cross (1999); Fu et al. (2009); Apeagyei et al. (2013); Kim et al. (2009); Kim et al. (2012); Schwartz et al. (2017); Islam et al. (2018)
Temperature	Cross (1999); Yan et al. (2010); Kim et al. (2011); Diefenderfer et al. (2012); Iwanski et al. (2013); Arimilli et al. (2016); Graziani et al. (2016); Sangiorgi et al. (2017)
Humidity	Santagata et al. (2010); Fu et al. (2009); Gonzalez et al. (2009); Jenkins et al. (2007); Jenkins et al. (2012); Ben and Jenkin (2013); Cizkova et al. (2016); Guatimosim et al. (2018)
Wind	Kim et al. (2009); Kim et al. (2012); Modarres and Ayar (2014); Tia and Wood (1983); Roberts et al. (1984); Cohen et al. (1989); Niazi and Jalili (2008); Babagoli et al. (2016); Omrani and Modarres (2018)
Rainfall	Asphalt Institute (1998); Jenkins et al. (2007); Kim et al. (2011); Gao et al. (2014); Ojum et al. (2014); Li et al. (2016); Grilli et al. (2016)
Component Materials	He and Wong (2008); Du (2015); Xiao and Yu (2011); Iwanski et al. (2013); Modarres and Ayar (2016); Kim and Lee (2016); Arimilli et al. (2016)
Construction Features	He and Wong (2008); Du (2015); Xiao and Yu (2011); Iwanski et al. (2013); Modarres and Ayar (2016); Kim and Lee (2016); Arimilli et al. (2016)

Table 2.2 Summary of Laboratory Curing Methods

Curing Methods	Major Finding	References
Uncovered specimen	Covered specimens could simulate a few hours after CIR construction but uncovered specimens are more adaptable for long-term curing condition	Lee and Im (2008); Fu et al. (2010)
Semi-covered specimen		
Covered specimen		

Table 2.3 Summary of Laboratory Curing Conditions

Stabilizer Type	Curing Condition	References
Foamed Asphalt	60°C for 3 days	Bowering (1970); Bowering and Martin (1976); Lancaster et al. (1994); Maccarrone et al. (1994); Muthen (1998); Lane and Kazmierowski (2003); Hodgkinson and Visser (2004)
	40°C for 1 day (short-term) 40°C for 3 days (long-term)	Ruckel et al. (1982); Muthen (1998); Marquis et al. (2003)
	40°C for 1 days (short-term) 46°C for 3 days (long-term)	Jenkens and Van de Ven (1999)
	Ambient Temperature (1-28 days)	Ruckel et al. (1983); Saleh (2004); Nataatmadja (2001); Long and Theyse (2004); Long and Ventura (2004)
Asphalt Emulsion	25°C in mold for 15 hours (initial curing) 60°C for 3 days (final curing) 60°C for 60 days (long-term)	Sebaaly et al. (2004)
	60°C for 24 hours	Lee et al. (2001)
	60°C for 48 hours	Cross (2003)
	35°C and 20% relative humidity for 14 days for smaller specimens (≈120mm diameter and longer period for larger specimens	Serfass (2002)

Table 2.4 Current Practices for Control of Curing

Type of Curing Recommendation	**States**
Time Based	Iowa (14 days), Nevada (10 days), New York (10 days), Minnesota (3-14 days)
Moisture Content Based	Kansas (2.0%), Colorado (1.0%), Indiana (2.5%), Virginia (50% of optimum water content)
Both Time and Moisture Content Based	Colorado (maximum of 1% free MC, 10 days)

Table 2.5 Current Practices for Allowing Traffic on CIR Layer

Type of Recommendation	States
Time Based	Colorado (2 hours), Indiana (2 hours), Minnesota (2 hours)
Moisture Content Based	Virginia (50% of optimum water content)
Based on Stability Testing	Iowa (no specified test)
No Restriction	Nevada (emulsified asphalt fog seal application), Kansas (power brooming required), New York (brooming required)

The various characteristics that have been identified that directly affect performance of CIR materials are summarized in Table 2.6, including performance tests that have been employed to evaluate these properties.

Table 2.6 Critical Performance Characteristics of CIR Materials

Critical Performance Characteristics	Performance Tests	References
Stiffness	Resilient Modulus	Scholz et al. (1991); Sultan et al. (2016); Cross (1999); Fu et al. (2009); Apeagyei et al. (2013)
	Dynamic Modulus	Kim et al. (2009); Kim et al. (2012); Schwartz et al. (2017); Islam et al. (2018)
Indirect Tensile Strength	Indirect Tensile Strength	Cross (1999); Yan et al. (2010); Kim et al. (2011); Diefenderfer et al. (2012); Iwanski et al. (2013); Arimilli et al. (2016); Graziani et al. (2016); Sangiorgi et al. (2017)
Shear Strength	Triaxial	Santagata et al. (2010); Fu et al. (2009); Gonzalez et al. (2009); Jenkins et al. (2007); Jenkins et al. (2012); Ben and Jenkin (2013); Cizkova et al. (2016); Guatimosim et al. (2018)
Stability	Flow Number and Flow Time	Kim et al. (2009); Kim et al. (2012)
	Marshall and Hveem Stability	Modarres and Ayar (2014); Tia and Wood (1983); Roberts et al. (1984); Cohen et al. (1989); Niazi and Jalili (2008); Babagoli et al. (2016); Omrani and Modarres (2018)
Moisture Content		Asphalt Institute (1998); Jenkins et al. (2007); Kim et al. (2011); Gao et al. (2014); Ojum et al. (2014); Li et al. (2016); Grilli et al. (2016)
Durability	Tensile Strength Ratio	He and Wong (2008); Du (2015); Xiao and Yu (2011); Iwanski et al. (2013); Modarres and Ayar (2016); Kim and Lee (2016); Arimilli et al. (2016)

Table 2.7 and Table 2.8 summarize findings on various tools that have been employed for determination and prediction of the level of curing including in-situ determination devices and prediction equations and models.

Table 2.7 Tools for Quality Control and Determination of In-situ Level of Curing of CIR

Parameter	Devices	References
Stiffness and Strength	Light Weight Deflectometer (LWD) and Falling Weight Deflectometer (FWD)	Lee et al. (2011); Betti et al. (2017); Guatimosim et el. (2017)
	Ground Penetrating Radar (GPR)	Loizos and Plati (2007); Plati et al. (2010); Isola et al. (2013); Modarres et al. (2014); Mehranfar and Modarres (2020); Papavasiliou et el. (2010)
	Dynamic Cone Penetrometer (DCP)	Mohammad et al. (2003); Budge and Wilde (2007); Quirk and Guthrie (2011)
	Geogauge	Mohammad et al. (2003); Lee et al. (2009); Woods et al. (2012); Khosravifar et al. (2013); Lin et al. (2015)
Moisture Content	Nuclear Gauge	Thomas and Kadrmas (2003); Lee et al. (2016); Cox et al. (2016); Sebaaly et al. (2019)
	Time-Domain Reflectometer (TDR)	Woods (2011)

Table 2.8 Prediction Tools for Level of Curing of CIR

Prediction Tools	References
Moisture Loss Index	Woods et al. (2012)
Maturity-Stiffness Relationship	Kuna et al. (2016)
Michaelis–Menten (MM) model	Graziani et al. (2016); Graziani et al. (2018)

2.5.2 Major Findings from the State-of-the-Art Review

The aim of this literature review was to determine the state of the art and state of the practice for quality control and acceptance tools to assess the uniformity, curing behavior and the as-constructed performance of CIR pavements. It is important to establish critical performance characteristics of CIR materials in order to develop or repurpose existing test methods that can be used to measure the identified critical characteristics. In addition, tools currently used for field measurements of degree of curing of CIR as well as critical factors that impact CIR curing time are identified. The following preliminary conclusions were drawn from the review:

- Performance of CIR materials is typically evaluated in terms of two primary distresses: permanent deformation and moisture susceptibility. However, cracking may be an issue when considerable amounts of active fillers are used as stabilizers.

- The weather conditions (temperature, humidity, wind, rainfall) are significant factors that affect CIR curing and as such it will be vital to collect weather data to develop the predictive models. In addition, the mix composition and information regarding the various construction features should be considered.

- There are three different laboratory curing methods (uncovered, semi-covered, covered) for CIR materials. These methods could be applicable in simulating different stages of field curing, as well as curing pertinent to different locations.

- Different environmental curing conditions and durations have been used for CIR materials. However, studies have indicated that curing at 40°C could be ideal to expedite the laboratory curing process without significantly changing mixture properties.

- Currently, state DOTs that routinely use CIR typically use time-based or moisture-based curing specifications with minimal consideration of stiffness/strength gain requirements. Whereas some specifications allow traffic immediately on the compacted CIR layer, others provide some form of recommendation that do not directly characterize early age structural capacity during curing period. However, it is evident that to avoid premature damage, structural capacity requirements should be specified.

- There is a lack of consensus about the fundamental, engineering or empirical properties that are used to characterize CIR materials for pavement design and performance evaluation. Properties such as stiffness, strength, stability, moisture content and durability, have been identified to directly affect performance.

- Based on the literature review, deflection methods (such as, LWD or FWD) and DPS (GPR based measurement) are recommended for use in this study for monitoring in-situ properties of CIR layers during curing.

- There are existing predictive curing models for CIR materials. Whereas they do not take into all factors that could impact curing, they are a good starting point for developing a more robust predictive model.

CHAPTER 3: FIELD PROJECTS, MATERIALS AND TEST METHODS

This chapter first describes the CIR field projects selected for this study. Subsequently, details of the field material sampling and data collection is presented. This includes information such as the as-placed job mix formula for each test section, the recycling train setup, and existing pavement conditions. Timing for overlay placement on the field projects is documented and the various test methods employed in the study are discussed.

3.1 FIELD PROJECTS

Through a survey of local road agencies in Minnesota, well-informed practical considerations, and discussion with TAP, 6 CIR field projects were selected for the study. Figure 3.1 shows the geographical location of the selected projects with respect to the state counties. The details of the projects with their various attributes are listed in Table 3.1. The approved mix design information as well as the construction plans for these projects are included in Appendix B.

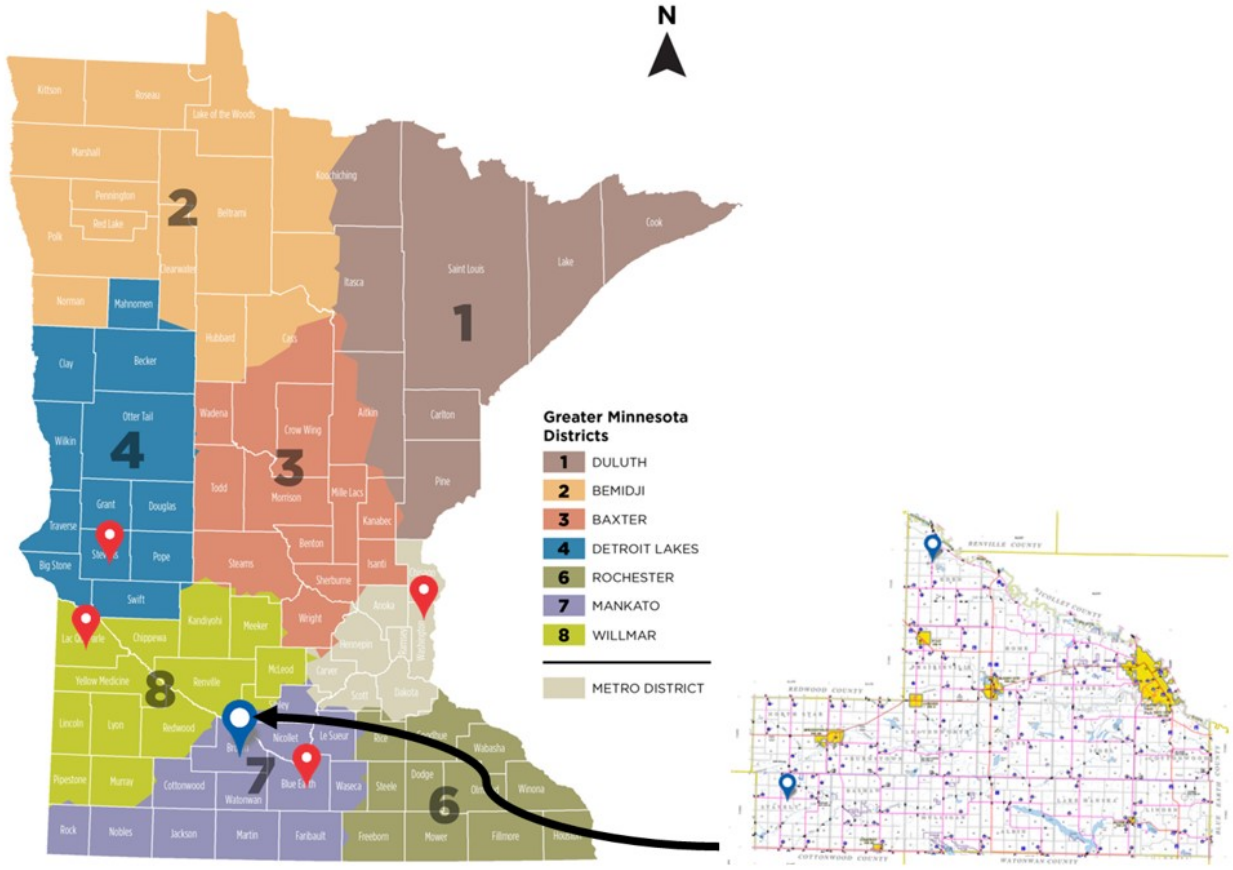

Figure 3.1 Geographical Location of CIR Field Study Projects

Table 3.1 Details of CIR Field Study Projects

Overseeing Agency	Project Name	MnDOT District (County)	Project Type	As-designed Mixture type and thickness	Location	Length (km/mi)	ADT in 2020
Brown County Highway Department	SAP 008-608-042	7 (Brown)	CIR Overlay	Engineered Emulsion (PG 58-28 base binder) 3% Target Asphalt Binder Content 2% Target Moisture Content 76mm (3inch) CIR	**CSAH 8** Between CSAH 30 and 10	6.1/3.8	95
	SAP 017-611-019 008-621-004	7 (Brown)	CIR Overlay	Engineered Emulsion (PG 58-28 base binder) 2.5% Target Asphalt Binder Content 2% Target Moisture Content 76mm (3inch) CIR	**CSAH 11** From U.S. HWY 71 to 490th AVE **CSAH 21** From 490th AVE to CSAH 3	1.6/1.0 8.0/5.0	180
Minnesota Department of Transportation	SP 8105-21	7 (Blue Earth)	Mill Bit. Surface CIR Overlay	Engineered Emulsion (PG 58-28 base binder) 2.25% Target Asphalt Binder Content 0.5% Cement 1.5% Target Moisture Content 76mm (3inch) CIR	**TH 30** From 140' East of TH22 to 1200' East of CSAH 1	33.3/20.7	960
	SP 8209-111	Metro (Washington)	Mill Bit. Surface CIR Overlay	Engineered Emulsion (PG 58-28 base binder) 2% Target Asphalt Binder Content 2% Target Moisture Content 76mm (3inch) CIR	**TH 95** From .1 Mile South of TH94 to .5 Mile North of County Road 14	7.6/4.7	13,800
	SP 3703-25	8 (La Qui Parle)	Mill Bit. Surface CIR Overlay	Engineered Emulsion (PG 58-28 base binder) 2% Target Asphalt Binder Content 0.5% Cement 2% Target Moisture Content 76mm (3inch) CIR	**TH 75** From .1 Mile North of TH212 to TH7	28.5/17.7	1000
	SP 7503-38	4 (Stevens)	Mill Bit. Surface CIR Overlay	Foamed asphalt (PG 52-34) 1.7% Target Asphalt Binder Content 0.5% Cement 76mm (3inch) CIR	**TH 28** From 350' West of 4th St. to Lyndale Ave	20.8/12.9	3300

3.2 MATERIAL SAMPLING AND DATA COLLECTION

3.2.1 Brown County Highway Department

3.2.1.1 CSAH 8

Construction Sequence, Time and Date: CIR construction and sampling from the identified test section on the project occurred on July 8, 2020. The timing of construction of the test section was between 8:30am and 9:00am.

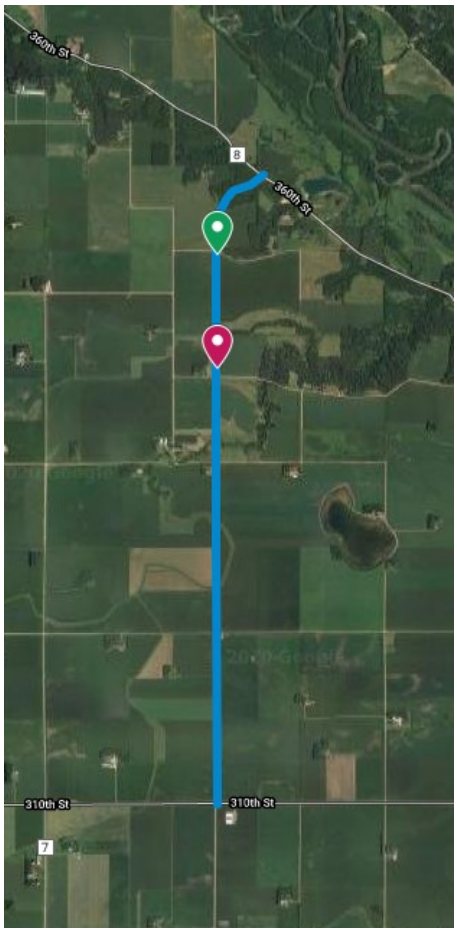

Figure 3.2 CSAH 8 View of the Project from Map (start of the section in green, end in red)

Test Section Description: The 305m (1000ft) test section is in the northbound lane. The total length of the project is shown in Figure 3.2 with the start and end of the test section indicated by the location pins. The GPS stationing coordinates indicates the start of the section at 556+79.00 and end at 566+83.00.

Weather Information: The weather was sunny throughout the construction day. The air temperature was about 25°C (77°F) and humidity was at about 79% with a wind speed of 12.9km/h (8mph). The weather data for the period of in-situ testing was extracted from the closest station to the project (Dacotah Ridge GC - KMNMORGA2) and is shown in Table 3.2.

Table 3.2 CSAH 8 Extracted Weather Data

Date	Average Temperature (°C)	Average Relative Humidity (%)	Average Wind Speed (km/h)	Accumulated Precipitation (cm)
7/8/2020	26.4	73	19.5	0
7/9/2020	24.3	75	8.4	0
7/10/2020	23	70	6.4	0
7/11/2020	22.3	81	5.6	0.79
7/12/2020	22.2	70	6.1	0
7/13/2020	23.7	72	18.7	0
7/14/2020	21	76	11.9	0.64
7/15/2020	19.6	71	2.3	0
7/16/2020	21.7	70	10.6	0
7/17/2020	25.7	78	13.0	0

Existing Pavement: The original structure was previous CIR with bituminous surface. The lane width of the pavement is 3.7m (12ft) with no shoulder. The construction plan involved recycling of the top 76mm (3inch). Prior to construction, the pavement had severe transverse cracks with average spacing of 7.6m (25ft) between cracks. There were also longitudinal cracks outside the wheel path (see Figure 3.4). The surface temperature of the pavement prior to milling was 30.8°C (87.5°F).

Figure 3.3 CSAH 8 Existing Pavement Distresses

Recycling Train Setup: The recycling train flowchart and a picture of a portion of the setup is shown in Figure 3.4.

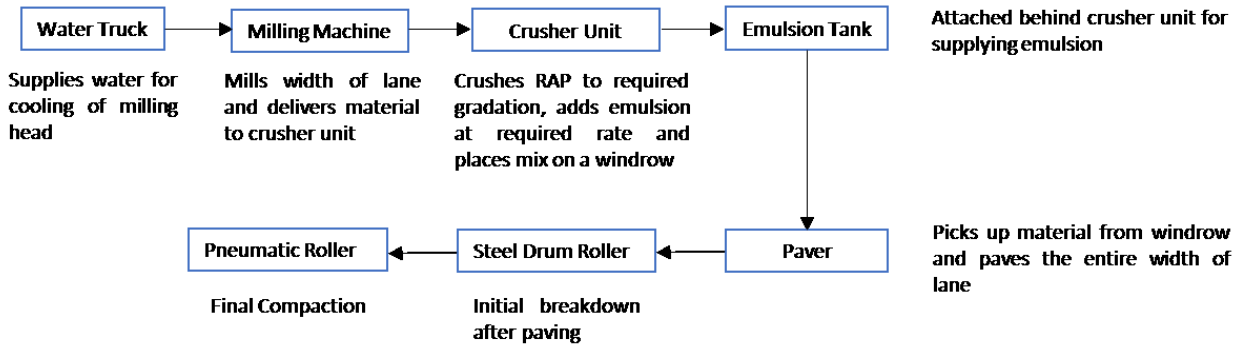

Figure 3.4 CSAH 8 Recycling Train Setup

As-placed Mix Design: The final as-placed CIR job mix formula is shown in Table 3.3.

Table 3.3 CASH 8 Job Mix Formula

Parameters	Attributes
Method of Asphalt Binder Delivery	Emulsion
Type and Grade of Emulsion	CIR-EE (PG 58-28 Base Binder)
Target Amount of Bituminous Material	1.5%
Type and Amount of Mineral Stabilizing Agent	N/A
Stabilizing Depth	76mm (3inch)
Added Amount of Moisture	1.5%
Target Density	1959kg/m^3 (122.3pcf)

Timing of Overlay Placement: Overlay of the roadway started on August 11, 2020.

3.2.1.2 CSAH 11/21

Construction Sequence, Time and Date: CIR construction and sampling from the identified test section on the project occurred on July 15, 2020. The timing of construction of the test section was between 11:15am and 11:50am.

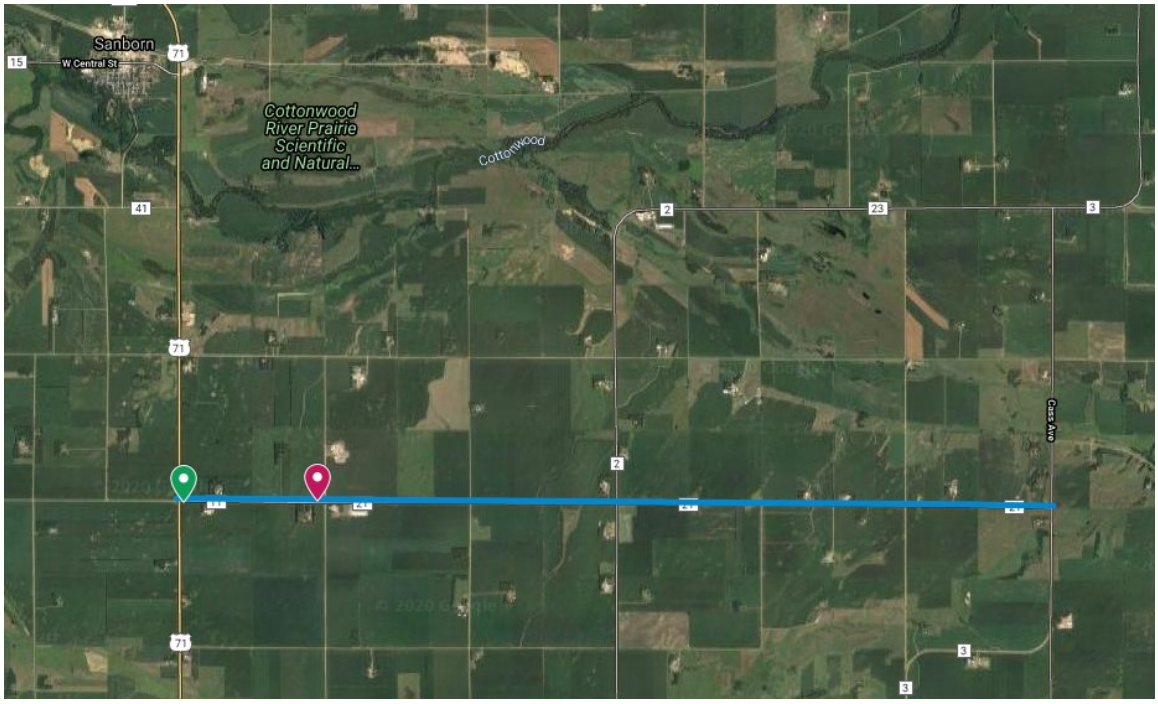

Figure 3.5 CSAH 11/21 View of the Project from the Map (start of the section in green, end in red)

Test Section Description: The test section was identified on westbound lane of the road. This is a joint project between Brown and Cottonwood Counties. However, the section starts and ends in the Cottonwood County portion before the intersection with 490th Ave as can be seen from Figure 3.5. The corresponding GPS stationing goes from the start of the test section at 246+49.50 to the end at 256+53.00.

Weather Information: The weather was cloudy during construction. The air temperature was at 22°C (72°F). Humidity was at 67% with a wind speed of 4.8km/h (3mph). Furthermore, the weather data for the period of in-situ testing was extracted from the closest station to the project (Schoer1Jrarm-KMNWABAS12). This information is given in Table 3.4.

Table 3.4 CSAH 11/21 Extracted Weather Data

Date	Average Temperature (°C)	Average Relative Humidity (%)	Average Wind Speed (km/h)	Accumulated Precipitation (cm)
7/15/2020	19.1	79	2.4	0
7/16/2020	22.1	76	8	0
7/17/2020	26.3	83	8.7	0
7/18/2020	25.7	84	11.7	1.5
7/19/2020	22.2	75	10.5	0
7/20/2020	21.6	81	3.5	0.43
7/21/2020	20.9	85	8.9	0.36
7/22/2020	18.8	81	4.2	0
7/23/2020	20.8	84	8.5	0
7/24/2020	26.4	83	10.9	0

Existing Pavement: The original pavement included a microsurfacing over 127mm (5inch) thick HMA on an underlying gravel base. The lane width of the pavement is 3.7m (12ft) with no shoulders. The construction plan involved recycling of the top 76mm (3inch). Prior to construction, the pavement had severe fatigue and transverse cracks (Figure 3.6). The temperature of the pavement prior to milling the test section was 29°C (85°F).

Figure 3.6 CSAH 11/21 Existing Pavement Distresses

Recycling Train Setup: The recycling train is as shown in the flowchart in Figure 3.7. It was the same construction crew as the CSAH 8 project and with a similar setup (see Figure 3.4).

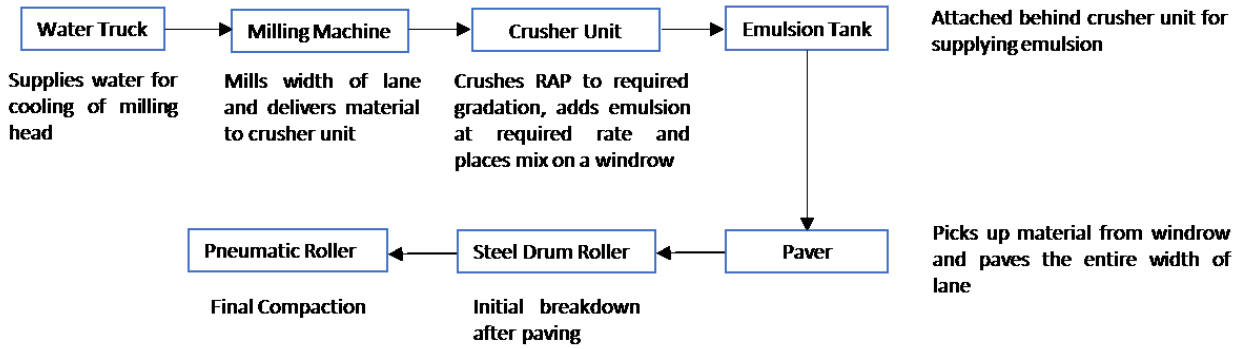

Figure 3.7 CSAH 11/21 Recycling Train Setup

As-placed Mix Design: The final as-placed CIR job mix formula is as shown in Table 3.5.

Table 3.5 CASH 11/21 Job Mix Formula

Parameters	Attributes
Method of Asphalt Binder Delivery	Emulsion
Type and Grade of Emulsion	CIR-EE (PG 58-28 Base Binder)
Target Amount of Bituminous Material	1.9%
Type and Amount of Mineral Stabilizing Agent	N/A
Stabilizing Depth	76mm (3inch)
Added Amount of Moisture	1.5%
Target Density	1937kg/m^3 (120.9pcf)

Timing of Overlay Placement: Overlay of the roadway resumed on September 1, 2020.

3.2.2 Minnesota Department of Transportation

3.2.2.1 TH 28

Construction Sequence, Time and Date: CIR construction and sampling from identified test section of project occurred on July 22, 2020. The timing of construction of the test section was between 12:15pm and 12:55pm.

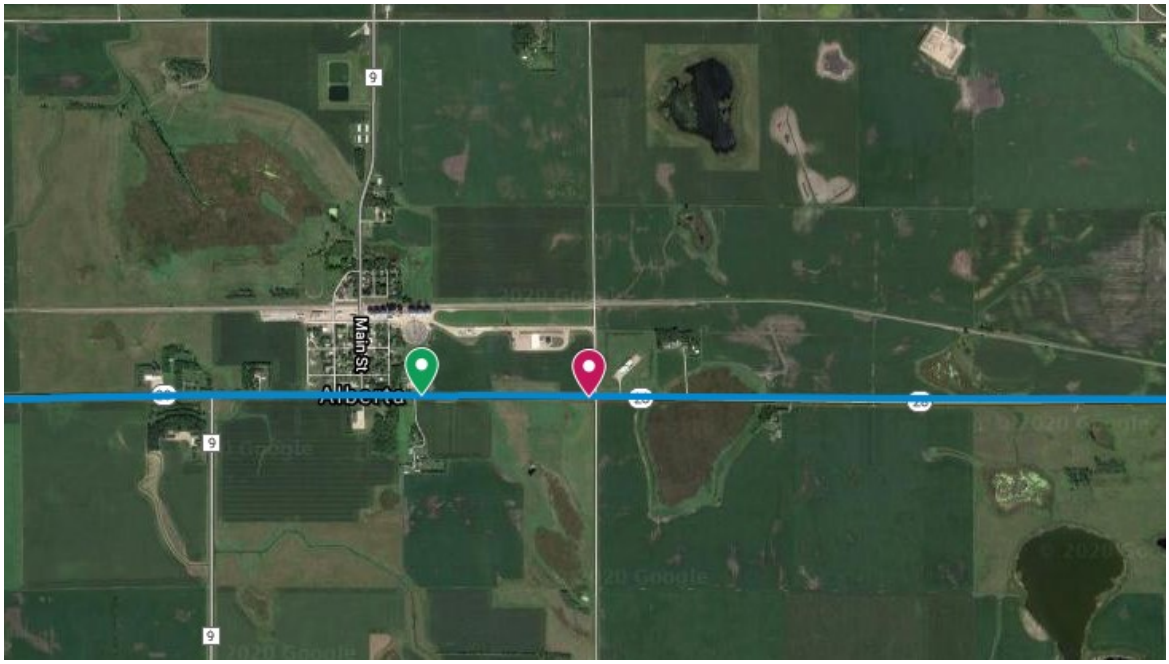

Figure 3.8 TH 28 View of the Project from the Map (start of the section in green, end in red)

Test Section Description: The test section was identified on westbound lane, starting at the city line of Alberta and going to the intersection with 540th Ave as can be seen in Figure 3.8. The corresponding GPS stationing goes from the start of the test section at 997+20.00 to the end at 1007+20.50.

Weather Information: The weather was sunny during construction. The air temperature was at 18.9°C (66°F). Humidity was at 62% with a wind speed of 8km/h (5mph). Furthermore, the weather data for the period of in-situ testing was extracted from the closest station to the project (University Addition - KMNMORRI13). This information is given in Table 3.6.

Table 3.6 TH 28 Extracted Weather Data

Date	Average Temperature (°C)	Average Relative Humidity (%)	Average Wind Speed (km/h)	Accumulated Precipitation (cm)
7/22/2020	19	81	1.3	0
7/23/2020	21.2	84	5.8	0
7/24/2020	27.3	84	9.6	0
7/25/2020	27.4	84	3.5	0.5
7/26/2020	23.6	80	2.8	0.8
7/27/2020	22.7	70	2.3	0
7/28/2020	23.6	70	1.1	0
7/29/2020	22.2	75	0.8	0

Existing Pavement: The original structure consisted of 127mm (5inch) HMA overlay on 254mm (10inch) concrete slab with underlying clay. The lane width of the pavement is 4.3m (14ft) with 0.6m (2ft) paved shoulders. The construction plan involved the milling of the first 51mm (2inch) of HMA and in-place recycling of the remaining 76mm (3inch). The concrete slab had 4.6m (15ft) joint spacing, which resulted in reflective cracks on the overlay (see Figure 3.9). There were also visible longitudinal cracks along the center of the lane. There was prior maintenance that involved sealing of all cracks and a few patches. The temperature of the pavement prior to CIR operation on the test section was 36°C (97°F).

Figure 3.9 TH 28 Pavement Condition after 2'' HMA milling operation

Recycling Train Setup: Due to paved shoulders and some turning lanes, the lane width of recycled pavement was wider than that accommodated by typical milling machine. Therefore, two milling machines were used to achieve the required width of 4.3m (14ft); smaller milling machine milling 0.6m (2ft) from roadway centerline and larger milling machine milling the remaining 3.7m (12ft). The recycling train setup is as shown in the flowchart in Figure 3.10.

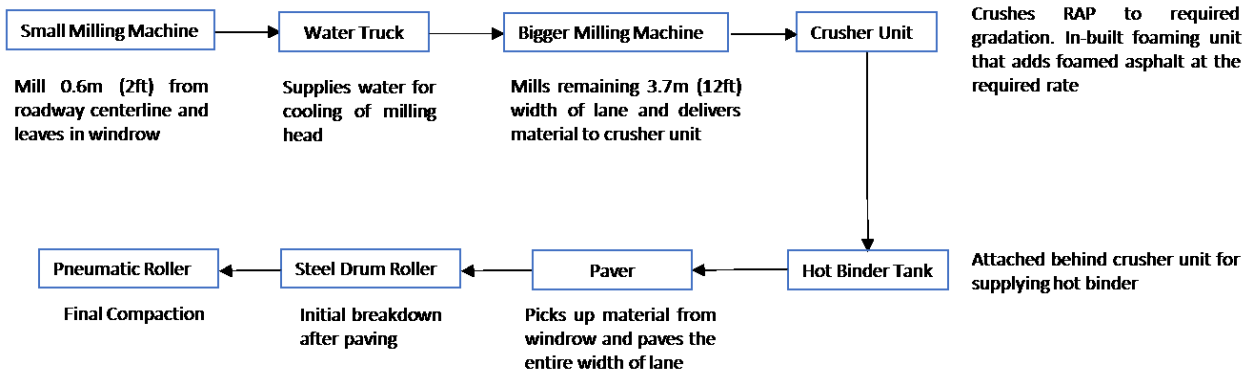

Figure 3.10 TH 28 Recycling Train Setup: Small Milling Machine on the left and Recycling Train Setup on the right

As-placed Mix Design: The final as-placed CIR job mix formula is as shown in Table 3.7.

Table 3.7 TH 28 Job Mix Formula

Parameters	Attributes
Method of Asphalt Binder Delivery	Foamed Asphalt
Grade of binder used for foaming	PG 52-34
Target Amount of Bituminous Material	2.5%
Type and Amount of Mineral Stabilizing Agent	N/A
Stabilizing Depth	76mm (3inch)
Added Amount of Moisture	3-4%
Target Density	2050kg/m^3 (128pcf)

Timing of Overlay Placement: The test section was overlaid on August 5, 2020.

3.2.2.2 TH 30

Construction Sequence, Time and Date: CIR construction and sampling started on the identified test section on the July 9, 2020. The timing of construction of the test section was between 9:24am and 10:30am.

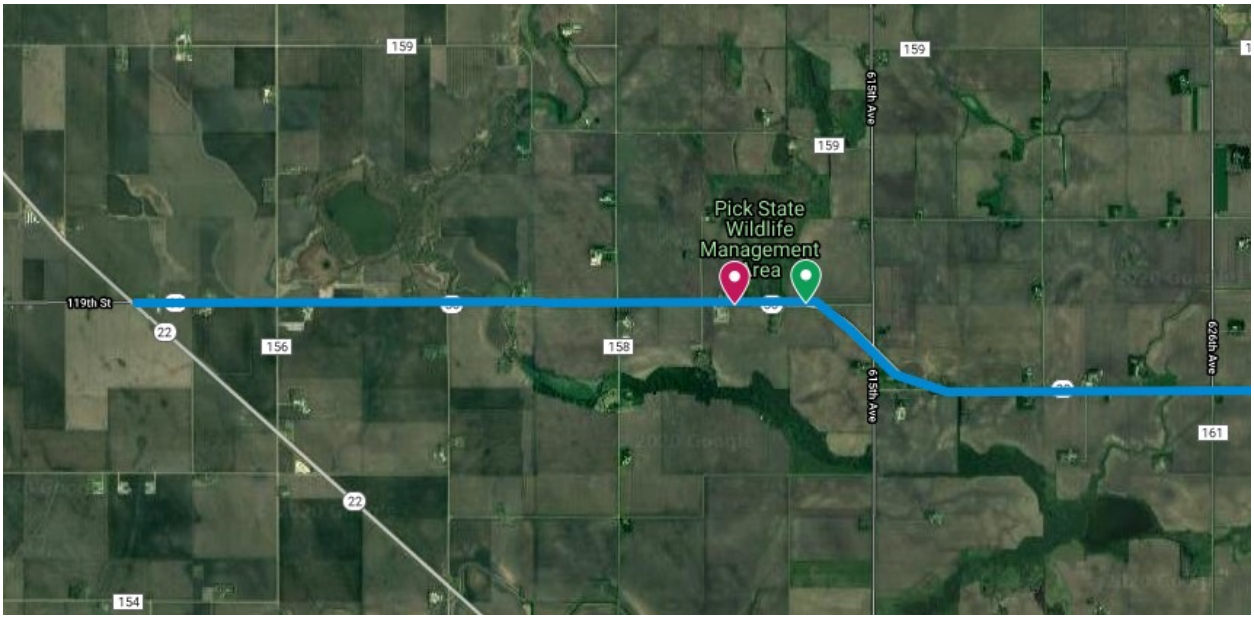

Figure 3.11 TH 30 View of the Project from Map (start of the section in green, end in red)

Test Section Description: The selected test section is on the westbound lane. The section is in the straight portion after the curvature next to the Pick State Wildlife Management Area (see Figure 3.11). The corresponding GPS stationing goes from the start of the test section at 1189+85.00 to the end at 1199+94.00.

Weather Information: Construction started right after a heavy rainfall that lasted for roughly an hour. There were puddles on the existing pavement resulting from the rain at the time of construction as can be seen in Figure 3.12. The air temperature was at 23°C (73°F). Humidity was at 99% with a wind speed of 9.7km/h (6mph). Subsequently, the weather data for the period of in-situ testing was extracted from the closest station to the project (Southern Minnesota Lake - KMNMNE147). This information is given in Table 3.8.

Figure 3.12 Test Section Condition Prior to Recycling Operation

Table 3.8 TH 30 Extracted Weather Data

Date	Average Temperature (°C)	Average Relative Humidity (%)	Average Wind Speed (km/h)	Accumulated Precipitation (cm)
7/8/2020	27.9	73	5.6	0
7/9/2020	22.2	88	3.1	1.27
7/10/2020	23.9	76	3.5	0.03
7/11/2020	22.9	82	3.7	1.22
7/12/2020	22.3	76	4	0
7/13/2020	23.1	76	9.5	0
7/14/2020	21.6	81	4.8	0.30
7/15/2020	19.2	79	1.8	0
7/16/2020	20.9	74	4.8	0
7/17/2020	25.4	82	7.9	0
7/18/2020	27.3	83	8.7	2.26
7/19/2020	24.1	71	6.8	0
7/20/2020	22.5	75	1.6	0
7/21/2020	22.4	80	5	0
7/22/2020	19.0	77	4.5	0
7/23/2020	20.9	79	4	0
7/24/2020	26.6	78	10.1	0

Existing Pavement: The original structure consisted of 254mm (10inch) HMA on a granular base. The total width of the pavement is 7.9m (26ft). The construction plan involved the removal of the first 76mm (3inch) of HMA and recycling of subsequent 76mm (3inch). Prior to construction, the pavement had severe transverse cracks with average spacing of 6.1m (20 ft) between cracks (see Figure 3.13). The temperature of the pavement prior to milling was at 25.8°C (78.5°F).

Figure 3.13 TH 30 Pavement Condition After Milling Operations

Recycling Train Setup: The contractors did not have a milling machine with a capacity to continuously mill the width recycled pavement in this segment. Therefore, two milling machines were used to achieve the required lane width of 4m (13ft); smaller milling machine milling 0.6m (2ft) from shoulder and larger milling machine milling the remaining 3.4m (11ft). The recycling train is as shown in the flowchart (see Figure 3.14).

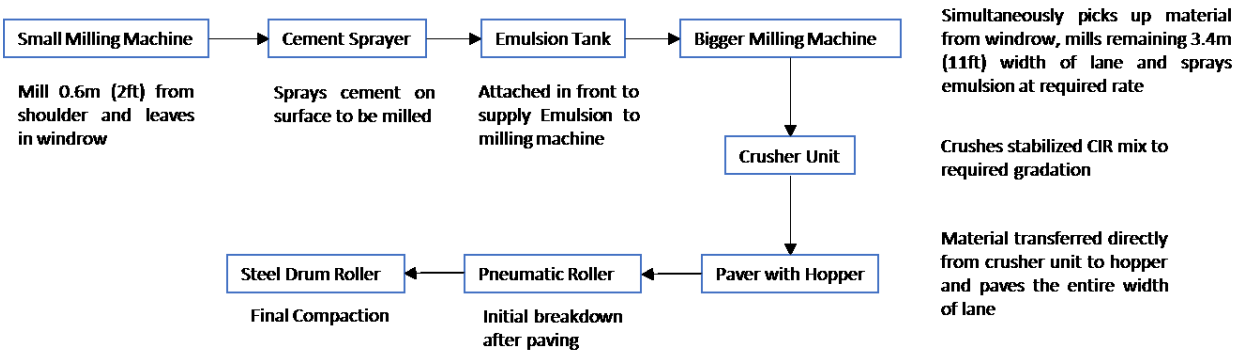

Figure 3.14 TH 30 Recycling Train Setup

As-placed Mix Design: The final as-placed CIR job mix formula is as shown in Table 3.9.

Table 3.9 TH 30 Job Mix Formula

Parameters	Attributes
Method of Asphalt Binder Delivery	Emulsion
Type and Grade of Emulsion	CIR-EE (PG 58-28 Base Binder)
Target Amount of Bituminous Material	2%
Type and Amount of Mineral Stabilizing Agent	0.5% Cement
Stabilizing Depth	76mm (3inch)
Added Amount of Moisture	1%
Target Density	1977kg/m^3 (123.4pcf)

Timing of Overlay Placement: The test section was overlaid on July 27, 2020.

3.2.2.3 TH 75

Construction Sequence, Time and Date: CIR construction started on the northbound lane going southward on July 12, 2020. The identified test section was constructed on July 17, 2020. The timing of construction of the test section was between 8:15am and 8:50am.

Figure 3.15 TH 75 Test Section with Prominent Pavement Distresses

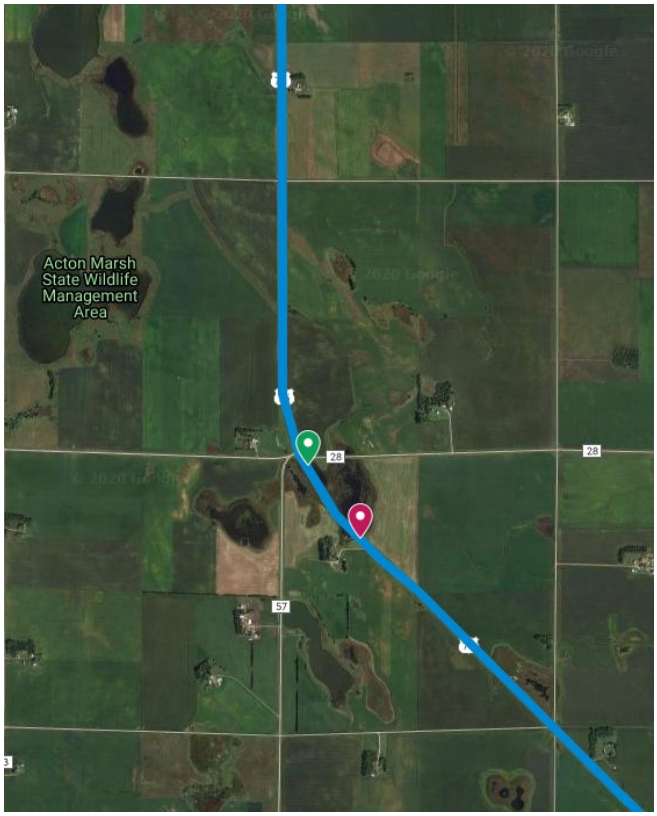

Figure 3.16 TH 75 View of the Project from Map (start of the section in green, end in red)

Test Section Description: The test section was identified on the northbound lane. The section is in the portion of the project north of Madison and starting at the intersection with 300th St. (see Figure 3.15 and Figure 3.16). The corresponding GPS stationing goes from the start of the test section at 111+79.00 to the end at 121+83.00.

Weather Information: The weather was sunny during construction. The air temperature was at 28.9°C (84°F). Humidity was at 69% with a wind speed of 6.4km/h (4mph). Subsequently, the weather data for the period of in-situ testing was extracted from the closest station to the project (NearChhtaPark-KMNMONTE4). This information is given in Table 3.10.

Table 3.10 TH 75 Extracted Weather Data

Date	Average Temperature (°C)	Average Relative Humidity (%)	Average Wind Speed (mph)	Accumulated Precipitation (in)
7/17/2020	26.8	81	3.4	0
7/18/2020	24.7	84	2.9	0.2
7/19/2020	22.8	69	2.7	0
7/20/2020	22.0	76	1.4	0.48
7/21/2020	20.7	85	2.1	0.15
7/22/2020	19.4	79	1.4	0
7/23/2020	21.9	80	4.2	0
7/24/2020	28.0	79	5.3	0
7/25/2020	28.3	80	2.7	0.08
7/26/2020	23.7	82	2.4	0.53
7/27/2020	22.8	69	1.4	0
7/28/2020	23.8	70	1.4	0
7/29/2020	22.4	75	1.1	0

Existing Pavement: The original structure consisted of 76mm (3inch) HMA overlay on 254mm (10inch) concrete slab and a gravel base. The total width of the pavement is 7.9m (26ft) including shoulders. The construction plan involved the recycling of the 76mm (3inch) HMA overlay with shoulders. The concrete slab had 6.1m (20ft) joint spacing, which resulted in reflective cracks on the overlay. There were also visible longitudinal cracks along the center of lane and all cracks were previously sealed (Figure 3.15). The temperature of the pavement prior to milling the test section was at 27.2°F (81°.

Recycling Train Setup: Due to greater than 3.7m (12ft) lane width of recycled pavement, two milling machines were used to achieve the required lane width of 4m (13ft); smaller milling machine milling 0.6m (2ft) from roadway centerline and larger milling machine milling the remaining 3.4m (11ft). The paving crew and equipment was same as the one on the TH 28 project (Figure 3.10**Error! Reference source not found.**) but with a cement sprayer right in front (Figure 3.18). The recycling train is as shown in the flowchart (see Figure 3.17).

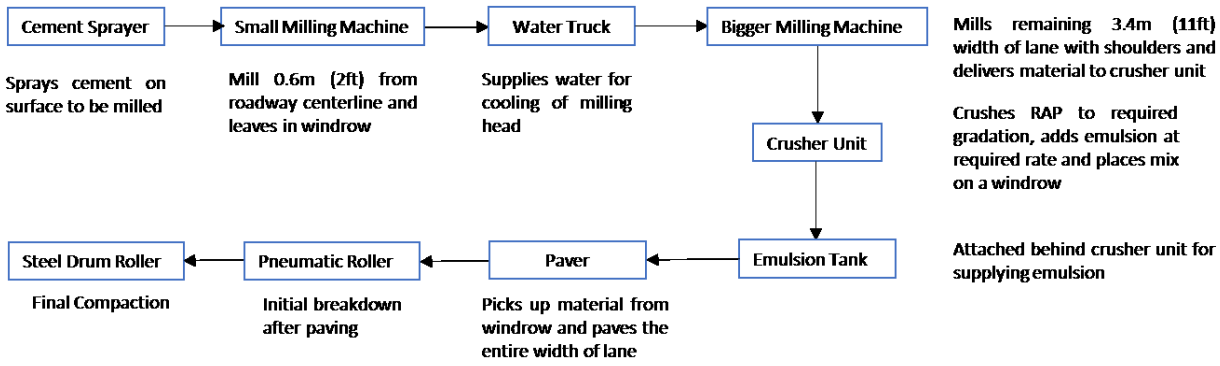

Figure 3.17 TH 75 Recycling Train Setup

Figure 3.18 TH 75 Cement Sprayer

As-placed Mix Design: The final as-placed CIR job mix formula is as shown in Table 3.11.

Table 3.11 TH 75 Job Mix Formula

Parameters	Attributes
Method of Asphalt Binder Delivery	Emulsion
Type and Grade of Emulsion	CIR-EE (PG 58-28 Base Binder)
Target Amount of Bituminous Material	1.7%
Type and Amount of Mineral Stabilizing Agent	0.5% Cement
Stabilizing Depth	76mm (3inch)
Added Amount of Moisture	1.5%
Target Density	2060kg/m^3 (128.6pcf)

Timing of Overlay Placement: The test section was overlaid on August 19, 2020.

3.2.2.4 TH 95

Construction Sequence, Time and Date: CIR construction started on the northbound lane going southward on July 10, 2020. The timing of construction of the test section was between 11:00am and 11:30am.

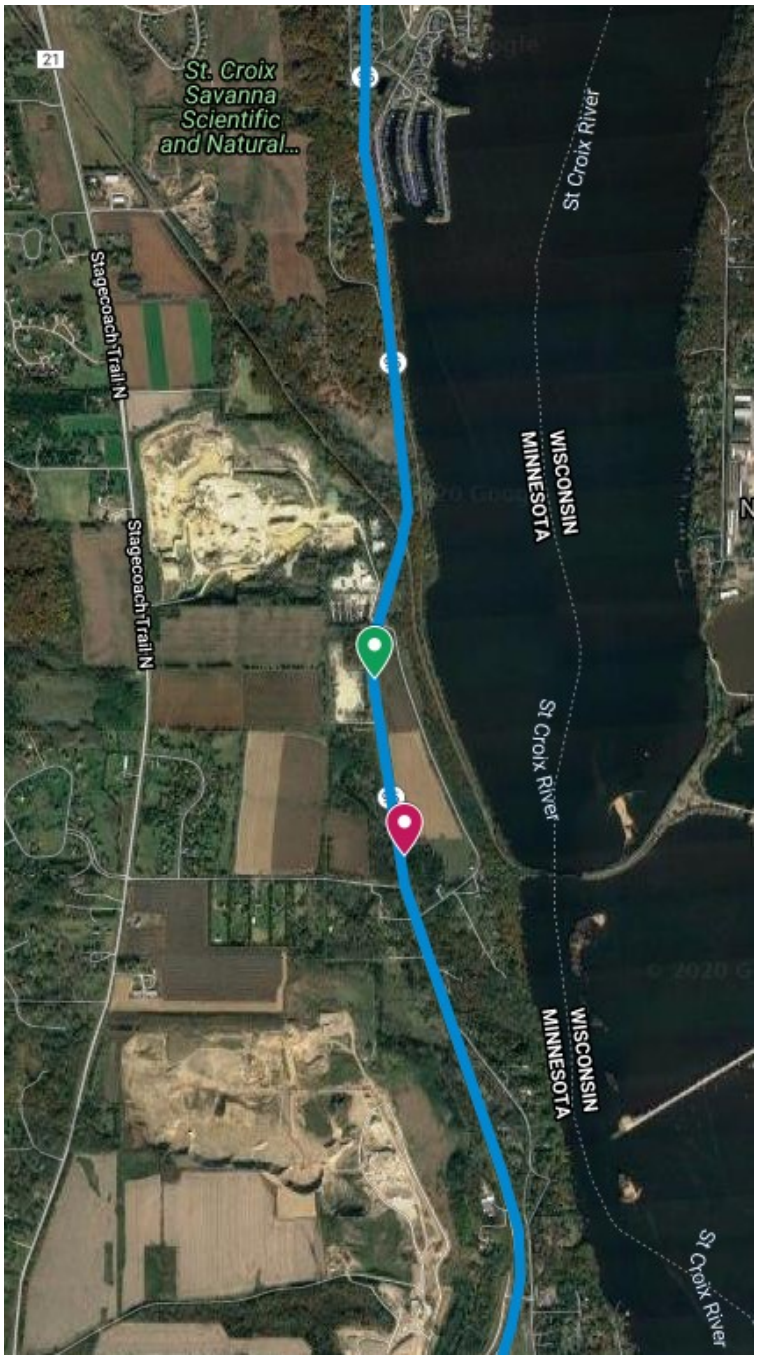

Figure 3.19 TH 95 View of the Project from Map (start of the section in green, end in red)

Test Section Description: The test section was identified on the northbound lane going southward. The section starts at the beginning of the southern half of the project, at the end of the curvature after the bridge and ends before the intersection with 22nd St N as can be seen in Figure 3.19. The corresponding GPS stationing goes from the start of the test section at 1099+04.50 to the end at 1108+96.00.

Weather Information: The weather was sunny during construction. The air temperature was at 22.2°C (72°F). Humidity was at 78% with a wind speed of 6.4km/h (4mph). Subsequently, the weather data for the period of in-situ testing was extracted from the closest station to the project (Wynstone-KMNSTILL13). This information is given in Table 3.12.

Table 3.12 TH 95 Extracted Weather Data

Date	Average Temperature (°F)	Average Relative Humidity (%)	Average Wind Speed (mph)	Accumulated Precipitation (in)
7/10/2020	22.1	99	0.8	0
7/11/2020	24.4	99	0.3	0
7/12/2020	17.4	99	0.2	0
7/13/2020	29.8	99	6.6	0.18

Existing Pavement: The original structure consisted of 178mm (7inch) HMA on a granular base. The total width of the pavement is 7.9m (26ft) including shoulders. However, only the driving lanes were recycled. The construction plan involved the milling of the first 51mm (2inch) of HMA (Figure 3.20) and recycling of subsequent 76mm (3inch). Prior to construction, the milled pavement had transverse cracks with average spacing of 4.3m (14ft) between cracks. There were also visible longitudinal cracks out of the wheel path (center of lane) and some patches. The temperature of the pavement prior to milling was at 38.1°C (100.5°F).

Figure 3.20 TH 95 Pavement Condition After 2'' HMA Milling Operations

Recycling Train Setup: The recycling train is as shown in the flowchart (Figure 3.21). The project had similar crew as the CSAH 8 and 11/21 but made use of intelligent compaction (IC) technology. Some of the equipment can be seen in Figure 3.21.

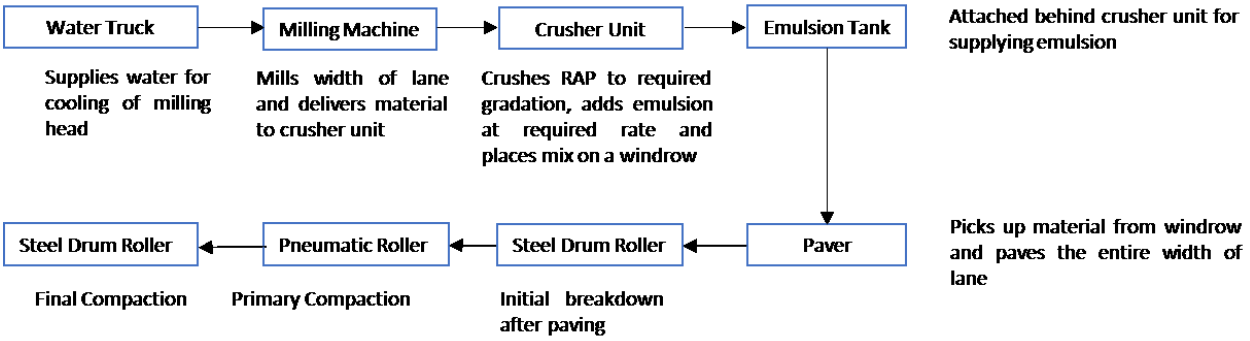

Figure 3.21 TH 95 Recycling Train Setup with IC Rollers

As-placed Mix Design: The final as-placed CIR job mix formula is as shown in Table 3.13.

Table 3.13 TH 95 Job Mix Formula

Parameters	Attributes
Method of Asphalt Binder Delivery	Emulsion
Type and Grade of Emulsion	CIR-EE (PG 58-28 Base Binder)
Target Amount of Bituminous Material	2%
Type and Amount of Mineral Stabilizing Agent	N/A
Stabilizing Depth	76mm (3inch)
Added Amount of Moisture	1.5%
Target Density	2058kg/m^3 (128.5pcf)

Timing of Overlay Placement: Overlay placement started 5 days after the CIR completion. Hence, the test section was overlaid on July 15, 2020.

3.3 TEST METHODS

3.3.1 Field (In-situ)

A series of in-situ tests were performed on the identified test sections during the initial curing duration for each of the six projects involved in this study. A team of MnDOT Office of Materials and Road Research (OMRR) personnel conducted the in-situ testing. The dates of testing for each project can be found in Table 3.14. The equipment used for these tests includes a Dielectric Profiling System (DPS), a Lightweight Deflectometer (LWD), a Nuclear Density and Moisture Gauge (NDMG), a Rapid Compaction Control Device Dynamic Penetrometer (RCCD), and a Surface Temperature Infrared Thermal Sensing Gun (TSG) (see Figure 3.22).

Figure 3.22 In-situ Testing Equipment

Each piece of equipment was used to take point measurements at eight uniformly spaced locations throughout the test section at 61m (200ft) longitudinal intervals, and 0.8m (2.5ft) and 2.6m (8.5ft) lateral offset from the centerline. These locations are referred to as “measurement location”. A schematic of the testing program, along with the standardized naming convention of the measurement locations can be found in Figure 3.23 and Figure 3.24. Except for TH28, testing was performed in the lane with increasing stationing and opposite travel direction. Note that the measurement location naming convention was dependent on the direction of testing. This means the “start” of the section is taken as the edge of the section where testing began and the measurement location on the left side of the lane closest to the “start” is always labeled “S11”.

Table 3.14 Testing Dates for Each Project

Project	Number of Testing Times	Testing Dates	Number of Day after CIR Paving
CSAH 08	4	7/8, 7/10, 7/15, 7/17	0,2,7,9
CSAH 11/21	4	7/15, 7/17, 7/21, 7/24	0,2,6,9
TH 28	3	7/23, 7/27, 7/29	1,5,7
TH 30	4	7/10, 7/16, 7/21, 7/24	1,6,11,14
TH 75	4	7/20, 7/23, 7/27, 7/29	3,6,10,12
TH 95	2	7/11, 7/13	1,3

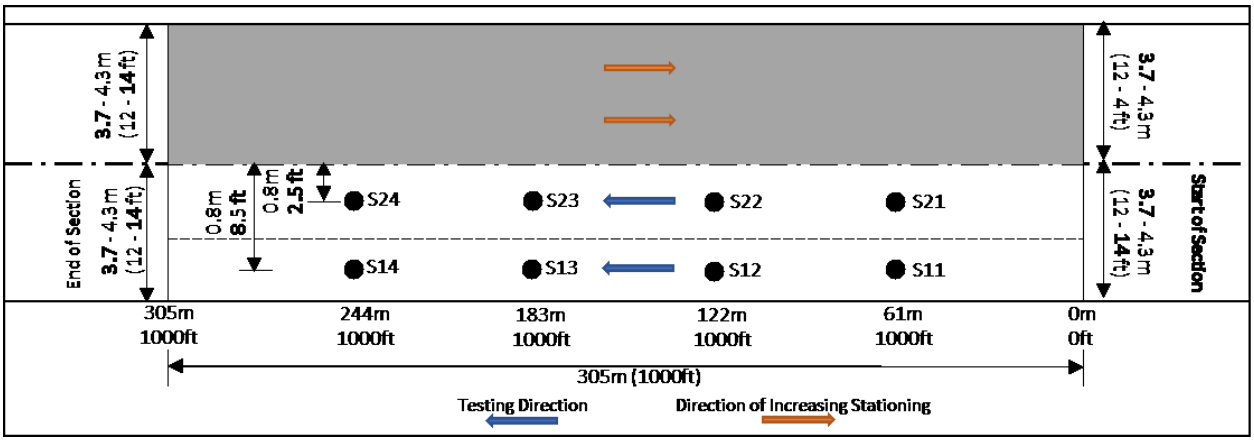

Figure 3.23 Typical Testing Diagram for a Test Section (Not Drawn to Scale)

The measurement locations were surveyed and marked with pavement marking paint on the first day of testing for each project. Real Time Kinematic (RTK) corrected GPS coordinates of the locations were captured using a Trimble R10 GPS system. All the testing was performed simultaneously to the extent that was possible: two OMRR team members performed the LWD, NDMG, and RCCD testing while one OMRR team member performed the DPS testing. The surface temperature of the measurement locations was captured before each point measurement. OMRR personnel collected the air temperature for each testing date using the weather application on their smartphones.

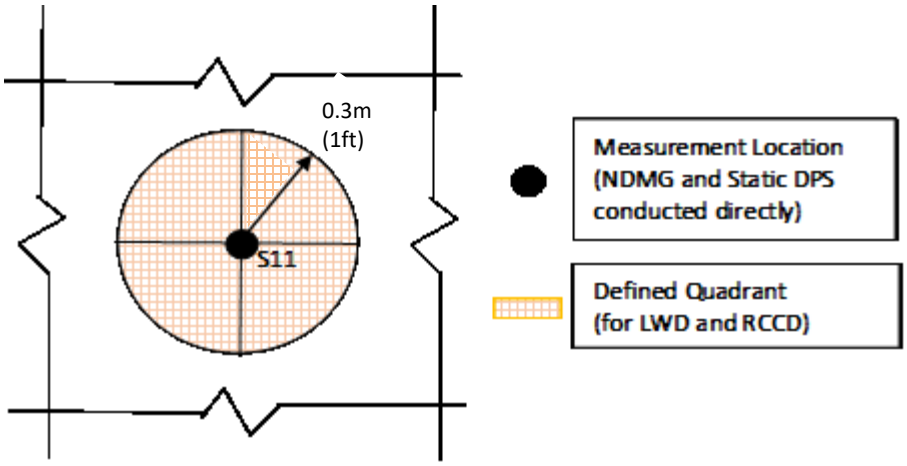

Figure 3.24 Schematic for the Testing Campaign on Each Measurement Location (S11 Example)

3.3.1.1 Lightweight Deflectometer (LWD)

The LWD was used to evaluate stiffness as curing progresses. The LWD equipment (Figure 3.25) is made up of three parts: a pole with a sliding drop weight, a base that is used to transfer the impact of the drop weight to the ground with a coupled load cell and an accelerometer that estimates deflection of the surface, and an electronic device that is used to display the measurement results. The base, which has a diameter of 150mm is placed on the measurement location. The pole is fit onto the base while a hook holds the drop weight at the top of the pole. The electronic device is connected to the base through a cable. Once the electronic device is switched on and ready to record, the weight is dropped on to the base three times. The electronic device records and displays the deflection of the surface for each drop as well as the average deflection and the estimated elastic modulus of the material.

Figure 3.25 Lightweight Deflectometer

The testing is done at multiple spots, located within 0.3m (1ft) radius of targeted measurement locations, to avoid retesting over already compacted spots. To ensure systematic distribution of the LWD measurement spots, four quadrants centered at the exact measurement location were drawn on the pavement surface and each quadrant received at least one LWD test (see Figure 3.24). Additional measurements were taken if a high degree of variability was observed around the location. The measurement at different locations was done to ensure any compaction from previous tests would not affect the results.

As testing is done in a non-temperature-controlled environment, corrections are required to account for temperature susceptibility of asphalt component of the CIR mixtures. There is literature available on different temperature correction methodologies for the LWD device; the methodology recommended by Chou et al. (2017) was employed in this project due to its demonstrated consistency. The stiffness modulus values measured using the LWD were corrected to a reference temperature of 35°C (95°F). The corrected stiffness is denoted as E_{35}.

3.3.1.2 Rapid Compaction Control Device (RCCD)

The RCCD (Figure 3.26) was also used to track the evolution of stiffness gain during curing. The RCCD measures the penetration depth of the penetrometer through the CIR material which is reflective of the stiffness/strength of the material. The RCCD testing procedure is as follows: place the device in the test location, step on the footholds, load the spring by pulling up on the plunger until a click is heard which indicates the loading spring is charged. At that point, the measuring rod is adjusted so the zero mark is aligned with a stationary measuring ring. The loading spring is then released by twisting the handle

counterclockwise. The penetration depth is obtained and manually recorded based on the alignment of measuring rod and ring.

Figure 3.26 Rapid Compaction Control Device

Only a single RCCD measurement was taken at each measurement location on each day of testing. For each measurement, the device was placed somewhere close to the center of the measurement location (see Figure 3.24). However, it was never placed closer than the edge of the center circle due to concerns that creating holes, even small ones, in the CIR surface would disrupt the static DPS point measurements. There is currently no existing procedure to correct for temperature sensitivity of RCCD measurements, therefore the test results are presented as measured.

3.3.1.3 Nuclear Density and Moisture Gauge (NDMG)

The NDMG was used to evaluate the moist density, dry density, bulk density, and percent moisture of the CIR material. However, for the purpose of this study, the percent moisture is of most interest to track the evolution of curing. The NDMG device used is a Seaman C-300 unit, depicted in Figure 3.27. All NDMG measurements were performed by a MnDOT certified operator. The unit was operated in “backscatter, touchable mode”, which means there was no air gap between the bottom of the meter and the CIR surface. After a short warm up period, the equipment was placed directly in the middle of a testing point with the display screen either perpendicular or parallel to the length of the test section.

Figure 3.27 Nuclear Density Moisture Gauge

Two NDMG measurements were taken at each measurement location on each day of testing (Figure 3.24). Once the first measurement was complete, the equipment was rotated 90 degrees and the second measurement was taken.

3.3.1.4 Dielectric Profiling System (DPS)

Ground Penetrating Radar (GPR) technology is a non-destructive testing technology that has shown promising results for rapid, full-coverage and continuous measurements of density in newly constructed bituminous pavements (Hoegh et al., 2019; Hoegh et al., 2020; Steiner et al., 2020; Zegeye-Teshale et al., 2020). A pertinent GPR application approach is the surface reflectivity method which consists of determining the surface dielectric ε_{AC} of the top bituminous mixture layer based on GPR reflection amplitudes obtained from a metal A_m and a newly constructed pavement surface A_0. Equation 3.1 is used to derive ε_{AC} :

$$\varepsilon_{AC} = \left(\frac{1 + \frac{A_0}{A_m}}{1 - \frac{A_0}{A_m}} \right)^2 \tag{3.1}$$

The ε_{AC} values can be converted to density using transfer (calibration) models generated from density-dielectric relationships. However, the primary objective of the present study is to assess the effectiveness of using surface dielectric to monitor the curing evolution of CIR mixtures. The determination of density is secondary.

GPR testing for this project was conducted using a push-cart Dielectric Profiling System (DPS) composed of a GSSI PaveScan data acquisition and control unit, three small-size dipole-type antennas, a distance measurement instrument (DMI) and a Global Positioning System (GPS) antenna receiver.

The DPS system unit can be seen in Figure 3.28. The same GPS receiver and controller equipment used to capture the measurement locations were used as part of the DPS unit. The receiver was mounted on the pushcart and connected to the control tablet through a wired connection. The receiver was used to stream GPS data to the tablet so that each dielectric measurement had an associated longitude and latitude.

Figure 3.28 Dielectric Profiling System

DPS testing was conducted according to the AASHTO PP 98-191 standard procedure. Accordingly, air and metal calibrations of the antennas were performed before each testing session.

A swerve test was performed to check if the antennas were properly calibrated and functioning. To perform a swerve test, continuous dielectric data was collected with the three antennas as the cart advances in a swerve pattern along the test section. Data was collected for 76m (250ft) in one direction, then 76m (250ft) in the opposite direction. The goal of this test was to get full and random coverage of the pavement mat with the three antennas. Properly calibrated and functioning antennas are expected to be collecting roughly the same range of dielectric values over the course of the test. Once the collection was complete, the median dielectric values of the antennas were compared. The goal was to have a relatively small range of values. The ideal is a range less than 0.1, but with the somewhat unpredictable nature of the makeup of CIR material, larger ranges were expected and seen. The range of each swerve test was manually recorded. The testing process continued once it was within the acceptable range, otherwise one or two additional swerve tests were performed. If these tests failed as well, the DPS unit was rebooted and calibration was performed again.

Once the swerve testing was complete, point measurements were taken at each of the measurement locations in the test section. These were time-based “static” DPS measurements where the center antenna was positioned directly over the measurement location (see Figure 3.24) and data was collected for 60s. Data was collected with each antenna, and the two outer antennas were spaced 2 ft. away from the center antenna. Because the measurement locations were located 0.8m (2.5ft) and 2.6m (8.5ft) away from the centerline at each of the specified intervals, data was collected 0.2m (0.5ft), 0.8m (2.5ft), 1.4m (4.5ft), 2m (6.5ft), 2.6m (8.5ft), and 3.2m (10.5ft) away from the centerline at the 61m (200ft), 122m (400ft), 183m (600ft), and 244m (800ft) locations along the test section. One static DPS test was

performed at each measurement location on each day of testing. The static DPS test configuration can be seen in Figure 3.29.

Figure 3.29 Positioning of the DPS Unit during Static DPS Test

Once the static tests were complete, continuous field surveys were taken. One survey was performed on each side of the test section for each day of testing. The survey would begin with the front wheels of the pushcart lined up on the starting edge of the test section, with the center of the right-most antenna 0.2m (0.5ft) away from either the centerline or the center of the test section, depending on which side of the section the survey was performed on. The starting edge of the test section was the marked line indicating the end of the test section closest to the "S11" and "S21" testing points (refer to Figure 3.23). This starting position can be seen in Figure 3.30. Once in the starting position, the measurement would begin. The cart advances in a straight line, using the measurement locations and other markers as positioning references. It was very important that the cart move in a straight line because the survey measurements were distance based and the starting station was specified. If the path of the cart wavered significantly, it would be difficult to line up the data from different runs next to each other because the stationing associated with the measurements would be incorrect. Data was collected along the entire length of the test section. The collection ended with the front wheel of the pushcart lined up on the ending edge of the section. The data collection was triggered by the DMI on the pushcart, so collection could be paused in the middle of the "run" to accommodate for moving of other testing equipment. The path was kept as clear as possible for these measurements as the GPR antennas are very sensitive.

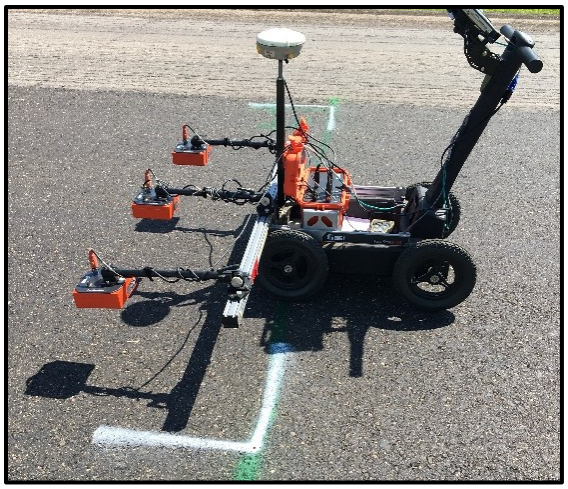

Figure 3.30 Beginning Position of a DPS Survey Measurement

Because the first set of testing for the OMRR team typically occurred on the day of construction (day 0) or the day after construction (day 1), the test section and its corresponding measurement locations were almost always set up and marked out before CIR could be laid in the opposite lane. Because of this, there were certain projects (TH28, TH30, and TH75) where the CIR in the opposite lane cut into the test section (joint overlapping) more than was anticipated. In these cases, the dielectric measurements of the antenna 0.2m (0.5ft) away from the centerline (i.e. the 0.2m (0.5ft) offset antenna) during the static and survey tests were often compromised. This is because the antenna would sometimes collect data over the newer CIR material, making the measurements not representative of the material in the test section. In these cases, normal data collection continued, but a note was made so the compromised data could be excluded during analysis. An example of this situation can be seen in Figure 3.31. This procedure was also followed for measurement locations that had cores drilled in their center. For these locations, the center antenna readings were excluded from data analysis.

Figure 3.31 Example of Compromised Data from Opposite Lane Paving

There are three types of raw DPS files: static, survey, and swerve. There is a raw data file for each static DPS point measurement taken for each project. For each of these static DPS files, the average, median, and standard deviation of the dielectric values gathered with each antenna was calculated. For each project, these summary statistics were gathered in a single table so that for each day of testing there were three entries for each measurement location, one for each antenna. There was also a raw data file for each swerve test. For each of these tests, the median dielectric value of the measurements gathered by each antenna was found and the range of those median values was calculated. The summary statistics for each swerve test were gathered in one table for each project. There was also a raw data file for each survey measurement. This means that for each day of testing on a project, there were two survey data files. The measurements taken during the two survey runs were combined into a single table based on stationing. The result was a single survey data table for each testing date for each project. Each test section was then split into lots of 46m (150ft) and summary statistics including average dielectric value, standard deviation, coefficient of variation, 10th percentile and 90th percentile was found for each lot for each day of testing. These statistics were calculated using the data from both sides of the test section. The summary statistics for each lot for each day of testing were gathered in a single table.

3.3.2 Laboratory

The various laboratory tests conducted to monitor curing in the laboratory are discussed in this sub-section.

3.3.2.1 Gravimetric Measurement

Primarily, the moisture evolution is tracked using gravimetric measurements. A digital scale with a 0.1g precision is employed (see Figure 3.32). The mass of each specimen is recorded immediately after compaction and subsequently measured on each testing day. Four specimens are measured on each testing day to determine average mass (moisture) loss. The mass loss is further expressed in terms of residual water using equation 3.2. Residual water (RW) is the transient moisture content of each specimen with reference to the IMC. The RW approaches an equilibrium amount close to but never to zero as it also accounts for moisture that may be lost during the compaction process or moisture chemically bound in the CIR. The equilibrium RW values tend to be higher with higher IMC.

$$Residual\ Water\ (\%) = \frac{M_w - (M_{ini} - M_{test})}{M_{ini} - M_{plate}} \times 100 \tag{3.2}$$

Where:

M_w = Mass of water for each specimen determined from mix design based on the IMC
M_{ini} = Initial mass of specimen with plate
M_{test} = Mass of specimen with plate at testing day
M_{plate} = Mass of plate

Figure 3.32 Digital Scale for Gravimetric Measurements

3.3.2.2 Laboratory Dielectric Measurement System

In the field, the applicability of the Ground Penetrating Radar (GPR) based technology to monitor curing evolution of CIR mixtures (using surface dielectric value as a parameter) was explored. Similarly, testing was conducted in the laboratory using a Laboratory Dielectric Measurement System (LDMS). The LDMS is composed of a GSSI PaveScan® antenna connected to a computer for data acquisition. The setup is as shown in Figure 3.33. Prior to measurements, calibration is done using a high-density polyethylene (HDPE) cylinder with a known dielectric value. The dielectric measurements were collected immediately after the gravimetric measurements using the same specimens and the average dielectric was determined. Due to fragileness of the specimens, dielectric measurements were not conducted immediately following compaction.

Figure 3.33 Laboratory Dielectric Measurement System (LDMS) Setup

3.3.2.3 Resilient Modulus Test

The resilient modulus (M_R) is used to evaluate stiffness and structural contribution of CIR materials. The M_R result can further be used as an input for pavement design, evaluation, and analysis. The M_R test was conducted in the laboratory in accordance with ASTM D7369. It involves the application of cyclic haversine

compressive load on the diametral plane of a cylindrical specimen. The horizontal and vertical deformations are measured and used to determine the Poisson's ratio using equation 3.3, and ultimately the M_R using equation 3.4. The test setup in the Universal Testing Machine (UTM) is shown in Figure 3.34. Three specimens were tested for each mixture at room temperature at the different curing times.

$$\mu = \frac{I4 - I1 \times \left(\frac{\delta_v}{\delta_h}\right)}{I3 - I2 \times \left(\frac{\delta_v}{\delta_h}\right)} \tag{3.3}$$

$$M_R = \frac{P_{cyclic}}{\delta_h t}(I1 - I2 \times \mu) \tag{3.4}$$

Where:

μ	=	Poisson's ratio
M_R	=	Resilient modulus, MPa
δ_v , δ_h	=	Recoverable vertical and horizontal deformation respectively, mm
$I1$, $I2$, $I3$, $I4$	=	Constants dependent on gauge length for measured deformations
P_{cyclic}	=	Cyclic load applied to specimen, N
t	=	Thickness of specimen, mm

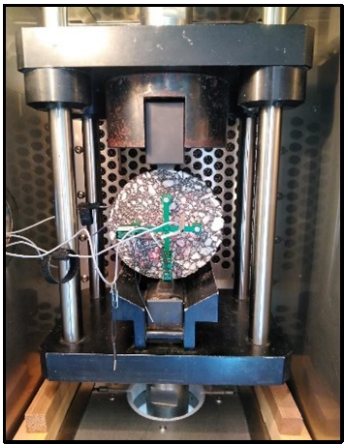

Figure 3.34 Resilient Modulus Test Setup in UTM

3.3.2.4 Indirect Tensile Strength Test

The indirect tensile strength (ITS) test is used for mechanical evaluation of CIR materials in terms of strength properties during the curing process. The ITS test was conducted following the ASTM D6931 standard. The procedure follows the application of a monotonic compressive load on the vertical diametral plane of a cylindrical specimen at a loading rate of 50mm/min. The peak load at failure is recorded to determine the ITS using equation 3.5. The typical test setup in the UTM is shown in Figure 3.35. Four replicates were tested at room temperature for each curing time.

$$ITS = \frac{2000 \times P}{\pi \times t \times D} \quad (3.5)$$

Where:

ITS	=	Indirect tensile strength, kPa
P	=	Peak load, N
t	=	Thickness of specimen, mm
D	=	Diameter of specimen, mm

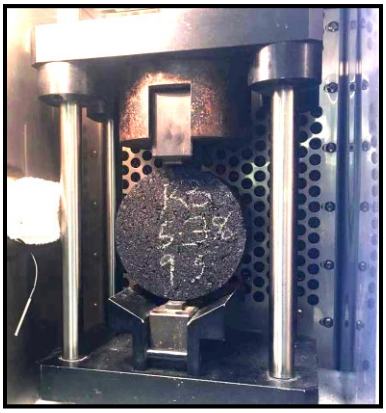

Figure 3.35 Indirect Tensile Strength Test Setup in UTM

3.3.2.5 Triaxial Shear Strength Test

The triaxial shear strength (TSS) test is used to evaluate the evolution of shear strength properties (bearing capacity) during the curing period. The TSS test is conducted by inserting the cylindrical test specimens into a mold equipped with an inflatable rubberized-plastic membrane (see Figure 3.36). The specimens used for TSS test are compacted to a height of 300mm (11.8 inch). A circular metal plate is placed on top of the mold and the test specimen is subject to a vertical axial compressive load until failure. This is done under displacement-controlled mode at a rate of 3mm/min. TSS testing is done at room temperature and the typical test setup in the Universal Testing Machine (UTM) is shown in Figure 3.37.

Figure 3.36 Components of Triaxial Shear Strength Testing Device

Figure 3.37 Triaxial Shear Strength Test Setup in UTM

The peak load at failure is recorded to determine failure stress using equation 3.6. The major principal stress at failure is then computed by accounting for the weight of the metal plate using equation 3.7.

$$\sigma_f = \frac{P_f}{\pi \times \frac{D^2}{4}} \tag{3.6}$$

Where:

σ_f = Failure Stress, kPa
P_f = Peak load, N
D = Diameter of specimen, mm

$$\sigma_1 = \sigma_f + \sigma_{dw} \tag{3.7}$$

Where:

σ_1 = Major principal Stress at failure, kPa
σ_{dw} = Pressure resulting from weight of metal, N

A series of tests are performed on specimens subjected to increasing lateral confining pressure. A linear regression is performed to obtain the relationship between the major principal stress at failure and confining stress as described in equation 3.8.

$$\sigma_1 = A \times \sigma_3 + B \tag{3.8}$$

Where:

σ_3 = Confining stress, kPa
A , B = Regression constants

Through use of the Mohr-Coulomb model, the shear failure envelope in terms of internal friction angle and cohesion can be determined. These are obtained from the regression constants using equation 3.9 and 3.10, respectively.

$$A = \frac{1 + sin\varphi}{1 - sin\varphi} \tag{3.9}$$

$$B = \frac{2 \times C \times cos\varphi}{1 - sin\varphi} \tag{3.10}$$

Where:

φ = Friction angle, degrees
C = Cohesion, kPa

3.4 LABORATORY EXPERIMENTAL DESIGN

The literature review conducted as part of this study highlighted the critical factors that may affect CIR mixture curing process. The factors include time, stabilizer type and amount, active filler type and amount, initial moisture content, compacted density, layer thickness, and weather conditions. The following sub-sections discuss how these factors were incorporated into study.

3.4.1 As-built Material and Curing Conditions

Material sampling and data collection were detailed such that pertinent information to replicate the as-built material and curing conditions in the lab were collected. The as-built characteristics were determined as follows (variations to these as-built conditions are discussed in a subsequent subsection):

- Stabilizer Type and Amount: In terms of the stabilizer type, all six projects followed the original plans from the approved mix design. However, slight changes were made to the stabilizer amount as construction progressed through the length of each project. Therefore, the stabilizer amount pertinent to the as-placed CIR mix on the identified test sections were recorded.

- Active Filler Type and Amount: These attributes were fully adopted from the approved mix design, as no changes were made to the job mix formula.

- Compacted Density and Layer Thickness: The density achieved through compaction was measured by the quality control personnel on each construction day for each of the six projects. This information was made available to the researchers. The densities applicable to the reference test sections were then extracted. In terms of the layer thickness, all six projects were stabilized to similar depth of 76mm (3inch). Subsequent information collected from local agencies and contractors suggests that this is the most typical stabilizing depth. Therefore, for simplicity, this factor is recommended to be kept constant in developing the CIR curing prediction model.

- Initial Moisture Content: The amount of moisture in the CIR mix consists of the existing in-situ moisture prior to recycling and added moisture associated with the recycling process. Therefore, to obtain a representative initial moisture content (IMC), the as-placed CIR loose mix was sampled. The IMC was then determined following ASTM D2216.

- Environmental Curing Condition: Climatic information was extracted from the weather station closest to each project. Since curing in the laboratory could only be done in a controlled temperature environment, all other environmental factors were monitored using sensor measurements. The average air temperature for the period of in-situ testing was calculated and used to simulate the curing process. The length of the period of in-situ testing for each of the six projects ranged from 3 to 15 days. The average air temperature was found to be similar for all six project locations and therefore a single curing temperature of 25°C was adopted for all mixtures.

- Curing Period/Duration: The choice of curing durations for testing to obtain the as-cured properties were informed by past research efforts and initial test trials. As a result, shorter curing durations were adopted for mixtures with active filler and those using foamed asphalt for stabilizing as opposed to emulsion.

The as-built material and curing conditions for the six projects is summarized in Table 3.15.

Table 3.15 As-built Material and Curing Conditions

Project [Stabilizer Type]	Stabilizer Amount	Active Filler [Type]	Density (kg/m^3)	IMC	Curing Temperature (°C)
TH 30 [Engineered Emulsion]	2.0%	0.5% [Cement]	1970	5.7%	25
TH 95 [Engineered Emulsion]	2.0%	-	2098	3.0%	25
TH 75 [Engineered Emulsion]	1.7%	0.5% [Cement]	2066	3.4%	25
TH 28 [Foamed Asphalt]	2.5%	-	2034	3.4%	25
CSAH 8 [Engineered Emulsion]	1.5%	-	1922	3.5%	25
CSAH 11/21 [Engineered Emulsion]	1.9%	-	1922	4.9%	25

3.4.2 Variations from As-built Conditions

To adequately capture the effect of the various curing factors, a partial factorial experimental design was developed with two treatment levels (low and high). This experimental design was developed using JMP Pro® statistical analysis software. Ultimately, at least three variations from the as-built material and curing

conditions from the six field projects were recommended in the experimental design. The following considerations were taken into account in selecting the value of the levels:

- Stabilizer Type: As it was possible to sample materials from field projects that employed the two most common stabilizer types (EE and FA) in the region, no further variations were required to capture the effect of this factor.

- Stabilizer Amount: It was observed that all six projects employed stabilizer amounts on the lower end of typical ranges used in stabilization. Therefore, a higher level within the range was specified to capture the contrast.

- Active filler Type and Amount: Field projects with and without active fillers were originally included in the study, with cement being the only type of active filler. However, lime kiln dust (LKD) was sampled from a different project that was not included in the study but in similar location to one of the study projects. Variations were then made within each project such that there is presence (high level) or absence (low level) of active filler, depending on as-built conditions. Except for the TH 30 project where both active filler types were used, either of cement or LKD was considered for each project. Additionally, different active filler amounts were explored.

- Density: Based on the QC data, it was observed that the density requirements were significantly higher for the state projects included in the study compared to the county projects. Therefore, for the state projects, a lower level was specified as a variation. A higher density was explored as a variation for the county projects.

- Initial Moisture Content: As a result of the weather conditions on the day of construction of the study test sections, the IMC varied between all six projects. On some of the projects, the reference test sections were constructed within a day or two of a rainfall event, which resulted in significantly higher IMC. These projects were therefore considered to be at a high level. Values within similar range were then specified as a higher level for the other projects with considerably lower IMC.

- Curing Temperature: The selected projects were constructed within the warmest period of the construction season. Therefore, the as-built condition was considered as the high level. The coolest temperature at which CIR operations is permitted in the DOT specifications was then selected for variation as the low level. The specified temperature is 15.6°C but was rounded to 15°C for simplicity.

- Moisture Reintroduction (Rainfall Effect): There were rainfall events during construction of some the field projects. Apparently, this may be a significant factor that alters the CIR curing process. Whereas rainfall cannot be directly simulated in the lab, a moisture conditioning protocol was employed to study the impact of reintroducing moisture to CIR layers while curing. The implementation of this protocol is discussed further in the next section.

Table 3.16 gives the details of the laboratory experimental plan with the values specified for the different factors. The first row of each of the six projects is the as-built material and curing conditions. The variations from these conditions are given in the subsequent rows. The naming convention for mixture identification is as follows: The first letter denotes the overseeing agency (D – MnDOT, B – Brown County); the second letter and following numbers denote the field project the material was sampled from; the last letter after the underscore indicates the different variations for each material (A – As-built; X, Y, Z are variation 1, 2 and 3 respectively). For each mixture variation, laboratory evaluation was done at least at four different times within the curing period, using at least three replicates each time.

Table 3.16 Laboratory Experimental Design

Project [Stabilizer Type]	Stabilizer Amount	Active Filler [Type]	Density (kg/m^3)	IMC	Curing Temperature (°C)	Mix ID
TH 30 [Engineered Emulsion]	2.0%	0.5% [Cement]	1970	5.7%	25	DT30_A
	2.0%	0.5% [Cement]	2082	3.0%	15	DT30_X
	3.0%	-	1970	3.0%	15	DT30_Y
	3.0%	-	2082	5.7%	25	DT30_Z
	2.0%	0.5% [LKD]	1970	5.7%	25	DT30_A(L)*
TH 95 [Engineered Emulsion]	2.0%	-	2098	3.0%	25	DT95_A
	3.5%	-	1922	3.5%	15	DT95_X
	3.5%	1.0% [Cement]	2098	3.5%	25	DT95_Y
	2.0%	1.0% [Cement]	1922	3.0%	15	DT95_Z
TH 75 [Engineered Emulsion]	1.7%	0.5% [Cement]	2066	3.4%	25	DT75_A
	3.0%	-	2066	3.4%	15	DT75_X
	1.7%	-	1970	5.0%	15	DT75_Y
	3.0%	0.5% [Cement]	1970	5.0%	25	DT75_Z
TH 28 [Foamed Asphalt]	2.5%	-	2034	3.4%	25	DT28_A
	3.5%	0.5% [Cement]	2034	3.4%	15	DT28_X
	3.5%	-	1954	5.0%	25	DT28_Y
	2.5%	0.5% [Cement]	1954	5.0%	15	DT28_Z
CSAH 8 [Engineered Emulsion]	1.5%	-	1922	3.5%	25	BC08_A
	3.0%	0.5% [Cement]	2002	3.5%	25	BC08_X
	1.5%	-	2002	4.5%	15	BC08_Y
	3.0%	0.5% [Cement]	1922	4.5%	15	BC08_Z
CSAH 11/21 [Engineered Emulsion]	1.9%	-	1922	4.9%	25	BC11_A
	3.0%	-	2002	3.0%	25	BC11_X
	1.9%	1.0% [LKD]	2002	4.9%	15	BC11_Y
	3.0%	1.0% [LKD]	1922	3.0%	15	BC11_Z

*A(L) signifies it is As-built condition but with LKD instead of Cement.

3.4.3 Specimen Fabrication and Curing Simulation

The overall goal of the specimen fabrication process is to mimic the CIR mixtures from the constituent materials and simulate the in-situ curing in the laboratory as closely as possible. A significant outcome of literature review that was conducted as part of this study was the identification of methods applicable in that regard.

3.4.3.1 Mixing and Compaction

Prior to mixing, the constituent materials were prepared as follows:

- RAP: The RAP was sampled from different portions along the length of the project; this increased the chances of an uneven distribution of moisture in the material. Therefore, the RAP was dried for at least 48 hours before mixing.
- Emulsion: The IMC determined as described in previous subsection represents total moisture content in CIR material, thus includes moisture from emulsion. Therefore, to account for this, the MC of the emulsion sampled from the projects were determined following the ASTM D7497 procedure. Additionally, prior to mixing, the emulsion was conditioned to similar temperature measured at the time of field sampling.
- Foamed Asphalt: The foamed asphalt was produced in the laboratory using the Wirtgen foaming device (Model WLB10S (see Figure 3.38). The design water application rate and asphalt temperature for foaming as used in field were employed in the laboratory.

Figure 3.38 Wirtgen Foaming Device (Model WLB10S)

The proportions of the constituent materials including the RAP, stabilizing agent (Emulsion or Foamed Asphalt), water and active filler were determined and batched individually. The CIR mixtures were produced by initially adding the active filler (when used) to the RAP and mixing with water for 1 minute,

then the stabilizing agent was added and mixed for additional 4 minutes. Figure 3.39 shows the Wirtgen twin-shaft pugmill mixer (Model WLM30) used for mixing.

Figure 3.39 Wirtgen Pugmill Mixer (Model WLM30)

Following mixing, compaction was done using the Wirtgen Vibratory Hammer (Model WLV1 (see Figure 3.40). Lower densities were compacted in 2 lifts while higher densities were compacted in 3 lifts. The compaction mold has a diameter of 152mm and all specimens were compacted to a height of 75mm, similar to field layer thicknesses.

Figure 3.40 Wirtgen Vibratory Hammer (Model WLV1)

3.4.3.2 Curing and Moisture Conditioning

As indicated previously, curing was done at two different temperatures. To simulate curing at 25°C, a forced draft oven was used. A curing room fitted with an air conditioner was employed to simulate curing at 15°C. Throughout the curing period, the temperature and relative humidity were monitored and recorded using a Bluetooth based sensor. As shown in Figure 3.41, all specimens were cured uncovered to accelerate the curing process. Metal plates were used at the base for easier handling after compaction and to prevent material loss while curing.

Figure 3.41 CIR Specimen Curing in Oven (at 25°C)

As initially highlighted, a moisture conditioning protocol following the AASHTO T283 procedure was adopted. The methodology is as follows:

- Companion CIR specimens were fabricated, weighed, and cured simultaneously.
- After four days of curing, one group of the CIR specimens is moisture conditioned using a vacuum desiccator (see Figure 3.42). The desiccator is filled with water to about 25mm above the specimen, a 250mm mercury vacuum pressure is applied for 5 mins and the specimens are left submerged for another 5 mins.
- Following conditioning, the specimens are reweighed and placed back to cure under similar conditions as the control group.

Figure 3.42 Vacuum Desiccator for Moisture Conditioning

3.5 SUMMARY OF MATERIAL SAMPLING AND TEST METHODS

3.5.1 Summary of Field Projects

Through a well-informed decision-making process and consultation with the TAP, six CIR pavement projects were identified for in-situ evaluation of curing, material sampling, and collection of field data. The projects are listed in Table 3.17, categorized by overseeing agency.

Table 3.17 CIR Field Study Projects

Agencies	Recommended Projects
MnDOT	SP 8105-21 (TH 30)
	SP 8209-111 (TH 95)
	SP 3703-25 (TH 75)
	SP 7503-38 (TH 28)
Brown County	SAP 008-608-042 (C.S.A.H. 8)
	SAP 017-611-019 / 008-621-004 (C.S.A.H. 11/21)

3.5.2 Summary of Field Project Material and Construction Attributes

Slight adjustments from the approved mix design parameters were adopted in most of the field projects. Table 3.18 summarizes the as-placed CIR mix attributes from the six field projects. Using the CSAH 8 project as baseline, the distinct characteristics of the other five projects are highlighted in red.

Table 3.18 Field Projects As-placed CIR Mixture Attributes

Parameters	Attributes					
	CSAH 8	CSAH 11/21	TH 28	TH 30	TH 75	TH 95
Method of Asphalt Binder Delivery	EE	EE	FA	EE	EE	EE
Target Amount of Bituminous Material	1.5%	1.9%	2.5%	2%	1.7%	2%
Type and Amount of Mineral Stabilizing Agent	N/A	N/A	N/A	0.5% Cement	0.5% Cement	N/A
Added Amount of Moisture	1.5%	1.5%	3-4%	1%	1.5%	1.5%
Stabilizing Depth (in)	3	3	3	3	3	3
Target Density (pcf)	122.3	120.9	128	123.4	128.6	128.5

3.5.3 Summary of Testing Campaign

A summary of the field and laboratory testing that were conducted as part of this study to evaluate curing are summarized in Table 3.19, organized by relevant measured property.

Table 3.19 Testing Campaign

Property	Field (In-situ) Tests	Laboratory Tests
Moisture Content	Nuclear Density and Moisture Gauge	Gravimetric Measurement
	Dielectric Profiling System	Laboratory Dielectric Measurement System
Mechanical	Lightweight Deflectometer	Resilient Modulus
		Indirect Tensile Strength
	Rapid Compaction Control Device	Triaxial Shear Strength

CHAPTER 4: FIELD (IN-SITU) TESTING RESULTS

Result of the in-situ testing conducted on the six field projects are presented in this chapter, organized by project. The average values of the test results (including temperature corrected moduli) are presented in the ensuing figures with error bars indicating one standard deviation from the measured mean values. The individual station and point results on each test section is included in Appendix C. The measured properties are plotted on the vertical axis while the time (in days) is plotted on the horizontal axis; the day of construction of test section is denoted as day 0 and the axis extends until the last day of testing.

4.1 CSAH 8

The result of NDMG and static DPS tests on CSAH 8 are presented in Figure 4.1. The applicability of both devices in detecting change in moisture content on this project is evident, although not pronounced and a similar trend is observed. Between day 0 and 2, as curing progresses, there is a decrease in % moisture measured using the NDMG and a corresponding decrease in dielectric which is also an effect of a decrease in moisture content. However, between day 2 and 7, an increase in moisture content is observed which could be attributed to the rain occurring on days 3 and 6. It is most likely that the rain on day 6 had the most effect on this moisture content increase. Subsequently, after day 7, there is a reduction in moisture content until the last day of testing (day 9) which makes sense as no other rainfall occurred within this period.

Figure 4.2 shows the result of the LWD and RCCD testing on the field project. The measured LWD E_{35} consistently increases as curing progresses with time to the last day of testing. Consequently, the penetration measured with the RCCD decreases with time, which is also an indication of the increase in stiffness/strength. However, between day 7 and 9, an increase in penetration is observed. This change could be artifact of not correcting for temperature sensitivity, as the surface temperature during day 9 testing was higher compared to day 7. It is however noteworthy for this project that the impact of higher moisture content due to rain on measured stiffness is outweighed by the increase in stiffness associated with curing as observed on day 7.

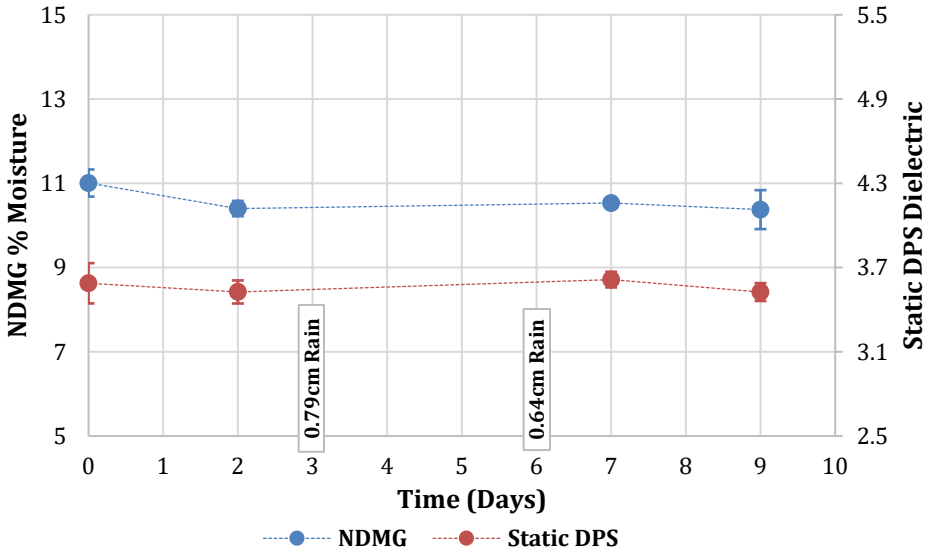

Figure 4.1 CSAH 8 Moisture Content Evolution

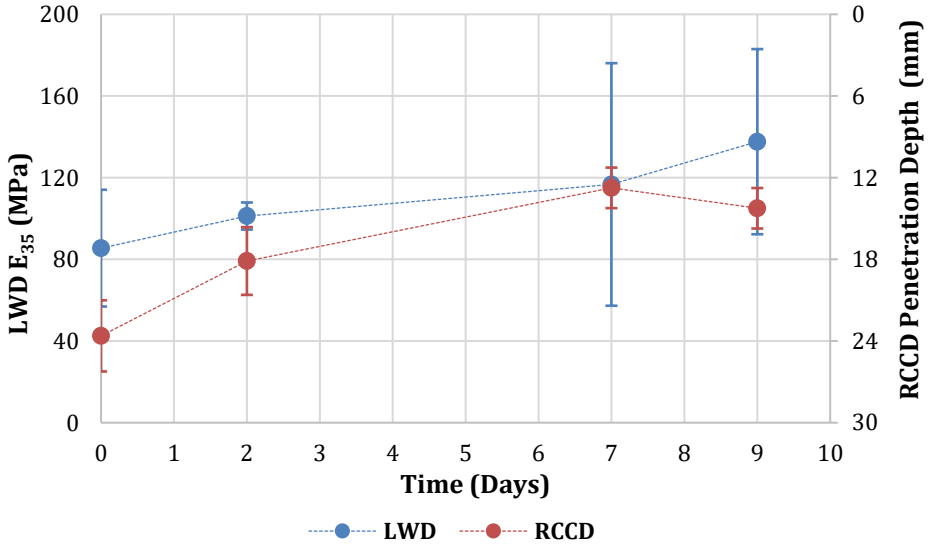

Figure 4.2 CSAH Stiffness Evolution

4.2 CSAH 11/21

As shown in Figure 4.3, there is a high degree of change in moisture content measured with NDMG and static DPS tests on CSAH 11/21 project, especially during the early stages of curing. However, the two devices show different trends as curing progresses. Between day 0 and 2, there was a decrease in % moisture and dielectric which is expected as there was no rain. There were however rainfall events on days 3, 5 and 6 prior to testing on day 6. The static DPS dielectric measurements was able to capture the increase in moisture content due to the rain. On the other hand, the NDG shows a consistently decreasing

% moisture. A hypothesis to this disparate trend is that the static DPS does not differentiate between surface moisture and moisture within the CIR layer, whereas the NDMG can, as the device is in direct contact with the pavement layer during testing. The dielectric remained almost constant between day 6 and 9 even though there were no further rainfall between those days, however, the NDMG kept detecting a decrease in moisture content. It is likely that there is a limiting moisture content beyond which changes in dielectric for a material may be minimal as other material components dominate the measured value.

The result of the LWD and RCCD testing on the CSAH 11/21 field project is shown in Figure 4.4. The measured E_{35} increases progressively with time and consequently the RCCD penetration. However, the increase in penetration between day 6 and 9 could also be an indication of sensitivity of RCCD testing at higher temperature. Similarly, for this project, the negative effect of a higher moisture content due to rain (detected by static DPS) on the gain in stiffness from curing was not significant as observed on day 6.

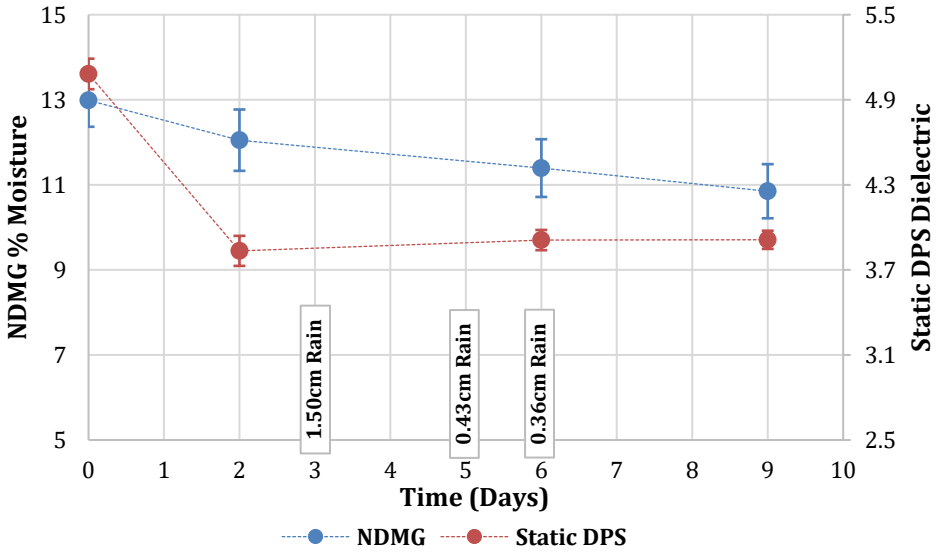

Figure 4.3 CSAH 11/21 Moisture Content Evolution

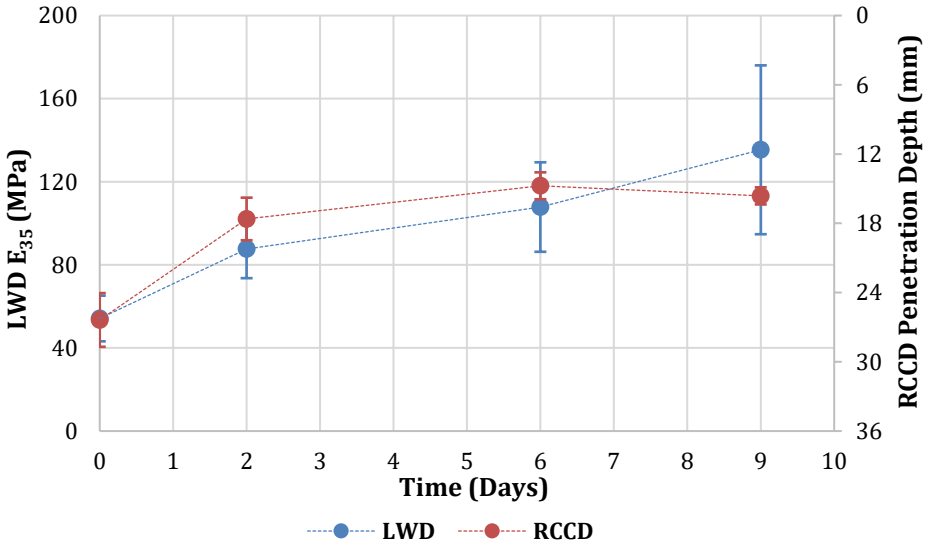

Figure 4.4 CSAH 11/21 Stiffness Evolution

4.3 TH 28

Figure 4.5 shows minimal change in moisture content on the TH 28 project as measured using both the NDMG and static DPS tests. It is noteworthy that this project utilized foamed asphalt as a stabilizing agent as opposed to the previous projects already discussed that use asphalt emulsion. It was not possible to test day 0, so it is unknown how much the moisture content in the foamed asphalt changed in the first day. However, it is expected to cure quicker than emulsion. Therefore, the research team planned on conducting tests on CIR with foamed asphalt in laboratory, with measurements made also on day 0 for comparative purposes. The rainfall on days 3 and 4 resulted in a slight increase in moisture content measured on day 5 as compared to day 1. The NDMG shows that on day 7 the moisture content begins to slightly decrease which makes sense, as there was no further rainfall. On the other hand, the static DPS does not follow the same trend as the average dielectric value increases. There is a higher variability with the static DPS test result with this project compared to others; therefore, the increase in dielectric between day 5 and 7 may be an artifact of testing variability.

The result of the LWD and RCCD testing on the TH 28 field project is shown in Figure 4.6. It can be observed that between day 1 and 5, E_{35} initially shows a slight decrease and consequently the RCCD penetration increases. The decrease in stiffness could be attributed to the sensitivity of this layer to the presence of higher moisture content due to the rain. Stiffness begins to increase as shown by the LWD E_{35} and RCCD penetration on day 7, potentially as a result of decreasing moisture.

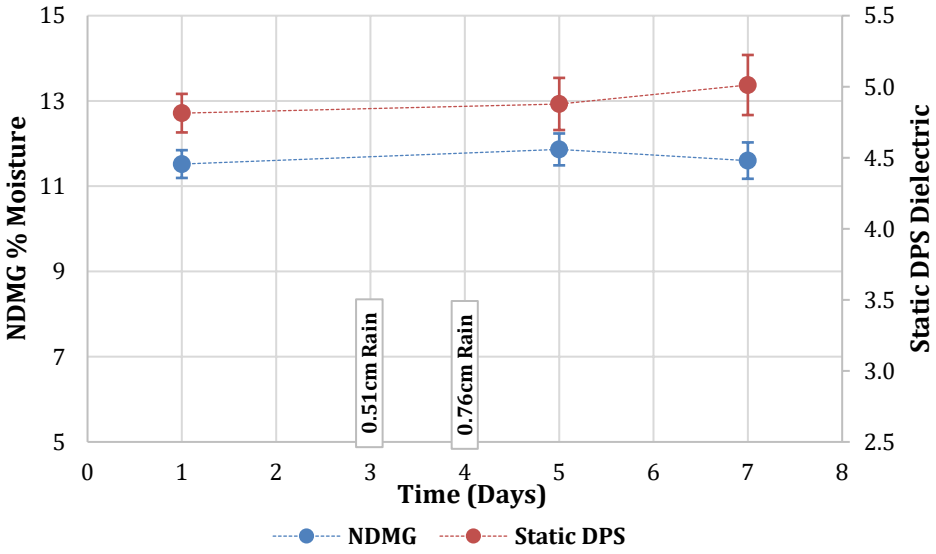

Figure 4.5 TH 28 Moisture Content Evolution

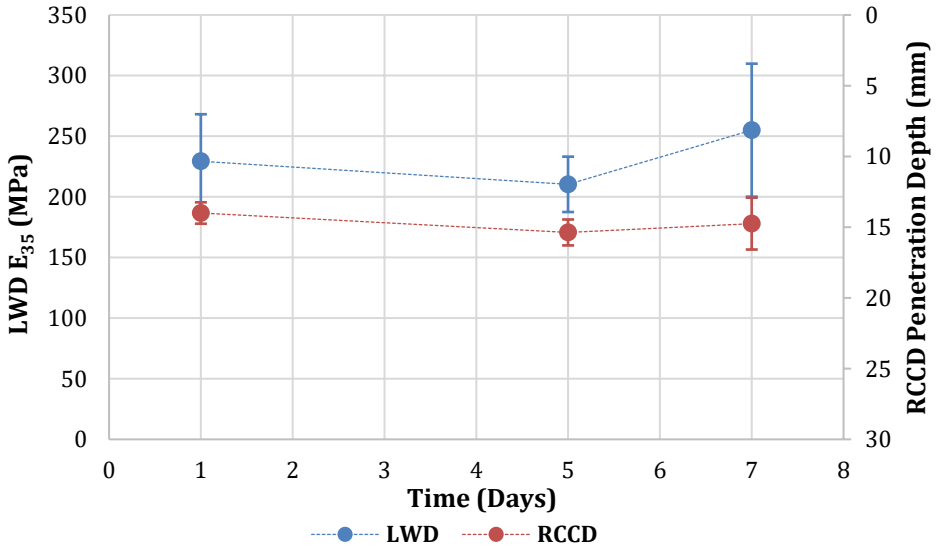

Figure 4.6 TH 28 Stiffness Evolution

4.4 TH 30

Testing was conducted at 4 different occasions on TH 30 project. Figure 4.7 shows that there was a similar trend in the moisture content measured using both the NDMG and static DPS tests, with a significant decrease between day 1 and day 6. The rainfall events between testing days did not seem to significantly affect the rate of moisture content reduction with this project. The hydration of the active filler employed in this project could be a reason for this trend as some of the moisture could be utilized for this purpose in addition to evaporation. After day 6, little to no change in moisture content is observed even with the

rainfall occurring on day 9. This suggests that the layer might be close to the limiting moisture content. A hypothesis for this observation is that the formation of the hydration products results in a decrease in permeability of this layer preventing rainfall from infiltrating and therefore excess surface moisture could runoff and evaporate faster.

Similar to the trend with moisture content, Figure 4.8 shows that there is a significant gain in stiffness (LWD E_{35} and RCCD Penetration) in the TH 30 CIR layer between day 1 and day 6. However, the measured trend with LWD E_{35} does not entirely agree with the RCCD penetration. The decrease in LWD E_{35} observed between day 6 and day 11 does not coincide with the fact that the rain on day 9 did not affect the moisture content of the layer on day 11. The trend with RCCD penetration is more plausible as it mirrors the trend in moisture content change; this suggests that there might have been an error associated with LWD testing on day 6. The variation in LWD test data on day 6 further reinforces this hypothesis. Additionally, there is a slight increase in stiffness at the later stage of curing (day 14) which could be indicative of further hydration of the active filler.

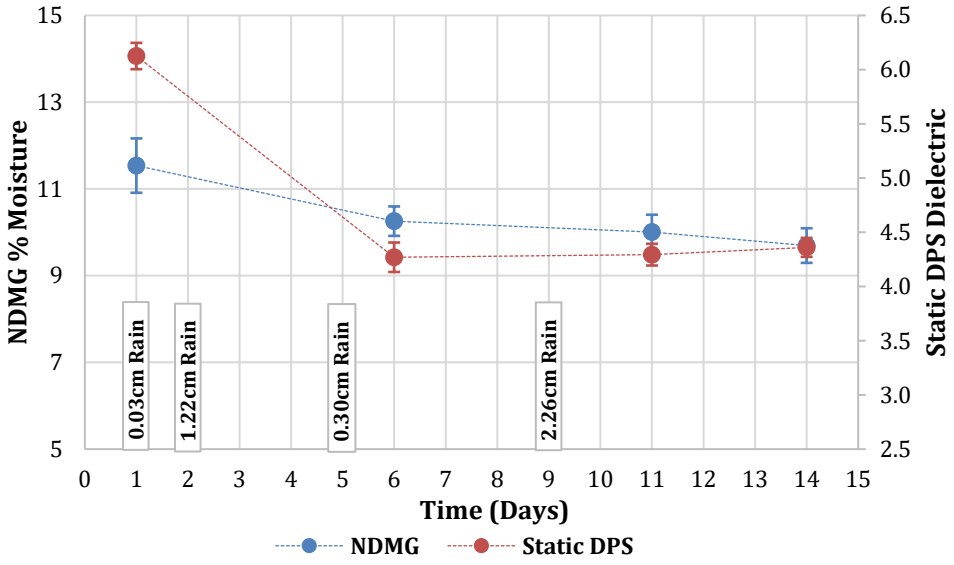

Figure 4.7 TH 30 Moisture Content Evolution

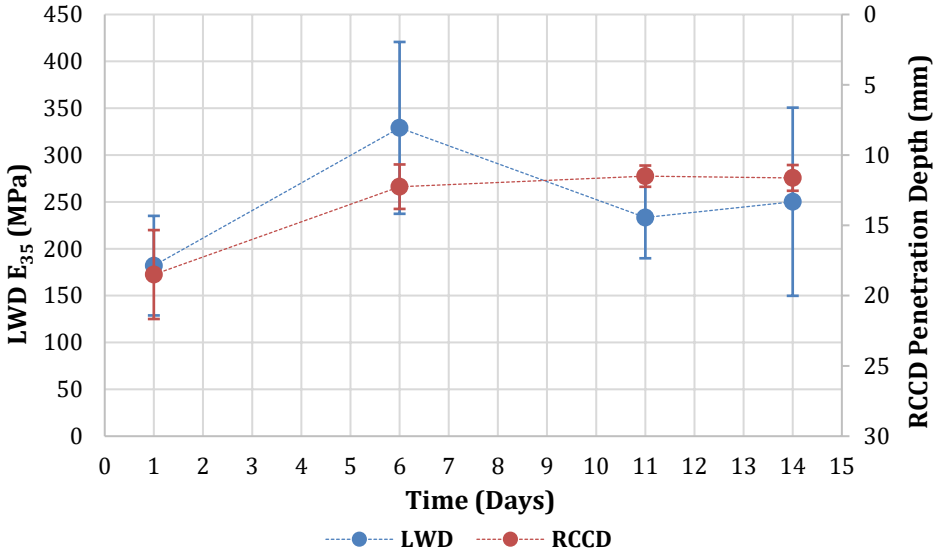

Figure 4.8 TH 30 Stiffness Evolution

4.5 TH 75

Due to timing of the TH 75 project, it was impossible to conduct testing on the initial test section until three days after construction. Therefore, a second test section constructed on a later date was defined along the length of the project to obtain representative properties during the earlier curing stages. Testing was conducted at four different occasions on the first test section. Figure 4.9 shows the results of the NDMG and static DPS tests. This project utilizes active filler in the CIR mix. There is no significant change in the moisture content of the CIR layer as time progresses, even with rainfall occurring between testing days. This further reinforces the impact of active filler in providing cementing action to prevent infiltration. The moisture content measured on day 0 at the second test section is slightly lower than the subsequent moisture content measured on the first test section which suggest that there might have been slight adjustments in mix design on the different construction day, which is typical for CIR projects.

The TH 75 project LWD and RCCD test results are presented in Figure 4.10. There is an abrupt change in measured LWD E_{35} and RCCD penetration between day 0 and 6. The LWD E_{35} shows a slight increase between day 6 and 10, but the RCCD penetration decreases; this could also be attributed to temperature sensitivity as testing on day 6 was done at a substantially lower temperature. The LWD E_{35} further shows a considerable increase at the later part of curing between day 10 and 12 which corresponds to the RCCD penetration. The testing temperature on both days are not significantly different and could be assumed not to influence the RCCD test results. This supports the hypothesis that there may be later hydration of active filler.

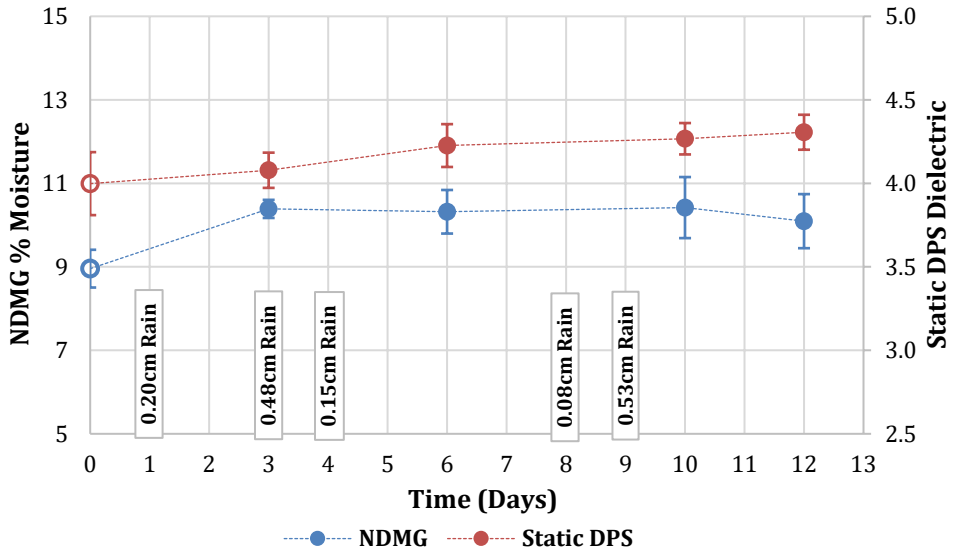

Figure 4.9 TH 75 Moisture Content Evolution (Day 0 from different section with open symbol)

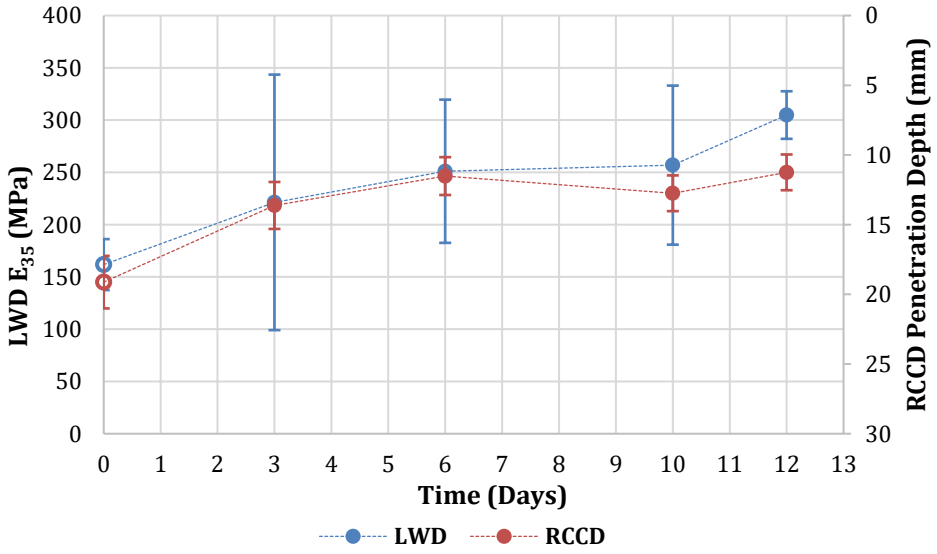

Figure 4.10 TH 75 Stiffness Evolution (Day 0 from different section with open symbol)

4.6 TH 95

The project on TH 95 was overlaid within 5 days of completion of CIR layer, therefore, it was only possible to conduct testing at two different occasions. The results of the NDMG and static DPS tests are shown in Figure 4.11 while that of the LWD and RCCD test results are presented in Figure 4.12. A slight decrease in moisture content of the CIR layer was observed between both testing days. It is likely that the magnitude of change would have been higher barring the minor rainfall occurring on day 3. As expected with curing,

there was also a significant gain in stiffness between both testing days as indicated by the increase in LWD E_{35} and decrease in RCCD penetration.

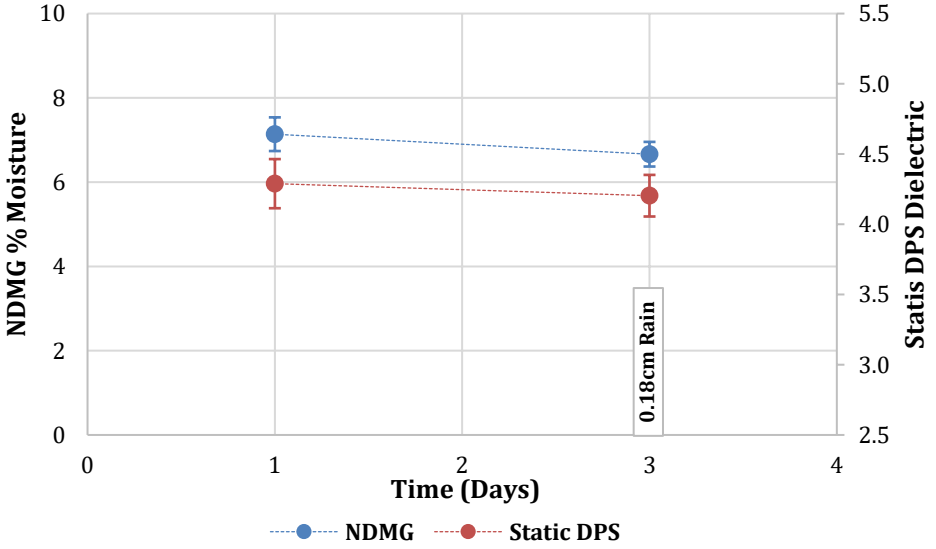

Figure 4.11 TH 95 Moisture Content Evolution

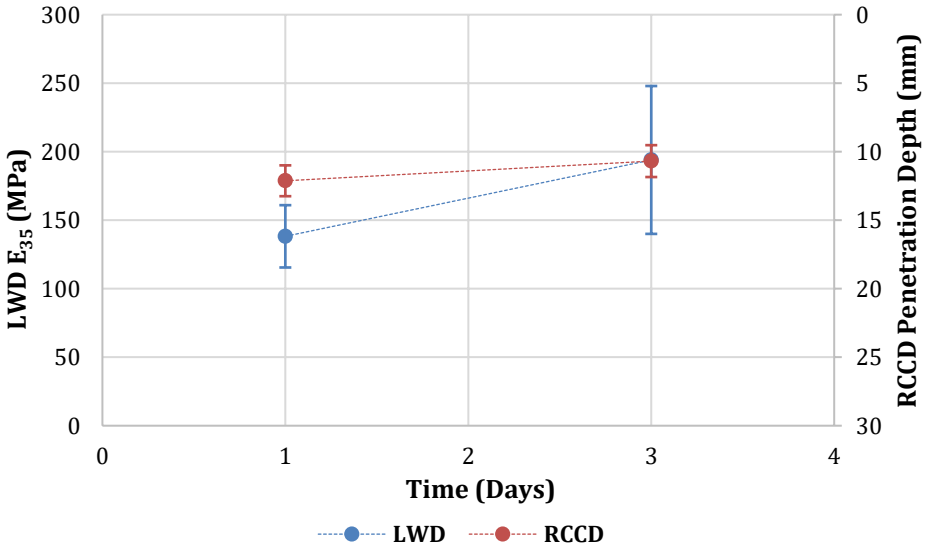

Figure 4.12 TH 95 Stiffness Evolution

4.7 DIELECTRIC PROFILING SYSTEM (SURVEY VS STATIC)

As shown in the previous sections, the DPS has promise in detecting changes in in-situ moisture content of the CIR layer as curing progresses. The two different approaches (survey and static) were employed for obtaining the DPS measurements. However, it is important to compare the approaches and identify which is most appropriate for the given conditions. The dielectric values measured on all the field projects using

both approaches are shown together in Figure 4.13, with values ranging between 3.5 and 6. For all of the results except one, it is evident that the measured values correlate well. Nevertheless, one significant observation is that there is less variability associated with the DPS survey approach as opposed to the static DPS measurements. This suggests that the survey method may be most suitable for test precision and repeatability.

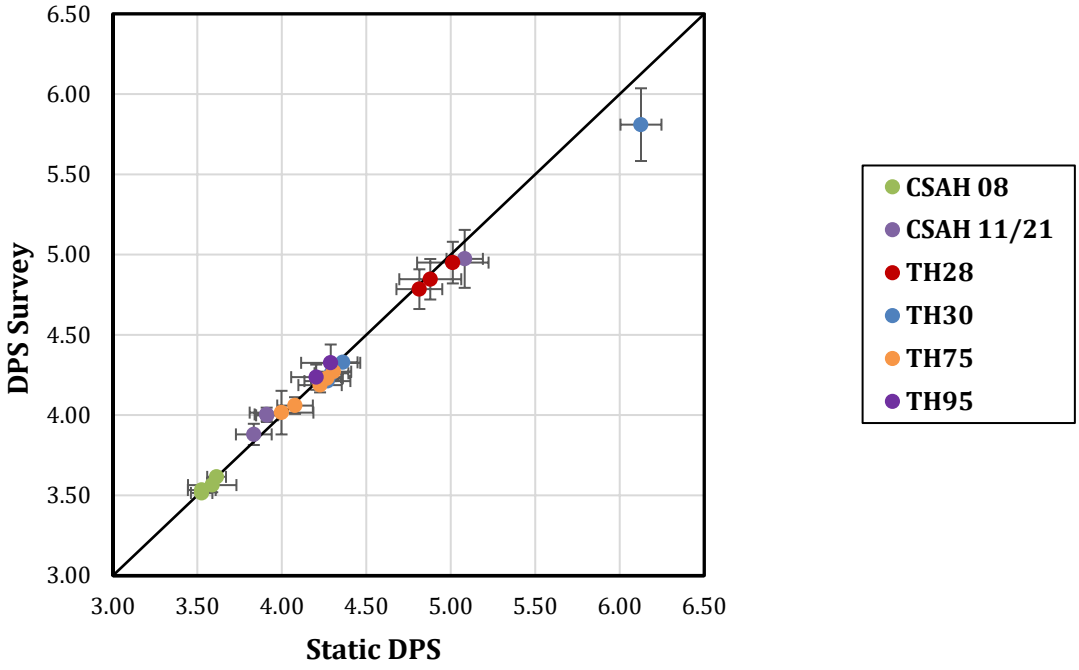

Figure 4.13 Comparison of DPS Measurement Methods

4.8 SUMMARY OF FINDINGS FROM IN-SITU TESTING

One primary objective of this study is to recommend a reliable in-situ strength/moisture content measurement method. In order to achieve this, the NDMG and DPS were explored to track the changes in in-situ moisture content. The LWD and RCCD devices were employed to assess the stiffness evolution. From the results presented, the following preliminary conclusions can be drawn:

- Generally, the NDMG and DPS show similar trend in moisture content change as related to curing. However, the DPS has a higher propensity of detecting increase in moisture content because of rainfall events. This is believed to be related to the fact that the DPS includes surface moisture in its measurement whereas the NDMG primarily measures moisture content within the layer.
- There is likelihood of a threshold in moisture content of CIR material beyond which further changes appear minimal and are not readily captured from the DPS dielectric measurements as other material components dominate the measured dielectric value.
- Rainfall did not seem to significantly affect the moisture content change in projects that employed active filler. One reason for this could be that some of this moisture is expended by hydration. The active filler is also believed to decrease permeability and prevent infiltration, allowing excess surface moisture to evaporate quicker.

- The LWD and RCCD were efficient in assessing the stiffness evolution as pertaining to curing. There is less measurement variability associated with the RCCD.
- Moisture content change resulting from rainfall events did not appear to significantly alter stiffness gain in the CIR mixtures stabilized using emulsion but seem to affect the project with foamed asphalt.
- Temperature corrections may be required for RCCD measurements. However, developing an approach for this is beyond the scope of this study.
- Comparison of DPS measurement methods suggests that the survey method may be more suitable than the static method for better test precision and repeatability.

CHAPTER 5: LABORATORY TESTING RESULTS

This chapter primarily discusses the effect of the various curing factors that were incorporated in the laboratory experimental design. The evaluation was done in terms of mechanical properties and moisture content evolution, using the laboratory tests described in Chapter 3. This chapter also presents the evolution of curing on a project-by-project basis.

Generally, similar trends were observed in the results of both the ITS and M_R tests. A select example can be seen using the results of two mixtures shown in Figure 5.1. Similarly, as demonstrated in Figure 5.2, the LDMS was observed to track the moisture content evolution to a comparable extent with the gravimetric measurements. The average values of the measured properties are plotted on the vertical axis while time (days) is plotted on the horizontal axis.

Discussions in this chapter are based only on the ITS test and gravimetric measurement results. A more detailed depiction of these results with measurement variability shown along with raw data for the M_R and LDMS test results can be found in Appendix D.

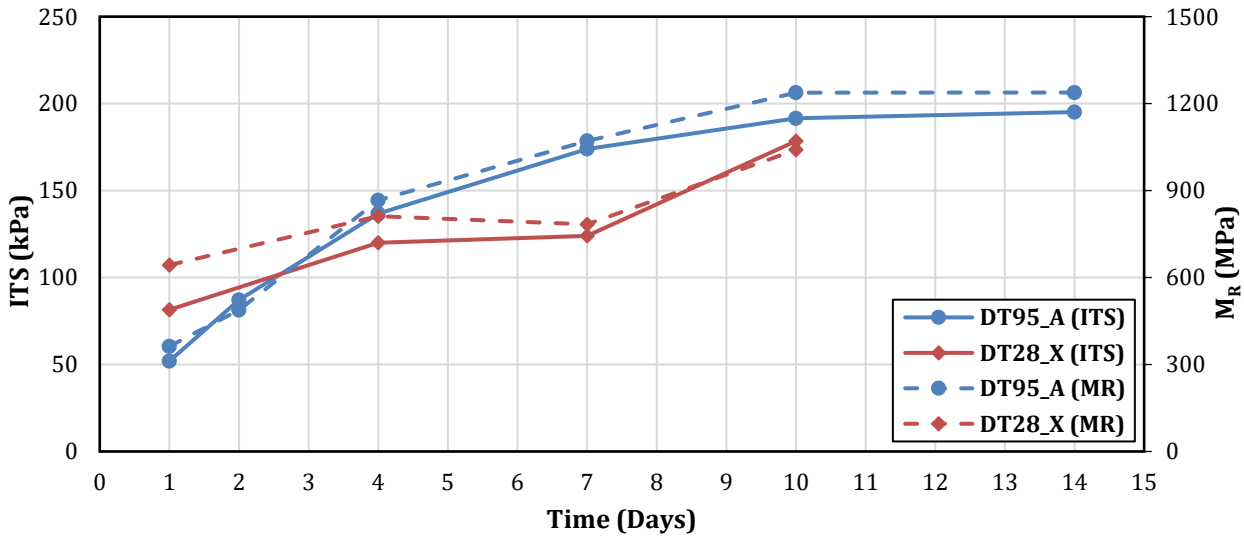

Figure 5.1 Example Correlation between ITS and MR Tests

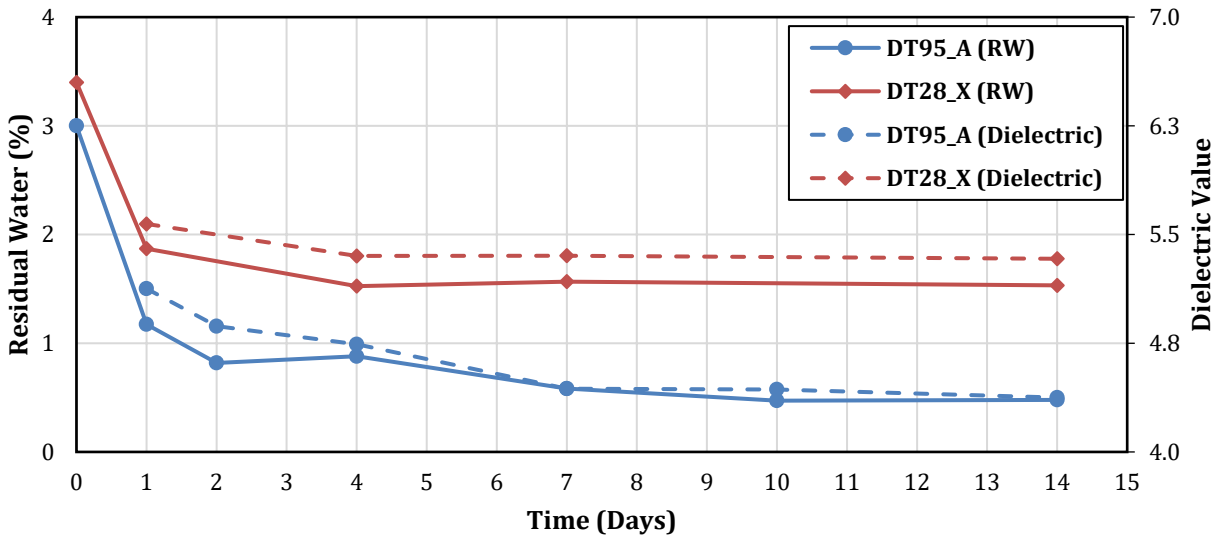

Figure 5.2 Example Correlation between Gravimetric and LDMS Correlation

5.1 EFFECT OF CURING VARIABLES (FACTORS)

The factors that may affect curing were integrated to design a partial factorial experiment. The resulting design requires altering more than one factor at a time to assess the cumulative effect. For this type of design, an extensive statistical analysis is required to isolate the main effect of each factor. The statistical analysis in developing the prediction model is discussed later. However, some preliminary observations can be made and are discussed in the following sub-sections.

5.1.1 Stabilizer Type and Amount

The effect of stabilizer type and amount can be investigated using the mixtures listed in Table 5.1. DT95_A and DT28_A had comparable mixtures attributes and with the prominent difference being stabilizer type. DT95_A and DT30_Z were both stabilized using EE and have comparable attributes. However, there are differences in the stabilizer amount and IMC. Whereas these two mixtures can be primarily used to assess the effect of stabilizer amount, there may be an interaction resulting from the difference in IMC. The result of the gravimetric measurement for the mixtures are presented in Figure 5.3 while the ITS result is shown in Figure 5.4. It can be observed that there is further gain in strength even after the mixtures have reached an equilibrium moisture condition. The effect of stabilizer type appears to be evident as DT28_A (even with slightly higher FA amount and IMC) reached equilibrium RW and final ITS value faster (by day 7) compared to DT95_A (which took over 10 days). On the other hand, after the first two days of curing, DT95_A and DT30_Z showed very similar trends as curing progresses. This suggests that stabilizer amount, if accompanied with an increase in IMC, may only have an effect in the early stages of curing, and subsequently may not be critical to the curing evolution.

Table 5.1 Mixtures for Assessing Effect of Stabilizer Type and Amount

Mix ID	Stabilizer Amount [Type]	Active Filler [Type]	Density (kg/m^3)	IMC	Curing Temperature (°C)
DT95_A	2.0% [EE]	-	2098	3.0%	25
DT30_Z	3.0% [EE]	-	2082	5.7%	25
DT28_A	2.5% [FA]	-	2034	3.4%	25

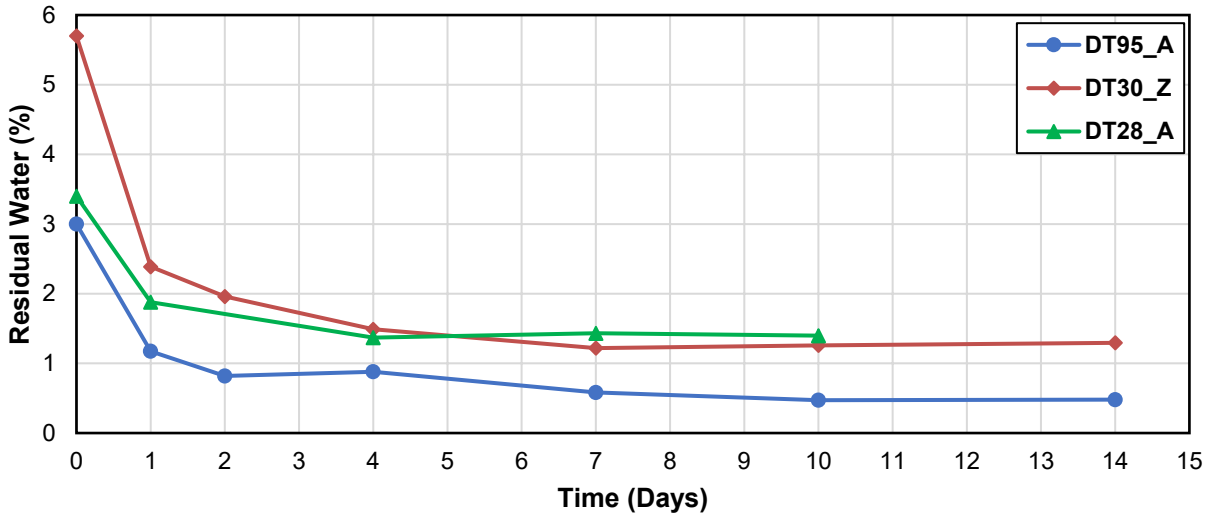

Figure 5.3 Gravimetric Measurement: Effect of Stabilizer Type and Amount

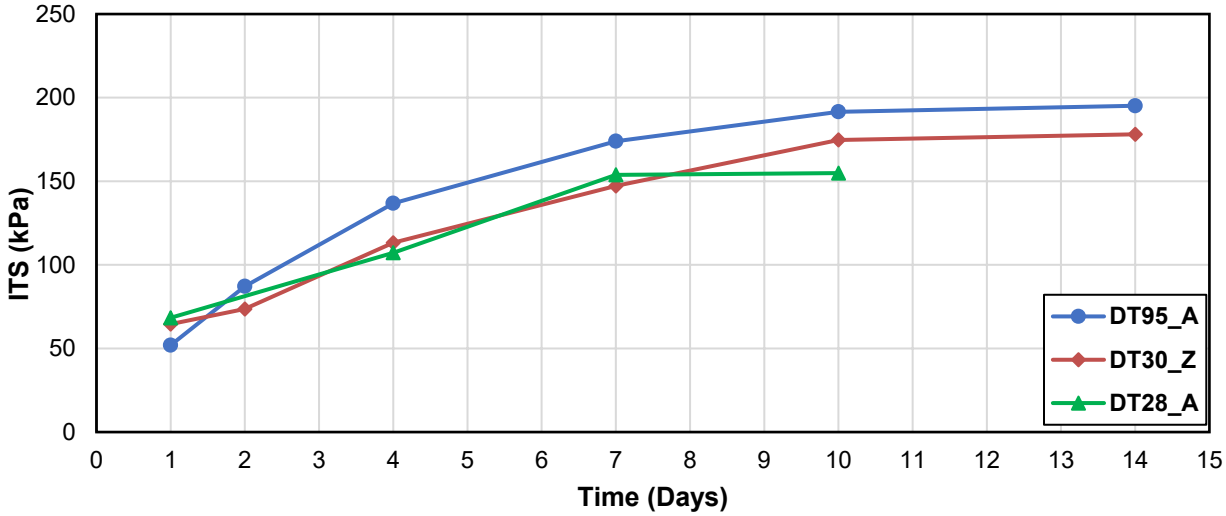

Figure 5.4 ITS Test: Effect of Stabilizer Type and Amount

5.1.2 Active Filler Type and Amount

Table 5.2 shows the attributes of the four mixtures used to assess the effect of active filler type and amount. There are slight differences in stabilizer amount and IMC between the mixtures, however, as previously reported, this may only be critical in the early curing stages. The gravimetric measurements for these mixtures are presented in Figure 5.5 while the ITS results are given in Figure 5.6. The results also show that a further gain in strength is observed after mixtures have attained moisture equilibrium. At similar dosage, the use of cement (DT95_Z) versus LKD (BC11_Z) as active filler results in faster curing with equilibrium RW and final ITS value achieved within 7 days. Irrespective of the difference in IMC, the trend with 0.5% cement (BC08_Z) is similar to that of 1% LKD (BC11_Z) and may take longer to reach the final properties. This suggests that to achieve a comparable curing rate when using active filler, higher amount of LKD is required as compared to cement. Ultimately, it can be observed that the absence of active filler requires an extended curing period to attain the equilibrium RW and final ITS value. Additionally, the higher the active filler amount, the faster the curing process.

Table 5.2 Mixtures for Assessing Effect of Active Type and Amount

Mix ID	Stabilizer Amount [Type]	Active Filler [Type]	Density (kg/m^3)	IMC	Curing Temperature (°C)
DT95_Z	2.0% [EE]	1.0% [Cement]	1922	3.0%	15
BC11_Z	3.0% [EE]	1.0% [LKD]	1922	3.0%	15
BC08_Z	3.0% [EE]	0.5% [Cement]	1922	4.5%	15
DT95_X	3.5% [EE]	-	1922	3.5%	15

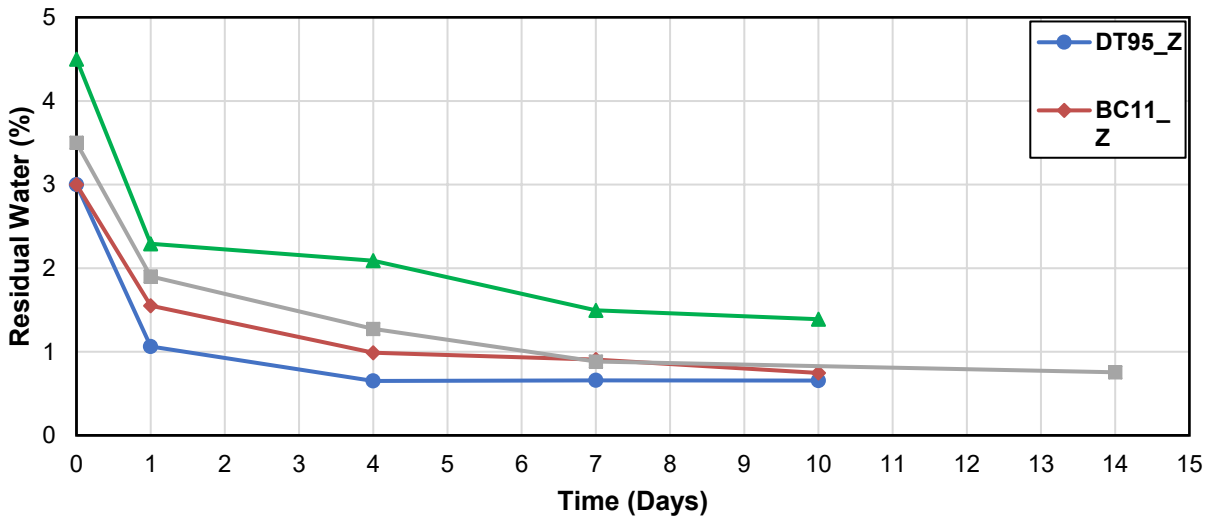

Figure 5.5 Gravimetric Measurement: Effect of Active Filler Type and Amount

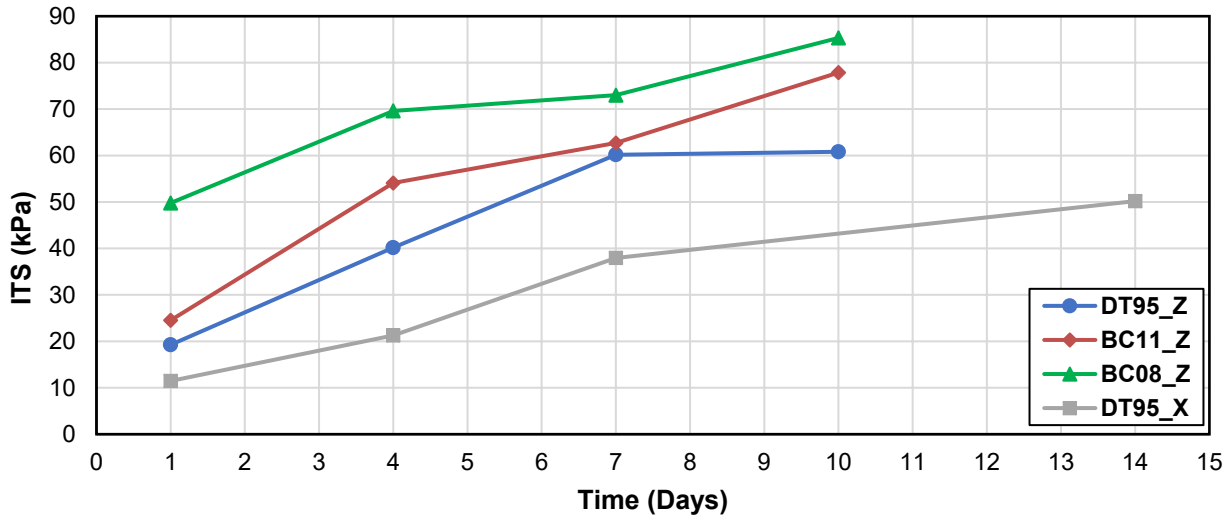

Figure 5.6 ITS Test: Effect of Active Filler Type and Amount

5.1.3 Density

Table 5.3 shows two mixtures with comparable attributes used to demonstrate the effect of density. There are slight differences in stabilizer amount and IMC which may not significantly affect the curing process after the early stages. The results for the gravimetric measurements and ITS tests are presented in Figure 5.7 and Figure 5.8, respectively. Evidently, density will significantly affect the final mechanical response after curing. However, the curing evolution appear to follow a similar trend. This suggests that density may not be a significant factor affecting the rate of curing.

Table 5.3 Mixtures for Assessing Effect of Density

Mix ID	Stabilizer Amount [Type]	Active Filler [Type]	Density (kg/m^3)	IMC	Curing Temperature (°C)
DT95_A	2.0% [EE]	-	2098	3.0%	25
BC08_A	1.5% [EE]	-	1922	3.5%	25

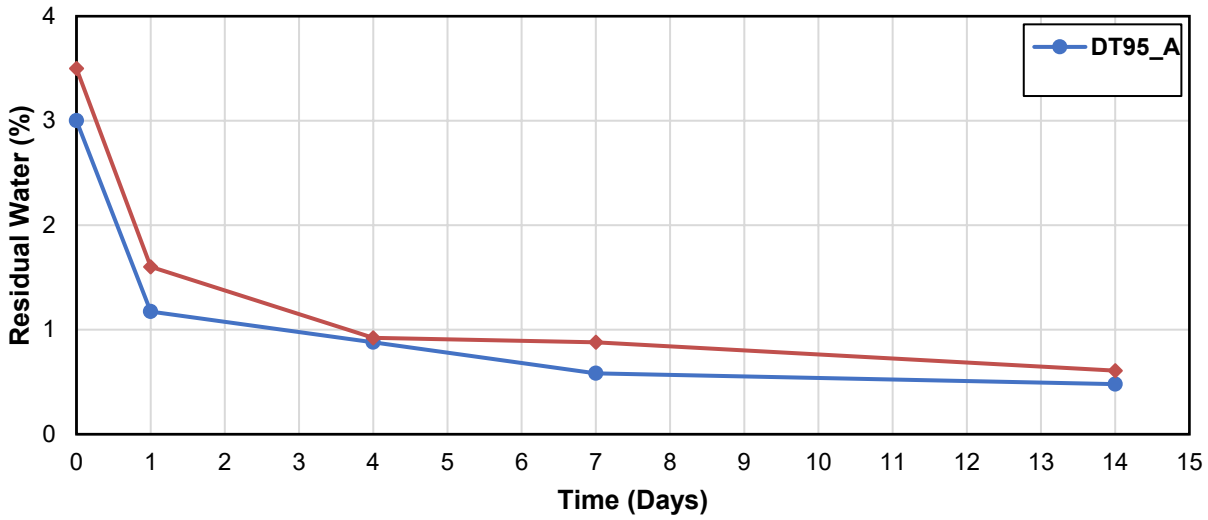

Figure 5.7 Gravimetric Measurement: Effect of Density

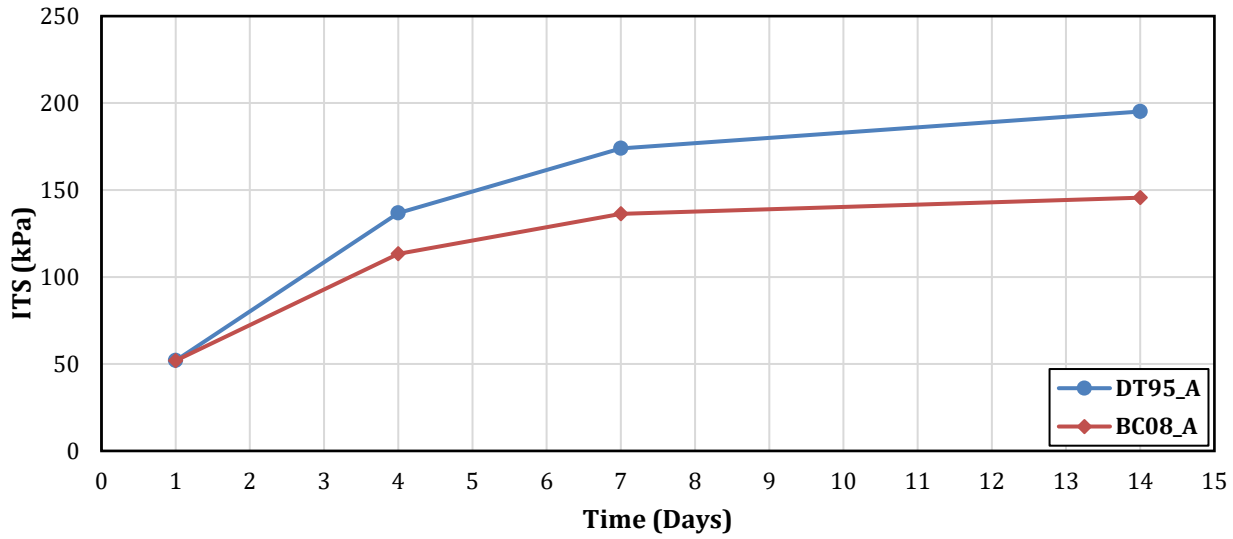

Figure 5.8 ITS Test: Effect of Density

5.1.4 Initial Moisture Content

To assess the effect of IMC, two mixtures with high IMC (DT30_Z and BC11_A) are compared to two with low IMC (DT95_A and BC08_A). The mixture variables are presented in Table 5.4; they have varying stabilizer amount and density. However, these factors have been identified in the previous subsections to have little to no effect on the evolution of curing. Figure 5.9 presents the gravimetric measurements of these mixtures whereas Figure 5.10 presents the ITS test results. Aside from the early curing stage, the trend in moisture (RW) evolution appear similar for all the mixtures with little to no changes after day 7. However, the ITS results show that mixtures with higher IMC (DT30_Z and BC11_A) gained more strength between days 7 and 14 compared to those with lower IMC (DT95_A and BC08_A).

Table 5.4 Mixtures for Assessing Effect of Initial Moisture Content

Mix ID	Stabilizer Amount [Type]	Active Filler [Type]	Density (kg/m^3)	IMC	Curing Temperature (°C)
DT95_A	2.0% [EE]	-	2098	3.0%	25
DT30_Z	3.0% [EE]	-	2082	5.7%	25
BC08_A	1.5% [EE]	-	1922	3.5%	25
BC11_A	1.9% [EE]	-	1922	4.9%	25

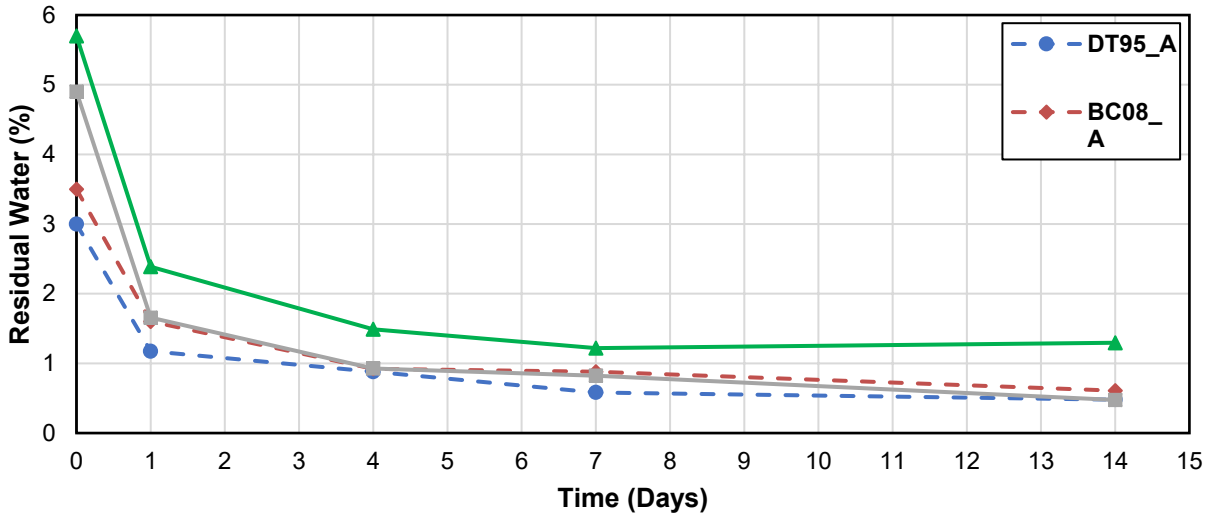

Figure 5.9 Gravimetric Measurement: Effect of Initial Moisture Content (dashed line: low IMC; solid lines: high IMC)

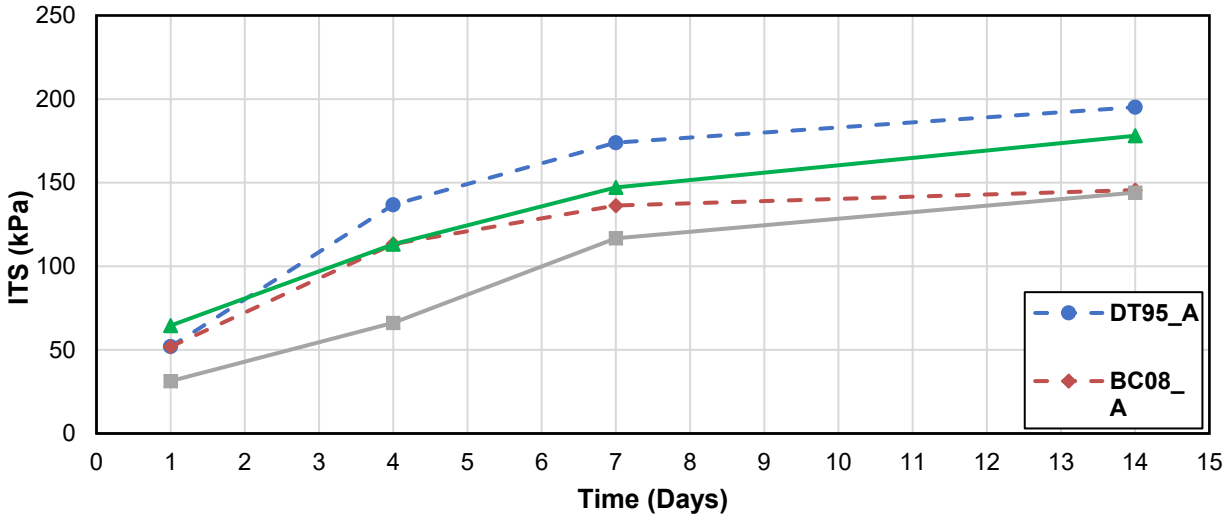

Figure 5.10 ITS Test: Effect of Initial Moisture Content (dashed line: low IMC; solid lines: high IMC)

5.1.5 Curing Temperature

Two groups of mixtures, with and without active filler as shown in Table 5.5, are used to investigate the effect of curing temperature. For the mixtures with active filler, the amount was similar. The result of the gravimetric measurements is presented in Figure 5.11 while the ITS result is shown in Figure 5.12. The data suggests that the curing temperature is not significant when there is no active filler. However, the curing temperature appears to accelerate the hydration process with active filler. At the 25°C temperature, DT75_Z mixture attains the equilibrium RW and final ITS value within 7 days. On the other hand, the hydration process appears to be slower when the BC08_Z mixture was cured at 15°C. This resulted in a more prominent gain in strength between days 7 and 10.

Table 5.5 Mixtures for Assessing Effect of Curing Temperature

Mix ID	Stabilizer Amount [Type]	Active Filler [Type]	Density (kg/m^3)	IMC	Curing Temperature (°C)
BC11_X	3.0% [EE]	-	2002	3.0%	25
DT75_X	3.0% [EE]	-	2066	3.4%	15
DT75_Z	3.0% [EE]	0.5% [Cement]	1970	5.0%	25
BC08_Z	3.0% [EE]	0.5% [Cement]	1922	4.5%	15

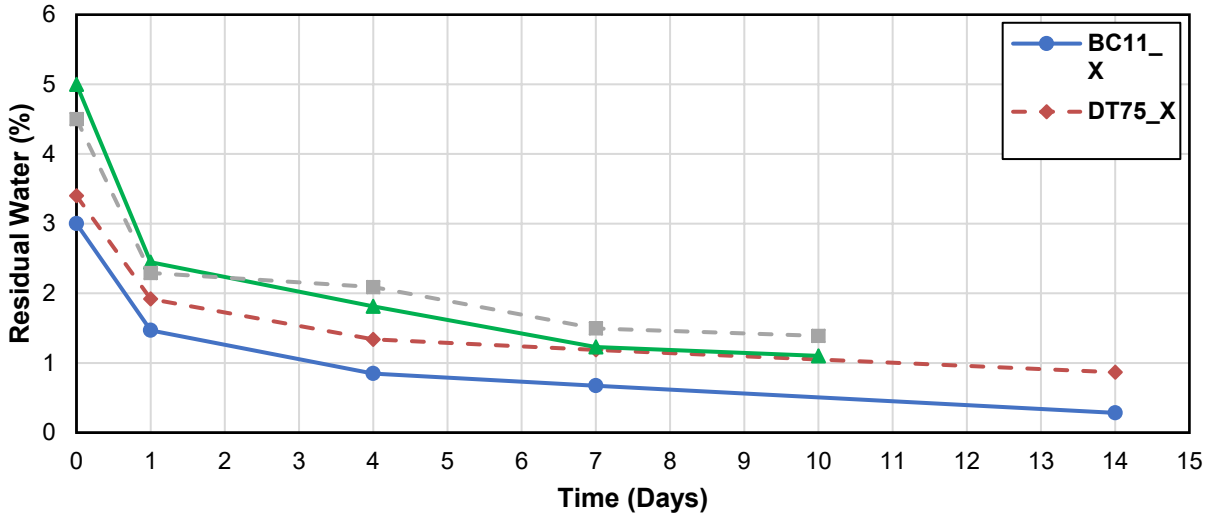

Figure 5.11 Gravimetric Measurement: Effect of Curing Temperature (dashed line: 15°C; solid lines: 25°C)

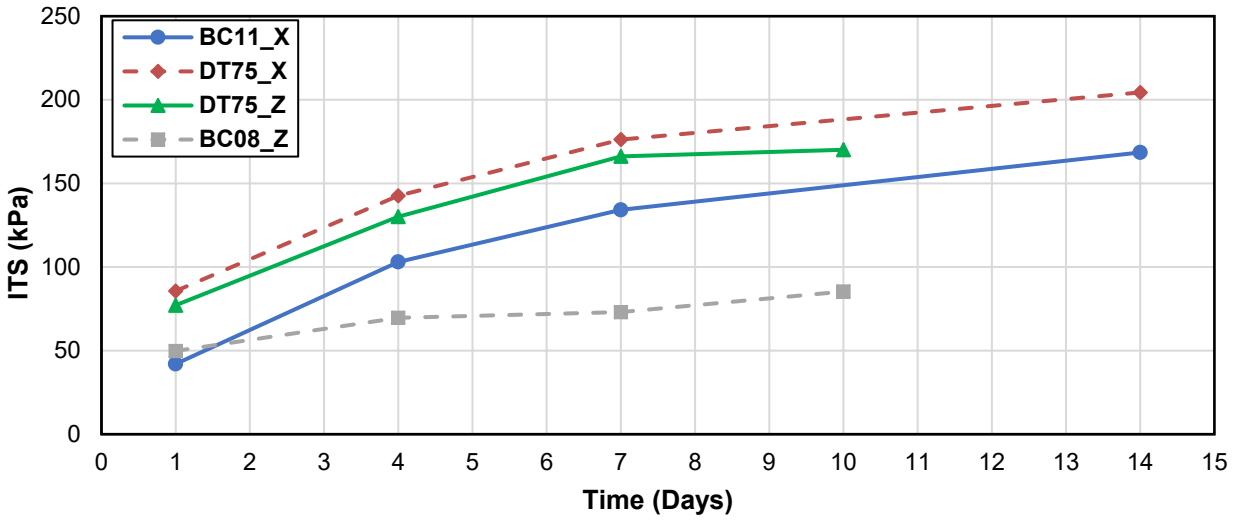

Figure 5.12 ITS Test: Effect of Curing Temperature (dashed line: 15°C; solid lines: 25°C)

5.1.6 Moisture Reintroduction (Rainfall Effect)

The moisture conditioning process introduced previously (in 3.3.2 was employed to study the effect of moisture reintroduction while curing. The intent is to simulate conditions similar to rainfall events during the early cure duration of CIR. This was done using two mixtures with and without active filler shown in Table 5.6. Figure 5.13 shows the result of the gravimetric measurement for these mixtures. Following the conditioning after four days of curing, more water infiltrated into the DT30_A mixture than the DT95_A, which is most likely an artifact of the lower density. However, due to the presence of active filler, the DT30_A mixture attains its equilibrium RW faster. From the ITS results shown in Figure 5.14, it is evident that the reintroduction of moisture results in significant decrease in strength for both mixtures. Subsequently, by day 10 of curing, the conditioned DT30_A mixture with active filler attains strength similar to the unconditioned specimen. On the other hand, the result suggests it may take more than 14 days for the conditioned DT95_A mixture ITS value is to match the unconditioned mixture. The reintroduction of moisture affects the short-term properties of the mixture but may not be detrimental once the equilibrium RW is reached. Therefore, it is likely that the conditioning process does not cause significant moisture damage to the CIR mixtures.

Table 5.6 Mixtures for Assessing Effect of Moisture Reintroduction

Mix ID	Stabilizer Amount [Type]	Active Filler [Type]	Density (kg/m^3)	IMC	Curing Temperature (°C)
DT30_A	2.0%	0.5% [Cement]	1970	5.7%	25
DT95_A	2.0%	-	2098	3.0%	25

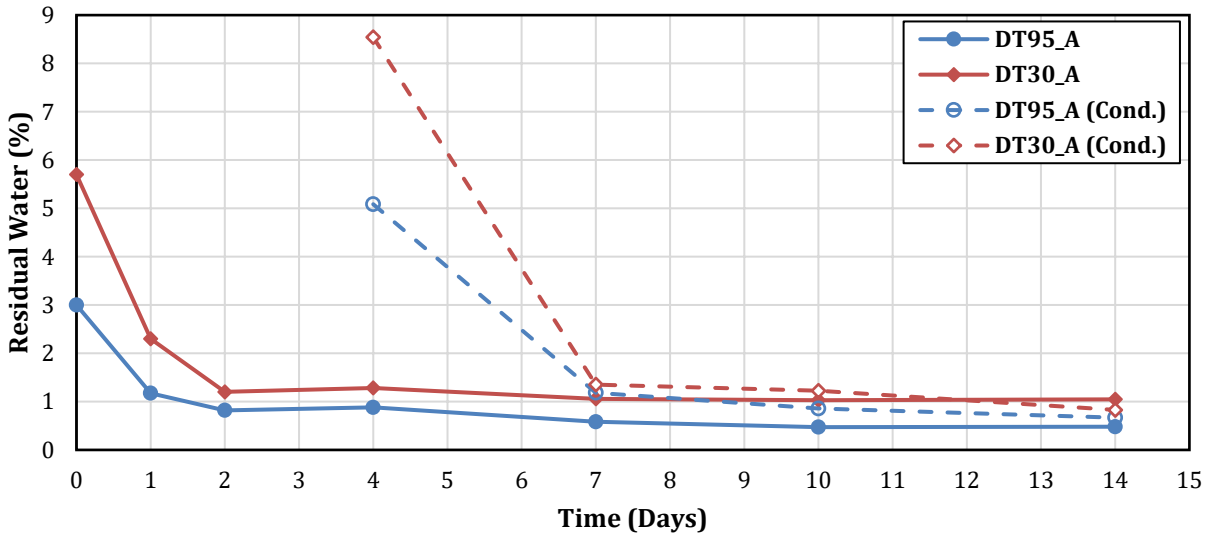

Figure 5.13 Gravimetric Measurement: Effect of Moisture Reintroduction (on Day 4)

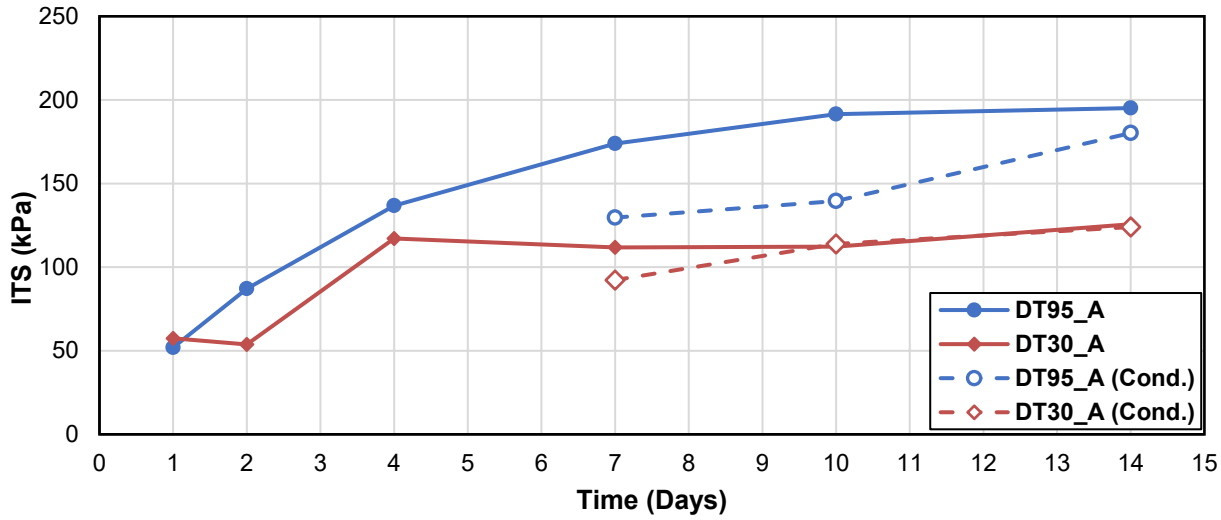

Figure 5.14 ITS Test: Effect of Moisture Reintroduction (on Day 4)

5.2 PROJECT-BASED RESULTS OF CURING EVOLUTION

This section discusses the evolution of curing as the factors are varied within the materials sampled from each of the field projects. The final mechanical properties that are achieved by a CIR mixture vary depending on the mix design. Therefore, for a clear comparative analysis, the mechanical properties (ITS) were normalized with respect to the final measured value. This assumes that the material has fully cured and achieved 100% of its final ITS by the last testing day. The moisture content values were not normalized as they typically tend to residual values within the same range. All comparative analyses conducted are with reference to the as-built conditions.

5.2.1 DT30

The mixture variations using DT30 sampled materials are given in Table 5.7. The gravimetric measurements and ITS results are shown in Figure 5.15 and Figure 5.16, respectively. The curing trend observed with the as-built CIR mixture (DT30_A) may have some errors as it was the first to be fabricated and tested in the laboratory. However, the general trend of decrease in moisture content and gain in strength was still observed as curing progressed. All mixtures appear to attain equilibrium RW within 4 – 7 days, however mixtures without active filler continue to gain strength. DT30_X cured the fastest likely due to the combination of lower IMC and active filler. After the first 2 days of curing, DT30_A, DT30_X and DT30_A(L) mixtures appear to reach similar RW and achieve more than 90% of their final ITS value by day 4. This suggests that the IMC may have an effect when active filler is used but this may only be minor. The absence of active filler is evident with DT30_Y and DT30_Z mixtures as they took longer than 7 days to reach the final ITS value. Additionally, with the absence of active filler, the IMC begins to play a significant role as DT30_Z cured the slowest.

Table 5.7 DT30 Mixture Variations

Mix ID	Stabilizer Amount [Type]	Active Filler [Type]	Density (kg/m^3)	IMC	Curing Temperature (°C)
DT30_A	2.0% [EE]	0.5% [Cement]	1970	5.7%	25
DT30_X	2.0% [EE]	0.5% [Cement]	2082	3.0%	15
DT30_Y	3.0% [EE]	-	1970	3.0%	15
DT30_Z	3.0% [EE]	-	2082	5.7%	25
DT30_A(L)	2.0% [EE]	0.5% [LKD]	1970	5.7%	25

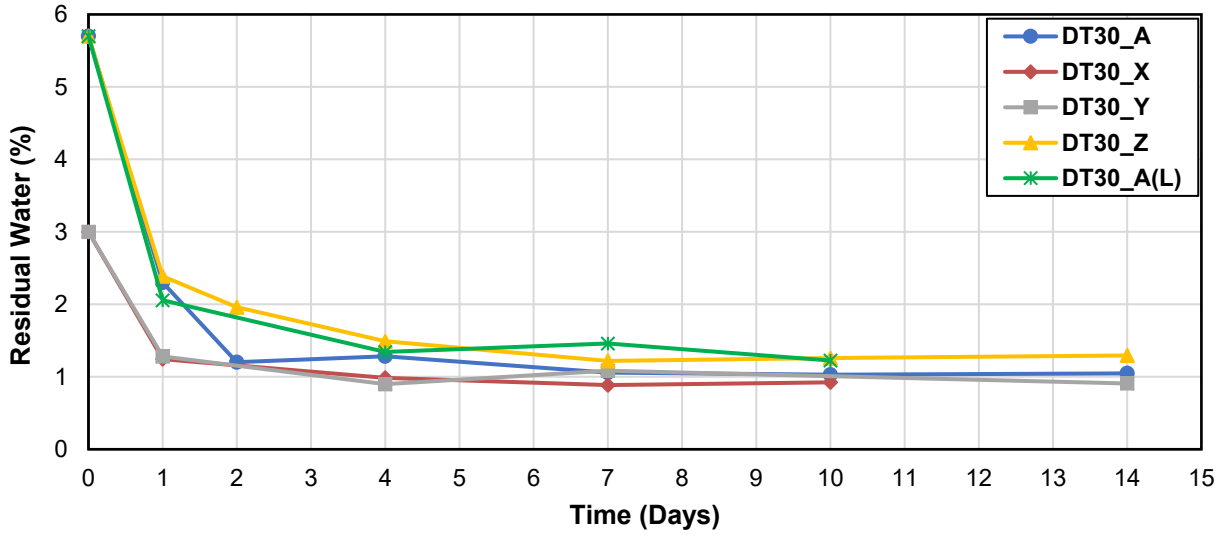

Figure 5.15 DT30 Gravimetric Measurements

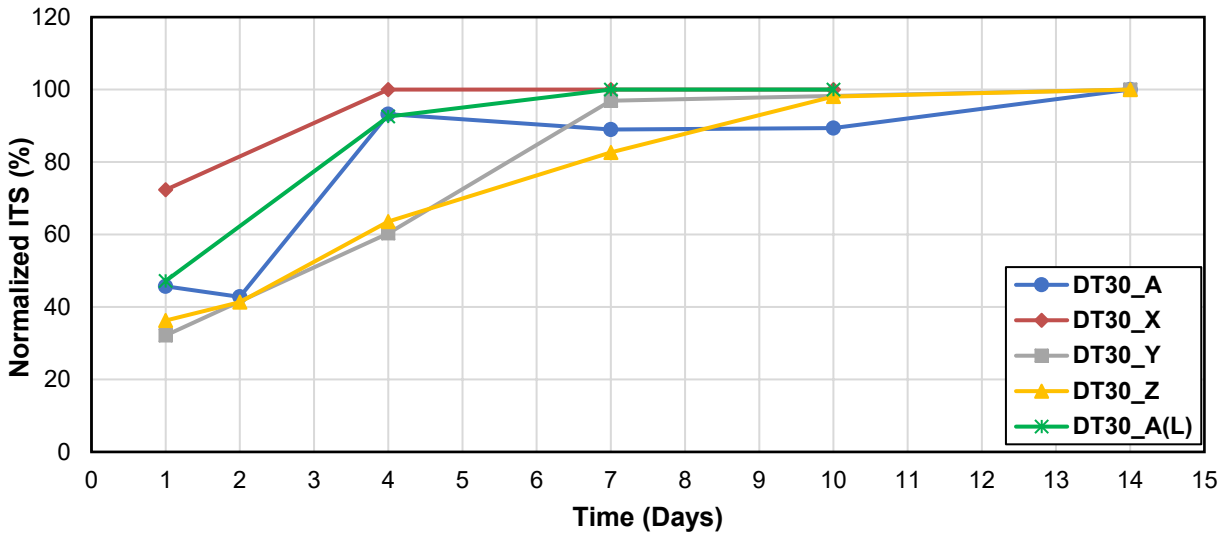

Figure 5.16 DT30 normalized ITS values (normalized with respect to last testing day)

5.2.2 DT95

Table 5.8 shows the mixture variations using DT95 sampled materials. The results of the gravimetric measurements and ITS tests for these mixtures are presented in Figure 5.17 and Figure 5.18, respectively. The equilibrium RW is achieved within 7 days of curing for all mixtures but gain in strength continues. The effect of the presence of active filler can also be observed with DT95_Y and DT95_Z curing faster than DT95_A and DT95_X. Furthermore, the effect of stabilizer amount and IMC also appears to be negligible when active filler is employed but the rate of strength gain is altered by both variables without active filler.

Table 5.8 DT95 Mixture Variations

Mix ID	Stabilizer Amount [Type]	Active Filler [Type]	Density (kg/m^3)	IMC	Curing Temperature (°C)
DT95_A	2.0% [EE]	-	2098	3.0%	25
DT95_X	3.5% [EE]	-	1922	3.5%	15
DT95_Y	3.5% [EE]	1.0% [Cement]	2098	3.5%	25
DT95_Z	2.0% [EE]	1.0% [Cement]	1922	3.0%	15

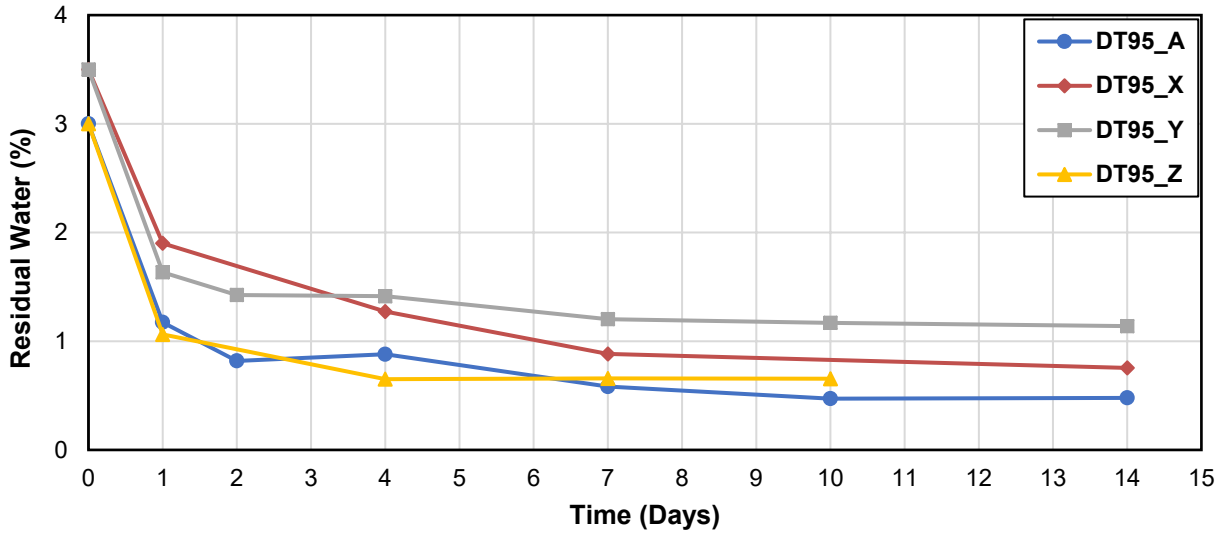

Figure 5.17 DT95 Gravimetric Measurements

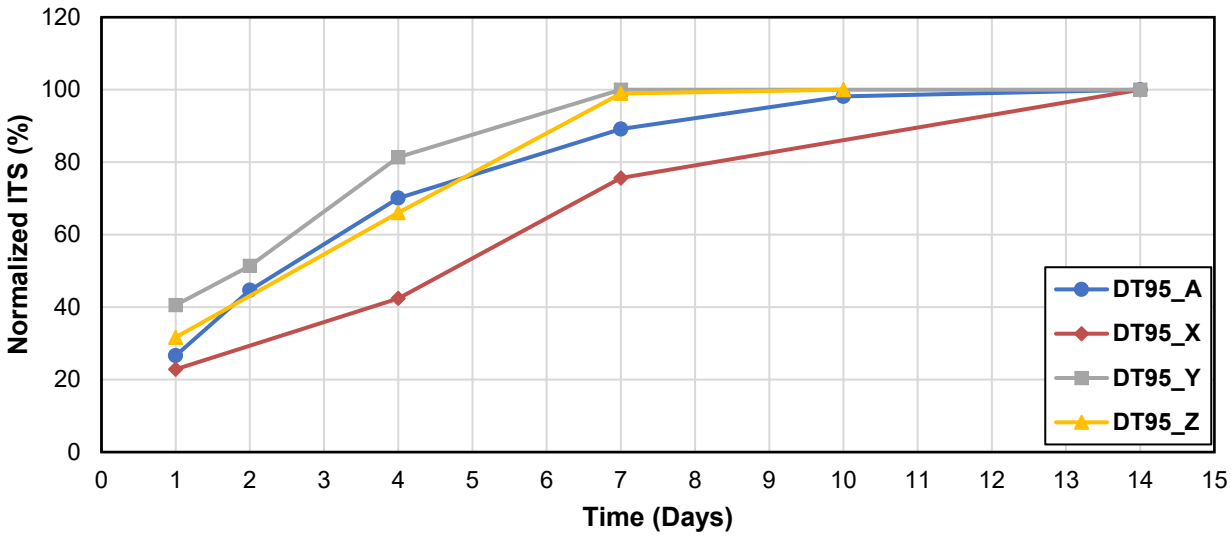

Figure 5.18 DT95 ITS Test

5.2.3 DT75

The mixture variations using DT75 materials is shown in Table 5.9. Figure 5.19 shows similar trends with previous projects in that equilibrium RW was achieved in all mixtures after 7 days of curing. Figure 5.20 further highlights the effect of active filler with final ITS value achieved within 7 days when active filler is used. Comparing DT75_X and DT75_Y, it is evident that a lower stabilizer amount accompanied with a higher IMC may result in a more dramatic change in strength evolution as curing progresses. However, this is not the case when active filler is present.

Table 5.9 DT75 Mixture Variations

Mix ID	Stabilizer Amount [Type]	Active Filler [Type]	Density (kg/m^3)	IMC	Curing Temperature (°C)
DT75_A	1.7% [EE]	0.5% [Cement]	2066	3.4%	25
DT75_X	3.0% [EE]	-	2066	3.4%	15
DT75_Y	1.7% [EE]	-	1970	5.0%	15
DT75_Z	3.0% [EE]	0.5% [Cement]	1970	5.0%	25

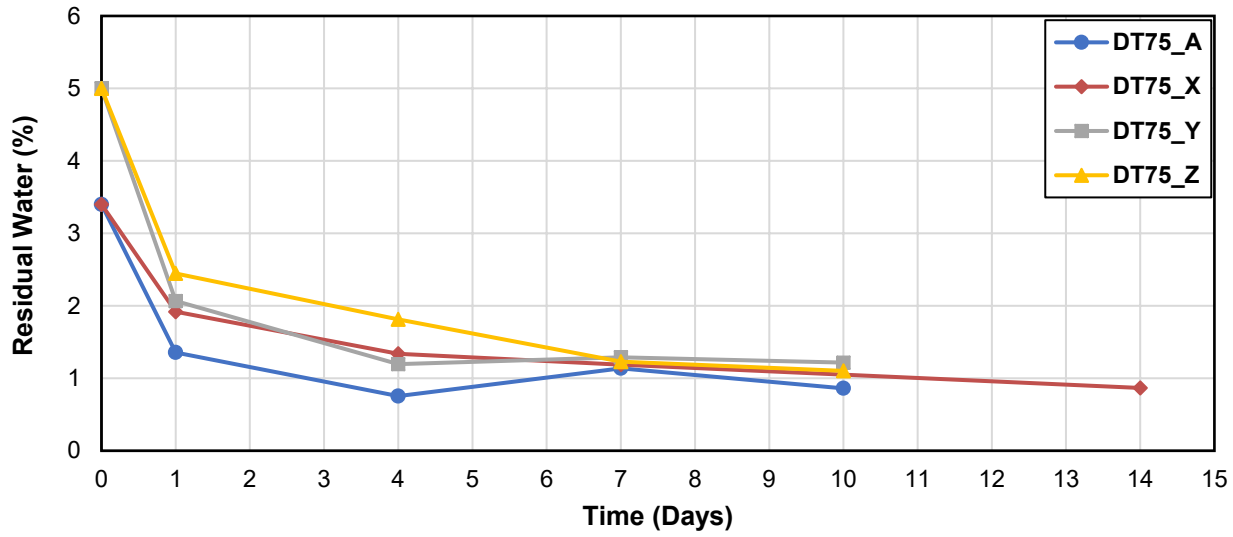

Figure 5.19 DT75 Gravimetric Measurements

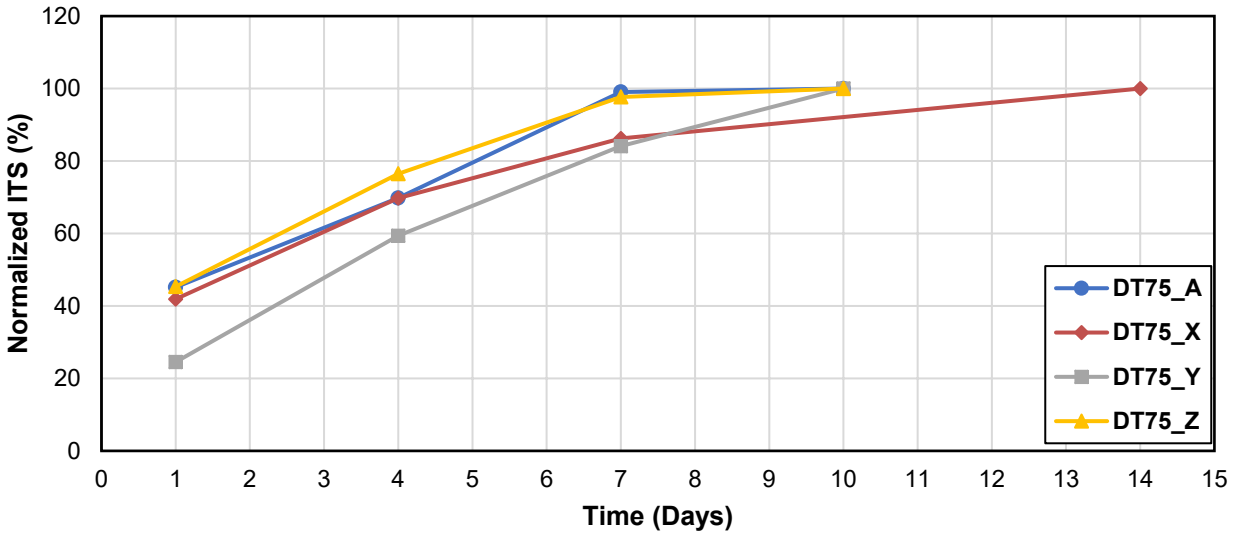

Figure 5.20 DT75 ITS Test

5.2.4 DT28

DT28 is the only project that utilized FA as a stabilizer. The mixture variations are shown in Table 5.10. As shown in Figure 5.21, only DT28_Y took longer than 4 days to achieve the equilibrium RW. This is likely due to the significantly higher IMC with no active filler present. Figure 5.22 shows that the trend with FA is similar to EE where gain in strength continues even after equilibrium RW has been achieved. It can be observed that curing at 15°C resulted in a delay in the hydration of active filler as DT28_X and DT28_Z continue to gain strength even after 7 days of curing. Ultimately, the as-built condition attained the final ITS value the fastest as a result of the lower FA amount and IMC together with curing at 25°C.

Table 5.10 DT28 Mixture Variations

Mix ID	Stabilizer Amount [Type]	Active Filler [Type]	Density (kg/m^3)	IMC	Curing Temperature (°C)
DT28_A	2.5% [FA]	-	2034	3.4%	25
DT28_X	3.5% [FA]	0.5% [Cement]	2034	3.4%	15
DT28_Y	3.5% [FA]	-	1954	5.0%	25
DT28_Z	2.5% [FA]	0.5% [Cement]	1954	5.0%	15

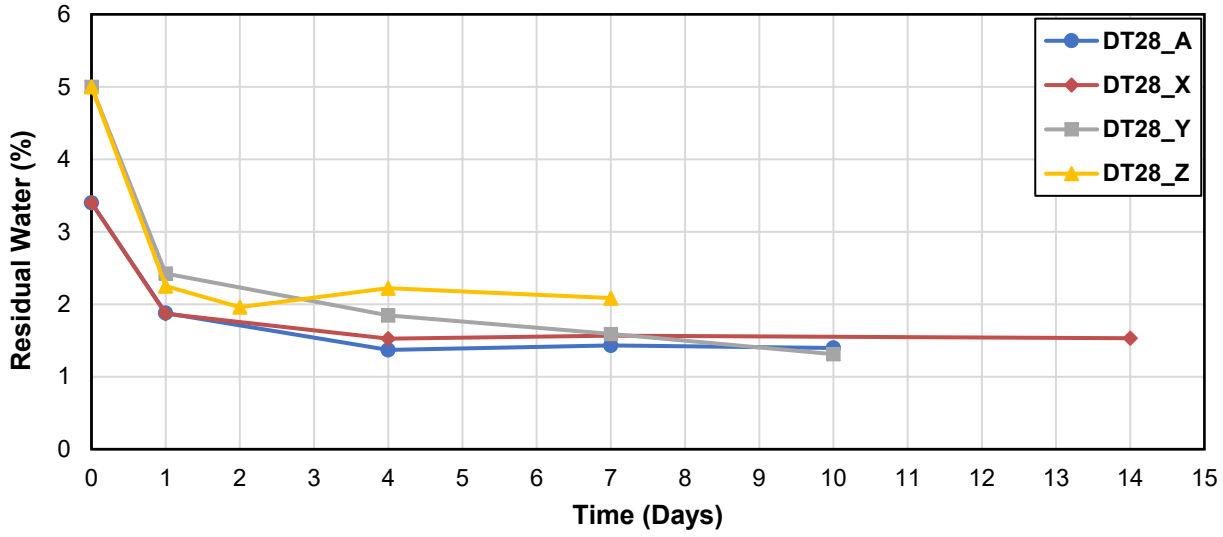

Figure 5.21 DT28 Gravimetric Measurements

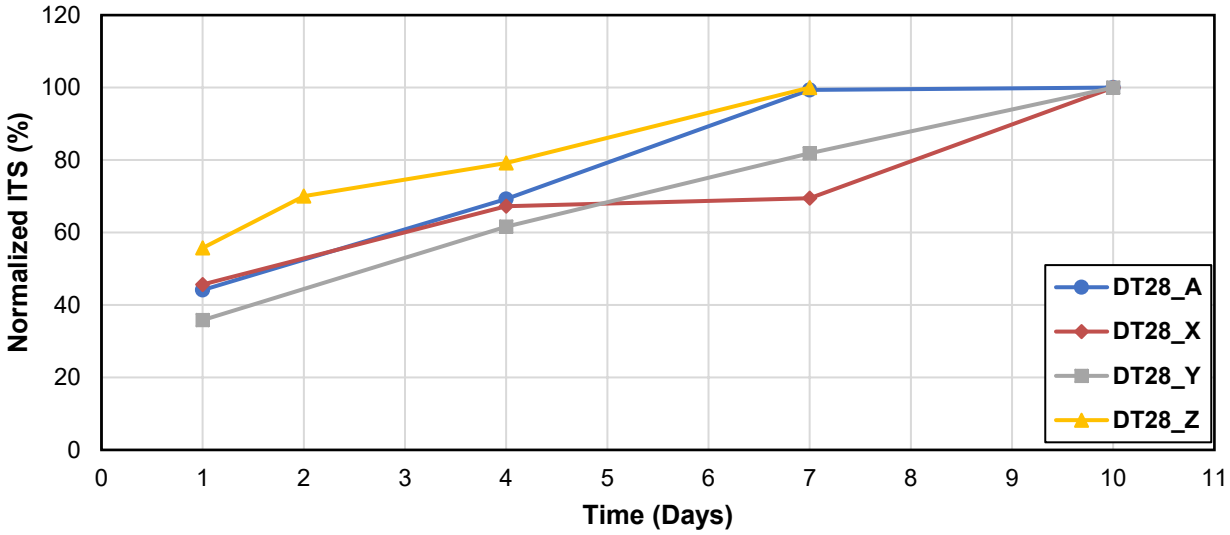

Figure 5.22 DT28 ITS Test

5.2.5 BC08

The variations for the BC08 materials are shown in Table 5.11. Figure 5.23 shows the gravimetric measurements while Figure 5.24 shows the ITS test results. The BC08_X mixture cured fastest because of the presence of active filler and curing temperature of 25°C. The delayed hydration of the active filler due to the low curing temperature is observed in BC08_Z with a pronounced gain in strength between day 7 and 10. Both mixtures without active filler (BC08_A and BC08_Y) follow a similar trend in terms of the moisture evolution, however, the ITS evolution differs which is evidence of the difference in IMC.

Table 5.11 BC08 Mixture Variations

Mix ID	Stabilizer Amount [Type]	Active Filler [Type]	Density (kg/m^3)	IMC	Curing Temperature (°C)
BC08_A	1.5% [EE]	-	1922	3.5%	25
BC08_X	3.0% [EE]	0.5% [Cement]	2002	3.5%	25
BC08_Y	1.5% [EE]	-	2002	4.5%	15
BC08_Z	3.0% [EE]	0.5% [Cement]	1922	4.5%	15

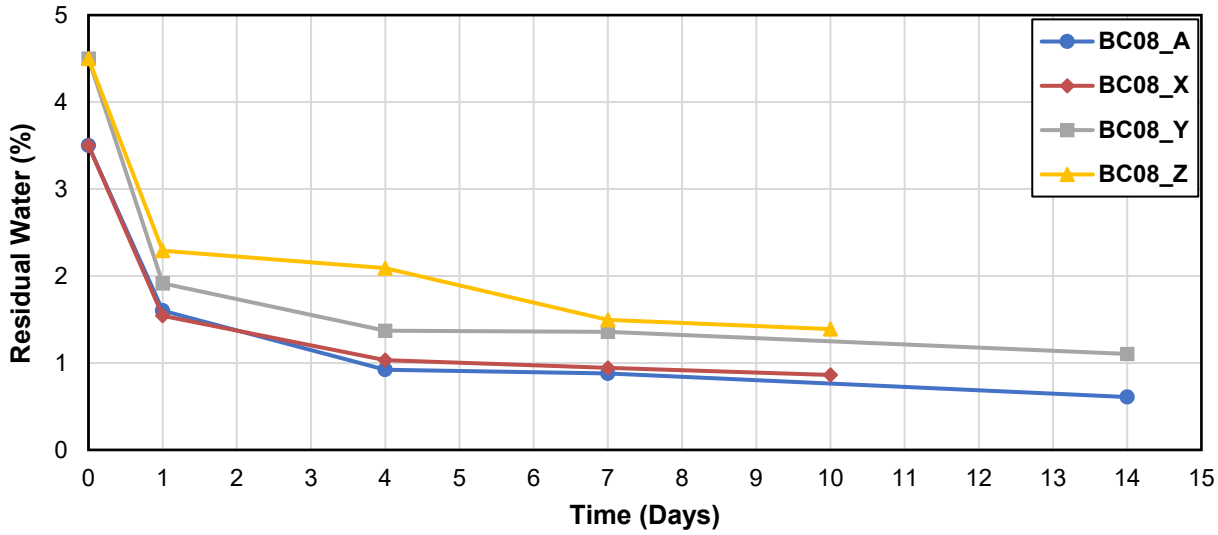

Figure 5.23 BC08 Gravimetric Measurements

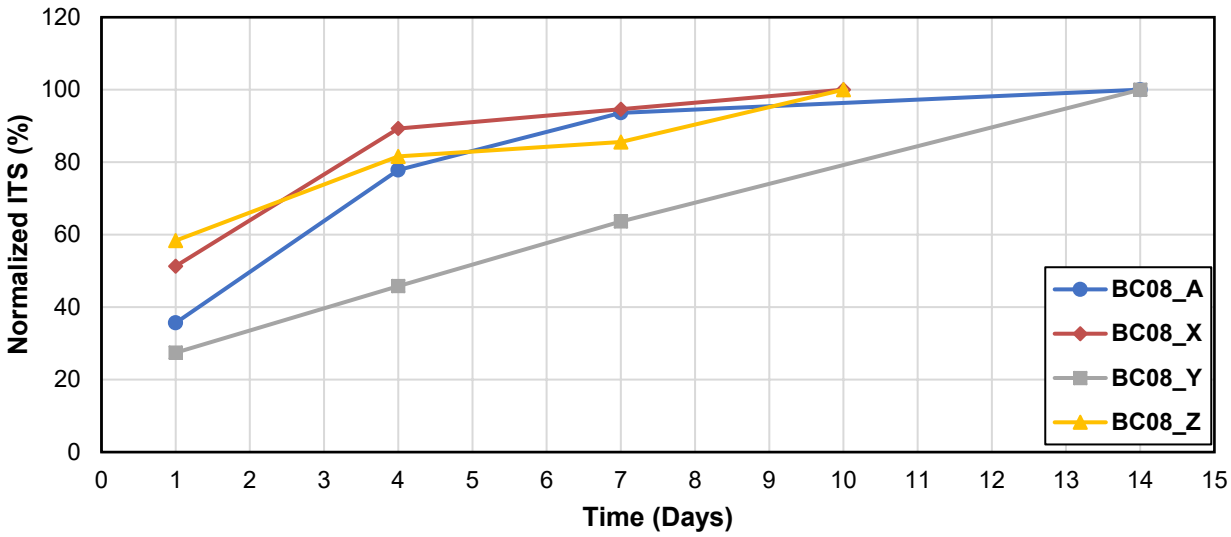

Figure 5.24 BC08 ITS Test

5.2.6 BC11

Table 5.12 shows the mixture variation for the materials sampled from BC11. LKD was used as active filler in this project as opposed to cement. Figure 5.25 and Figure 5.26 show that the benefit of active filler may not have been achieved due to the low curing temperature. Besides the effect of the IMC at the early curing stages, all the mixtures appear to follow a similar trend in terms of moisture and ITS evolution. For these materials, it takes more than 7 days to reach equilibrium RW.

Table 5.12 BC11 Mixture Variations

Mix ID	Stabilizer Amount [Type]	Active Filler [Type]	Density (kg/m^3)	IMC	Curing Temperature (°C)
BC11_A	1.9% [EE]	-	1922	4.9%	25
BC11_X	3.0% [EE]	-	2002	3.0%	25
BC11_Y	1.9% [EE]	1.0% [LKD]	2002	4.9%	15
BC11_Z	3.0% [EE]	1.0% [LKD]	1922	3.0%	15

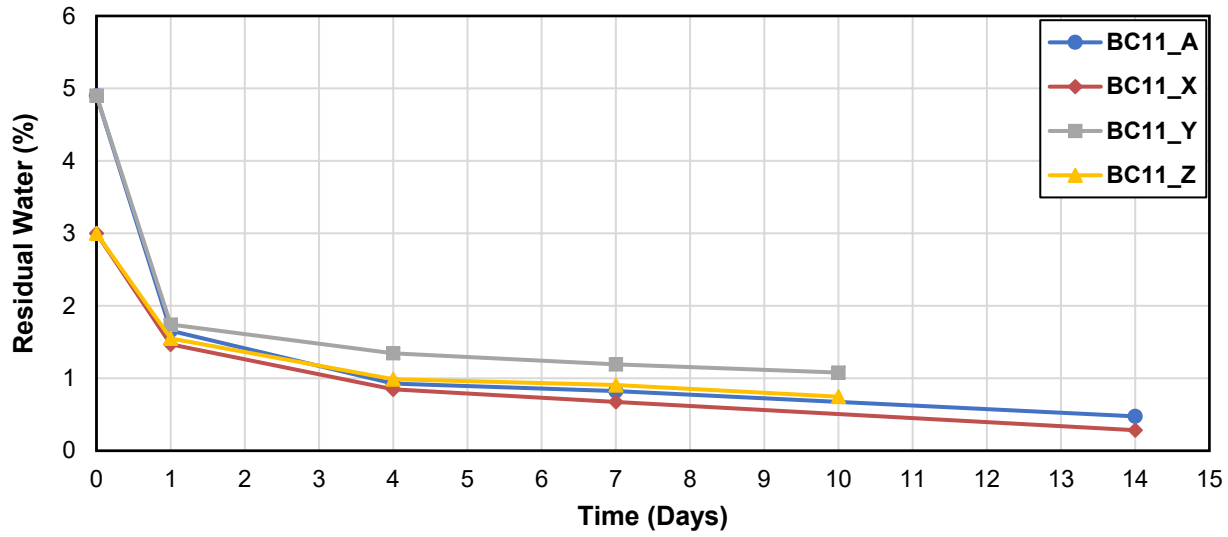

Figure 5.25 BC11 Gravimetric Measurements

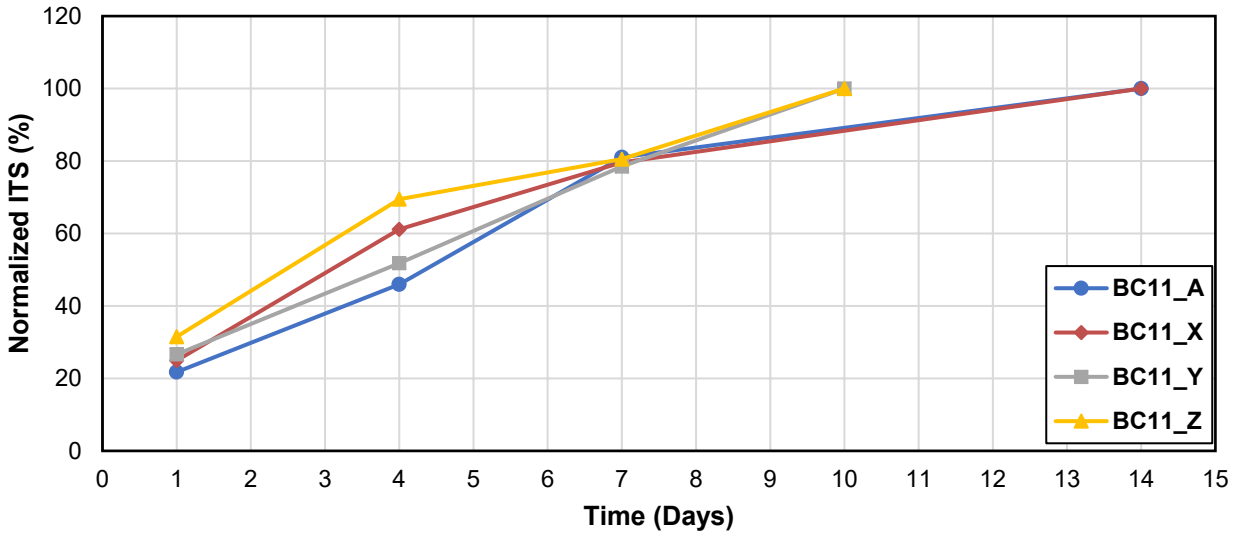

Figure 5.26 BC11 ITS Test

5.3 TRIAXIAL TEST RESULTS OF CURING EVOLUTION

The effect of the various curing factors on the evolution of the shear strength properties was evaluated using the TSS test. For each mixture, testing was done once during the early stage (after 5 days of curing) and once at the later stage (after 14 days of curing). To obtain the shear envelope at each curing stage, testing was conducted at three confining pressures (0 kPa, 35 kPa and 70 kPa), using one specimen for each confining pressure. Testing was done at only two curing times and using one specimen for each confining pressure due to limitations in amount of sampled component materials. Each test specimen requires about 29 lbs. (13 kg) of CIR loose mixture.

Only the as-built material and curing conditions of the six study projects (see Table 5.13) were evaluated using this test. Figure 5.27 and Figure 5.28 show the cohesion and friction angle, respectively, determined from the TSS testing for the six mixtures. Generally, a gain in cohesion can be observed as curing progresses, however there is no explicit trend in terms of the friction angle. These follow observations previously made by other researchers (Preti, 2021). The number above each bar in Figure 2.3 represents the percent change in cohesion between the two testing days. A lower percentage indicates that the final cohesion is attained sooner, which is an indication of faster curing. The DT95_EE_HL mixture exhibited the least amount of change in cohesion between the two testing days. It is likely that this is due to the relatively higher density (limits the amounts of voids/fluids between RAP particles) and lower IMC. The DT28_FA_HL mixture also showed a very low percent change in cohesion which confirms the faster curing of foamed asphalt compared to engineered emulsion. DT30_EE_LH(AF) and DT75_EE_HL(AF) are the only two mixtures that employed active filler at the same application rate. However, it is evident that the DT75_EE_HL(AF) mixture cured faster than the DT30_EE_LH(AF) mixture; this could similarly be a combined effect of a relatively lower IMC and higher density. On the other hand, BC08_EE_LL and BC11_EE_LH mixtures showed much higher degree of change in cohesion between the two testing days. It is not surprising as both mixtures were compacted to relatively lower densities and did not employ active filler.

Table 5.13 Mixtures for Assessing Evolution of Shear Strength Properties

Project [Stabilizer Type]	Stabilizer Amount	Active Filler [Type]	Density (PCF)	IMC	Curing Temperature (°C)	Mix ID
TH 30 [EE]	2.0%	0.5% [Cement]	123	5.7%	25	DT30_A
TH 95 [EE]	2.0%	-	131	3.0%		DT95_A
TH 75 [EE]	1.7%	0.5% [Cement]	129	3.4%		DT75_A
TH 28 [FA]	2.5%	-	127	3.4%		DT28_A
CSAH 8 [EE]	1.5%	-	120	3.5%		BC08_A
CSAH 11/21 [EE]	1.9%	-	120	4.9%		BC11_A

*EE – Engineered Emulsion, FA – Foamed Asphalt, IMC – Initial Moisture Content

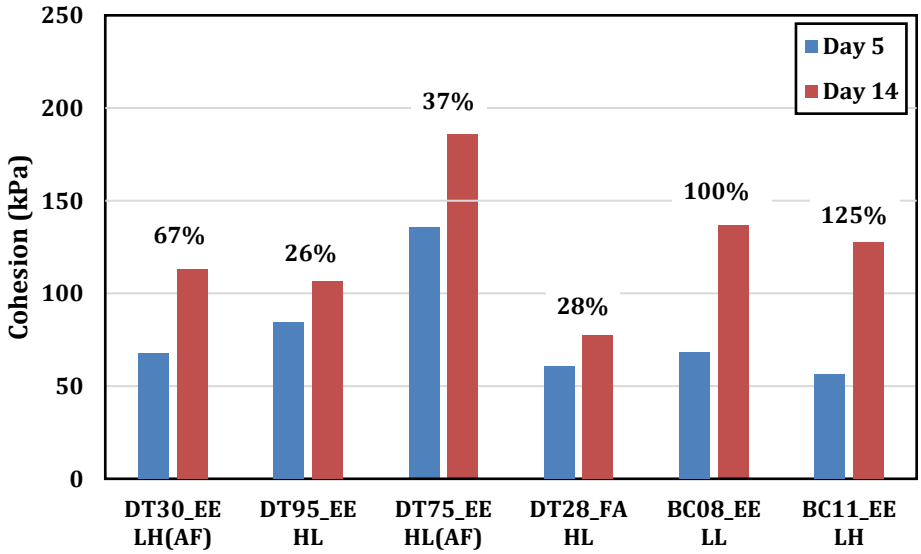

Figure 5.27 Cohesion Evolution (the amount of gain in percent is shown above the bars)

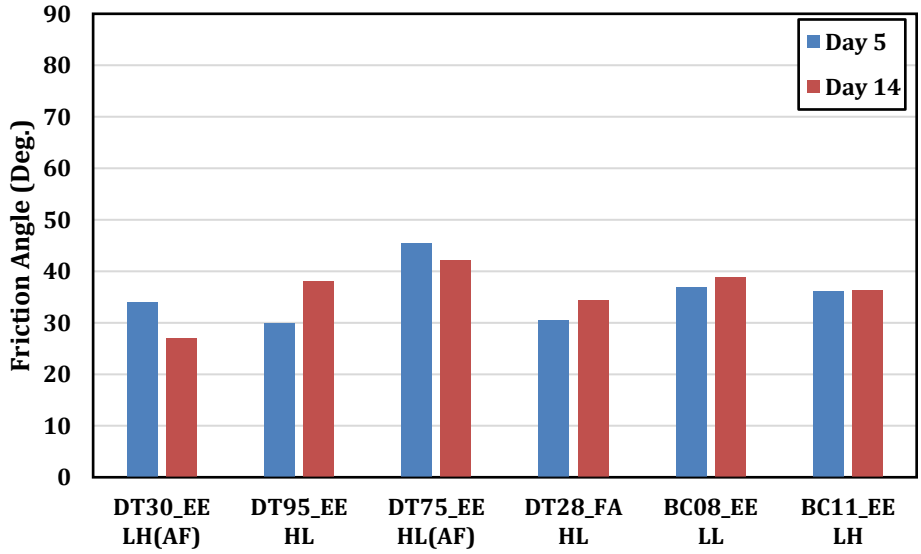

Figure 5.28 Friction Angle Evolution

5.4 SUMMARY OF FINDINGS FROM LABORATORY TESTING

Using the sampled materials, mixtures with as-built characteristics as well as variations to the as-built conditions were fabricated in lab to expand the dataset that will be used for a curing prediction model development. To do this, a partial factorial experimental design was developed to capture the effect of the various curing factors identified previously. Moisture evolution was tracked using gravimetric and LDMS measurements. The M_R and ITS tests were employed to assess the evolution of mechanical properties. A summary of laboratory testing effort is shown in Figure 5.29 Figure 5.32. These plot show results for all tested materials at different testing times. The intent of these plots is to not generate a specific conclusion, rather to demonstrate overall trends and to indicate need for statistical modelling to

develop curing prediction equation. As a supplementary laboratory CIR material characterization method, the triaxial shear strength test was conducted to evaluate the evolution of shear strength properties (bearing capacity) during the curing period. Due to limitations in quantity of sampled component materials, this was done only for the as-built material and curing conditions of the six study projects and at two different curing times (after 5 and 14 days of curing).

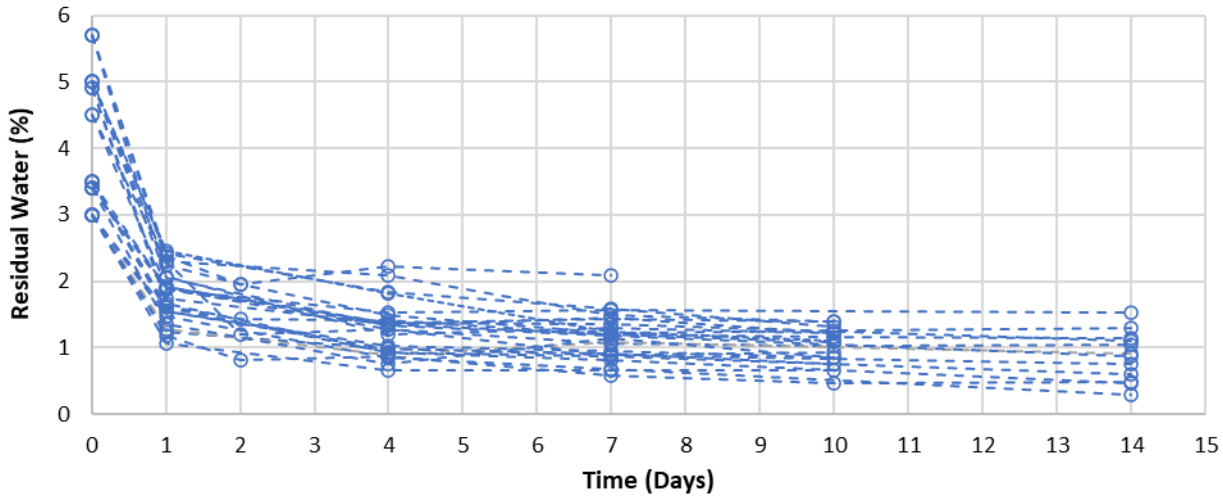

Figure 5.29 Summary of Gravimetric Measurements

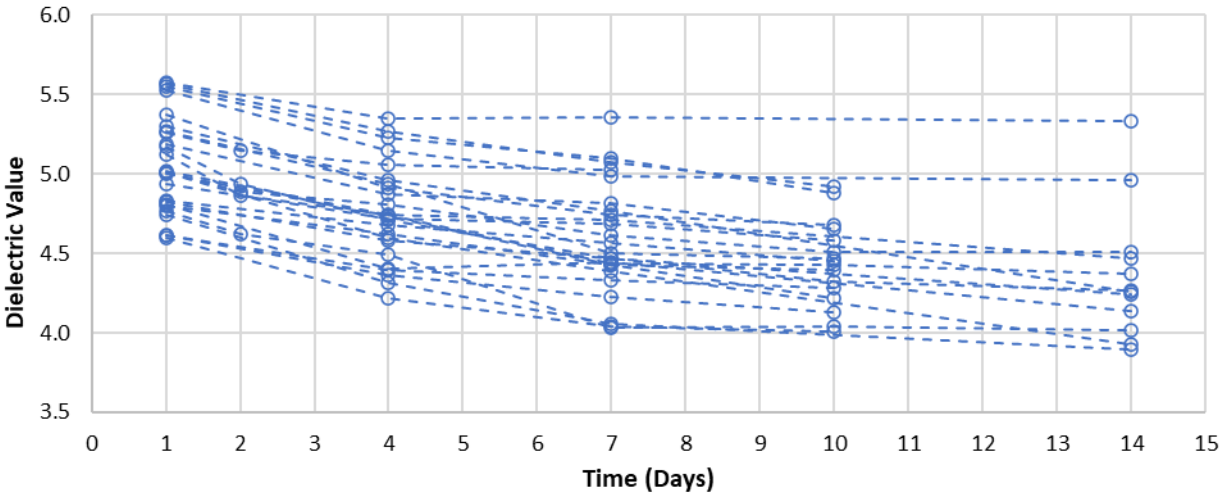

Figure 5.30 Summary of LDMS Measurements

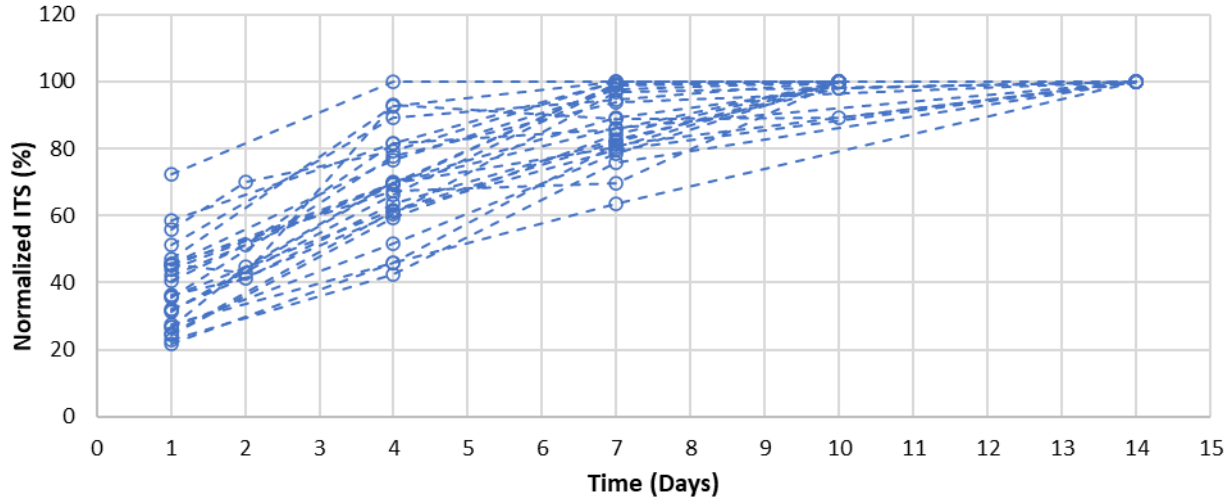

Figure 5.31 Summary of ITS Test

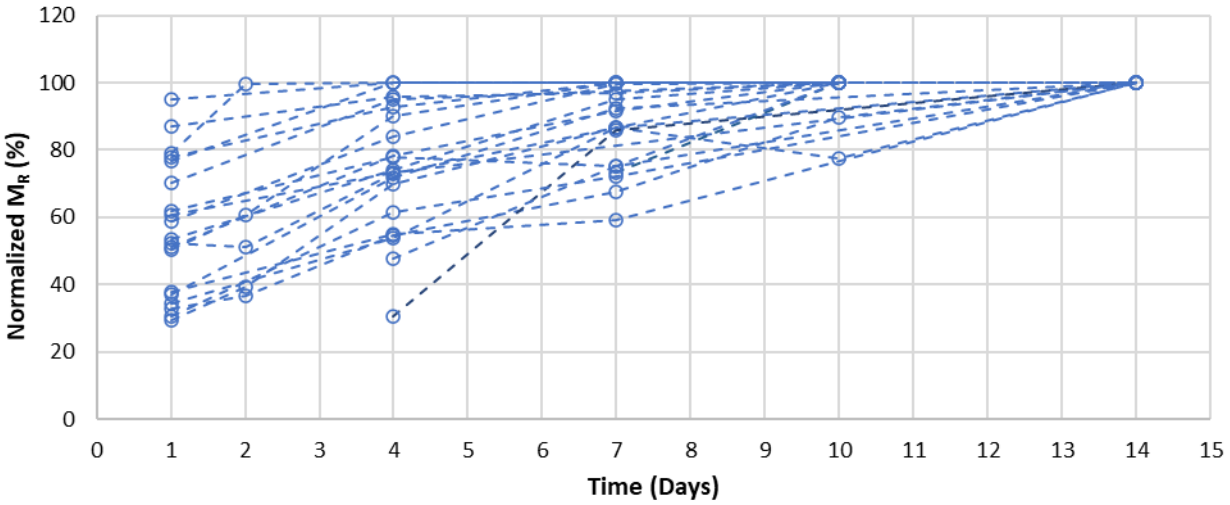

Figure 5.32 Summary of M_R Test

The following preliminary observations were made from the results presented:

- The LDMS shows promising results in tracking the moisture content evolution, comparable with the gravimetric measurements.
- The M_R and ITS tests show similar trends with evolution of mechanical properties.
- There is further gain in mechanical properties after the mixtures have reached an equilibrium moisture condition. This is more significant in the absence of active filler.
- Mixtures stabilized using foamed asphalt cure faster than those using engineered emulsion as a stabilizer.
- Stabilizer amount may only have an effect in the early stages of curing if associated with a difference in IMC. This however diminishes when active filler is employed.
- The higher the active filler amount, the faster the curing process. An extended curing period is required when active filler is not used.

- At similar dosage, the use of cement results in faster curing process compared to LKD. To achieve a comparable curing rate, higher amounts of LKD may be required.
- The data suggests that density (within the typical density variation range applicable to construction practices) is not a significant factor affecting the rate of curing.
- In terms of moisture evolution, IMC is most significant at the early stages of curing (up to first 3 days). However, mixtures with higher IMC tend to show a higher magnitude of change in mechanical properties as curing progresses.
- Effect of temperature (within range of typical temperatures encountered during construction season in Minnesota) may be insignificant to rate of curing when active filler is not used. However, with inclusion of active filler, hydration is accelerated at a higher curing temperature. At lower curing temperature, cement may hydrate at later stages of curing and result in improvement of mechanical properties at later times. On the other hand, the benefit of LKD might be lost if curing is done at lower temperature.
- The moisture conditioning protocol shows that density plays a role in the amount of moisture that can infiltrate the CIR layer. Reintroduction of moisture results in a significant decrease in strength of mixtures in the short term. After introducing moisture, moisture equilibrium is achieved faster when active filler is used in the CIR.
- Reintroduction of moisture may not be detrimental in the long-term once the equilibrium moisture condition is attained. Similar moisture conditions and mechanical properties with the unconditioned specimens can still be achieved after conditioning process. This suggests that the conditioning process does not cause significant moisture damage to the CIR mixtures.
- The TSS test can also be used to track the evolution of mechanical properties as curing progresses. However, contrary to previous observations, the data suggests that density plays a major role in the rate of gain in cohesion as pertaining to curing.

CHAPTER 6: CORRELATING FIELD AND LABORATORY RESULTS

It is apparent that there are several factors that may affect the curing evolution of CIR materials, however, some of these factors (such as wind speed, rainfall, and condition of underlying layer) are not easily implemented in a laboratory setup. Additionally, the limited field data is inadequate to reliably evaluate the effect of these factors. Therefore, it is paramount to establish a link between the laboratory and field curing conditions to translate the combined effect of these curing factors. Accordingly, this chapter describes the effort made in comparing and correlating the results of measurements obtained in the field and laboratory for the as-built material and curing conditions of the six study projects (see Table 6.1). The evaluation was done in terms of the evolution of both moisture content (MC) and mechanical properties. The following naming convention was adopted in this chapter for mixture identification: The first letter denotes the overseeing agency (D –MnDOT, B –Brown County); the second letter and following numbers denote the field project the material was sampled from; the letters after the first underscore indicates the stabilizer type (EE –Engineered Emulsion; FA –Foamed Asphalt); the two letters after the second underscore indicate the relative classification of the density and initial moisture content (IMC) respectively (L –Low; H –High); the presence of active filler is indicated in paratheses. For example, DT30_EE_LH(AF) is a mixture produced using materials sampled from MnDOT TH 30, with EE as stabilizer type, a relatively low in-situ density and high IMC, and also includes active filler. The results for the triaxial testing are presented in the following subsection.

Table 6.1 CIR Study Project As-built Material and Curing Condition

Project [Stabilizer Type]	Stabilizer Amount	Active Filler [Type]	Density (kg/m^3)	IMC	Curing Temperature (°C)	Mix ID
TH 30 [EE]	2.0%	0.5% [Cement]	1970	5.7%	25	DT30_EE_LH(AF)
TH 95 [EE]	2.0%	-	2098	3.0%		DT95_EE_HL
TH 75 [EE]	1.7%	0.5% [Cement]	2066	3.4%		DT75_EE_HL(AF)
TH 28 [FA]	2.5%	-	2034	3.4%		DT28_FA_HL
CSAH 8 [EE]	1.5%	-	1922	3.5%		BC08_EE_LL
CSAH 11/21 [EE]	1.9%	-	1922	4.9%		BC11_EE_LH

*EE – Engineered Emulsion, FA – Foamed Asphalt, IMC – Initial Moisture Content

6.1 MOISTURE CONTENT EVOLUTION

The nuclear density and moisture gauge (NDMG) and density or dielectric profiling system (DPS) were used to track the changes in in-situ MC. The NDMG directly measured the volumetric MC of the CIR layers, while the DPS indirectly tracks the change in MC by evaluating the change in material dielectric. One of the significant findings from chapter 4 was that the NDMG and DPS generally showed similar trend in terms of the in-situ MC changes during curing of CIR layers.

MC evolution was tracked in the laboratory using gravimetric measurements and laboratory dielectric measurement system (LDMS). Similar to the DPS, LDMS tracks the change in material dielectric. The DPS uses the surface reflectivity method to measure the dielectric constant while the LDMS uses the time-of-flight method. The LDMS showed promising results in tracking the MC evolution that was comparable with the gravimetric measurements. All subsequent results and analyses presented under this subsection use the average values of the replicate measurements. Detailed discussions on variabilities within in-situ test sections measurements as well as laboratory test replicates were discussed in chapters 4 and 5. The variabilities for both in-situ and lab measurements were low and within typical test method repeatability limits, thus use of averaged values for comparison purposes is deemed acceptable.

6.1.1 Direct Moisture Content Measurements

Both the NDMG and laboratory gravimetric measurement facilitated the direct evaluation of material MC. To precisely compare the results, the NDMG volumetric moisture content is converted to gravimetric units using equation 3.1.

$$Gravimetric\ MC\ (\%) = Volumetric\ MC\ (\%) \times \frac{\rho_w}{\rho} \tag{3.1}$$

Where:

ρ_w = Density of water (1000 kg/m^3)
ρ = Bulk density of material, kg/m^3

Table 6.2 presents the gravimetric IMC measured in the laboratory on the CIR loose mix (sampled during construction and stored in sealed bags), in comparison with the MC obtained from the contractor quality control (QC) data. The QC measurements were done immediately after compaction using the NDMG. Additionally, NDMG measurements were collected by the team from MnDOT Office of Materials and Road Research (OMRR). Due to construction scheduling, OMRR personnel were only able to obtain NDMG measurement on the day of construction for only two of the study projects. This information is included in

Table 6.2 for comparison.

Table 6.2 Comparison of Gravimetric Initial Moisture Content Measured in the Field and Laboratory

Project ID	Gravimetric Initial Moisture Content (%)		
	Laboratory	QC NDMG	OMRR NDMG
DT30_EE_LH(AF)	5.7	5.4	N/A
DT95_EE_HL	3.0	3.7	N/A
DT75_EE_HL(AF)	3.4	N/A	N/A
DT28_FA_HL	3.4	N/A	N/A
BC08_EE_LL	3.5	5.3	5.7

BC11_EE_LH	4.9	5.5	6.8

*N/A – Not Available; QC – Quality Control; OMRR – Office of Materials and Road Research

Based on the information presented in

Table 6.2, it is evident that the QC NDMG generally measured higher MC as compared to a direct gravimetric moisture content measurement. Small deviation between these two were expected for projects using active fillers, since gravimetric measurement would not account for water that is chemically bound to hydrated cement or lime. This is even more significant considering that the QC NDMG measures MC after compaction has been completed, with the propensity of the material to have lost some of its moisture during the compaction operation. NDMG measures moisture near the paved surface and all projects were constructed during relatively hot weather. Additionally, it can be observed that the OMRR NDMG measures an even higher MC compared to the QC NDMG. It is noteworthy that the OMRR measurements were taken several hours after compaction and a lower material MC should be expected. Ultimately, since the OMRR NDMG was used for subsequent field measurements, researchers developed a regression relationship between the laboratory measurements and OMRR NDMG measurements using the two data points from construction days (day 0). The regression relationship is a straight line in the form of equation 3.2.

$$y = ax + b \tag{3.2}$$

In this case, where:

x = OMRR NDMG MC (%)
y = Gravimetric MC (%)
a, b = Regression constants

The resulting regression constants are as shown in Figure 6.1. This is done to have direct comparison of the moisture evolution based on similar reference IMC.

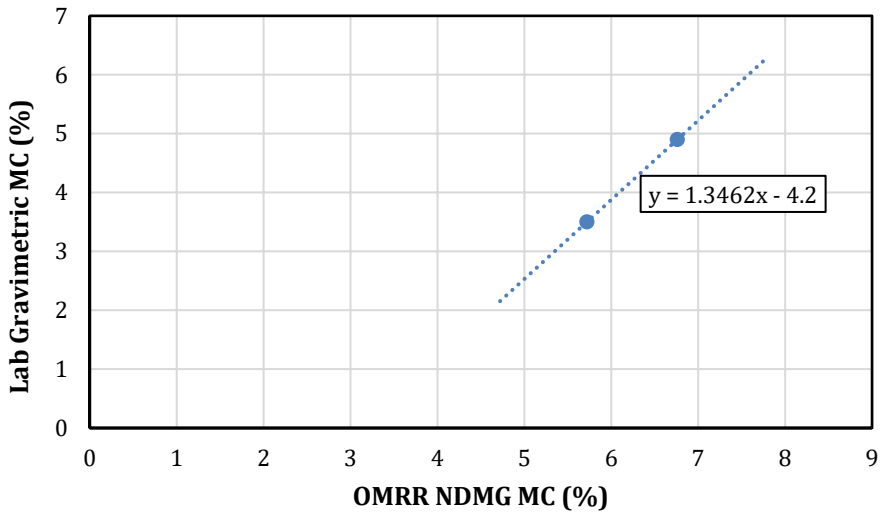

Figure 6.1 Regression Relationship between Laboratory and NDMG IMC

The regression equation was used to normalize all subsequent NDMG measurements. The normalized NDMG MC evolution is presented in Figure 6.2, in comparison with laboratory MC evolution. Except for DT28_FA_HL, the trend seems reasonable in terms of a continuous decrease in MC with time. However, it can be observed that the artifact of the higher MC measurements persists even after normalizing the NDMG data. The NDMG result shows that all projects except DT30_EE_LH(AF) and BC11_EE_LH , may have attained an equilibrium moisture condition by day 3. This is likely because both DT30_EE_LH(AF) and BC11_EE_LH projects had significantly higher IMC. This was not observed in the laboratory, as all projects had their MC stabilize between days 4 and 7. Generally, the data suggests that for most cases when IMC is lower, equilibrium moisture condition may be achieved faster in the field compared to the controlled laboratory environmental curing conditions. However, this trend reverses when the IMC is relatively higher.

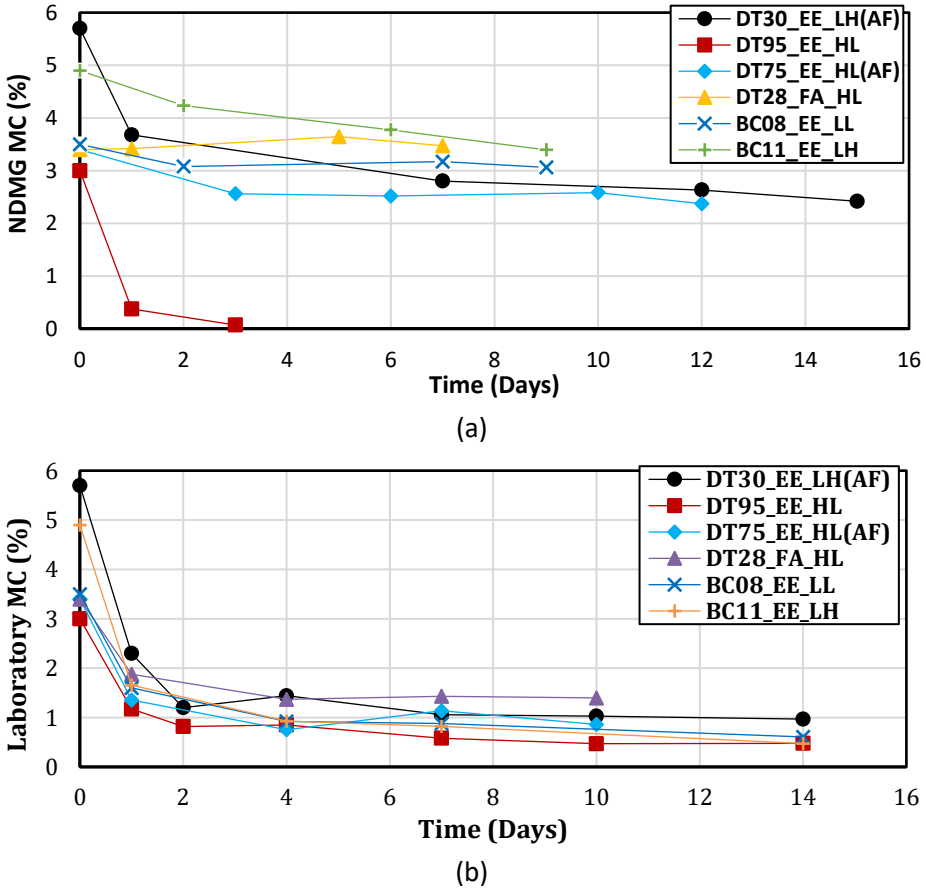

Figure 6.2 Moisture Content Evolution: (a) Normalized NDMG (b) Laboratory

6.1.2 Moisture Content Estimation from Dielectric Measurements

The DPS and LDMS were used to measure the material dielectric in the field and laboratory, respectively. Since it was not possible to obtain the dielectric measurements right after compaction, researchers explored the possibility of estimating the initial (Day 0) dielectric of the CIR materials prior to making comparisons. This is done to evaluate how the material properties change from day of construction.

Recall that in chapter 5, a moisture conditioning protocol was employed to study the effect of rainfall, using the DT30_EE_LH(AF) and DT95_EE_HL materials. LDMS was subsequently used to measure the material dielectric before and after conditioning. A linear regression relationship between the laboratory gravimetric MC and LDMS dielectric was then established for each material (form of equation 3.2) where:

x = Gravimetric MC (%)
y = LDMS Dielectric
a, b = Regression constants

The resulting values for the regression constants for the DT30_EE_LH(AF) and DT95_EE_HL materials are shown in Figure 6.3. The trend is very similar in terms of the slope of the regression line ($a - constant$) for both projects, however the intercept ($b - constant$) is material dependent. All other projects were then assumed to have $a - constant$ equivalent to the average of DT30_EE_LH(AF) and DT95_EE_HL. Using the unconditioned MC and dielectric values, the corresponding $b - constant$ for the other projects were computed.

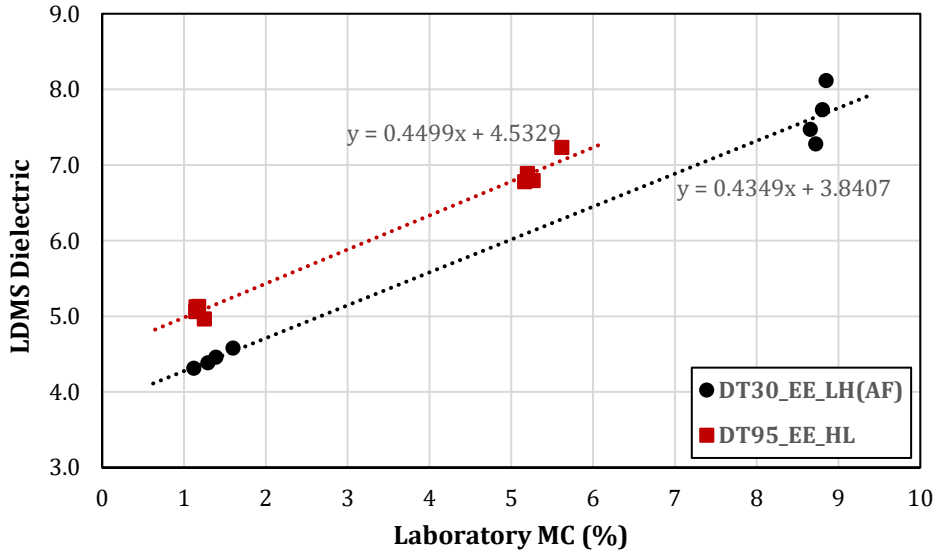

Figure 6.3 Dielectric and MC Relationship from Moisture Conditioning

This relationship was then used to estimate an initial dielectric value corresponding to the IMC, shown in Table 6.3. These values were assumed to be applicable to both field and laboratory measurements. The range of dielectric measured in the field and laboratory are also included in the table. Figure 6.4 shows a comparison of the dielectric evolution with respect to the DPS and LDMS.

Table 6.3 Summary of Dielectric Measurements

Project ID	IMC (%)	Estimated Initial Dielectric	DPS Dielectric Range (Measurement Days)	LDMS Dielectric Range (Measurement Days)
DT30_EE_LH(AF)	5.7	6.320	6.126 – 4.270 (Day 1 – 15)	4.767 – 4.015 (Day 1 -14)
DT95_EE_HL	3.0	5.883	4.289 – 4.203 (Day 1 – 3)	5.126 – 4.375 (Day 1 -14)
DT75_EE_HL(AF)	3.4	6.458	4.306 – 4.078 (Day 3 – 12)	5.554 – 4.877 (Day 1 -10)

DT28_FA_HL	3.4	6.243	5.012 – 4.814 (Day 1 – 7)	5.570 – 4.924 (Day 1 -10)
BC08_EE_LL	3.5	5.580	3.614 – 3.525 (Day 0 – 9)	4.740 – 3.895 (Day 1 -14)
BC11_EE_LH	4.9	6.446	5.082 – 3.834 (Day 0 – 9)	5.011 – 3.924 (Day 1 -14)

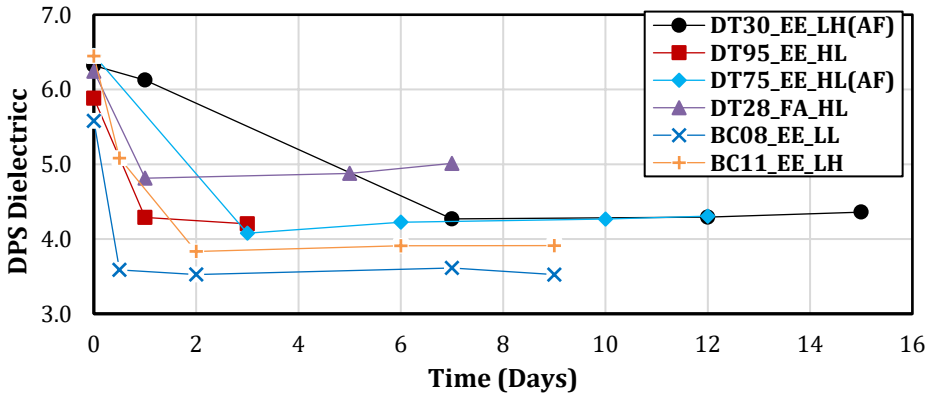

(a)

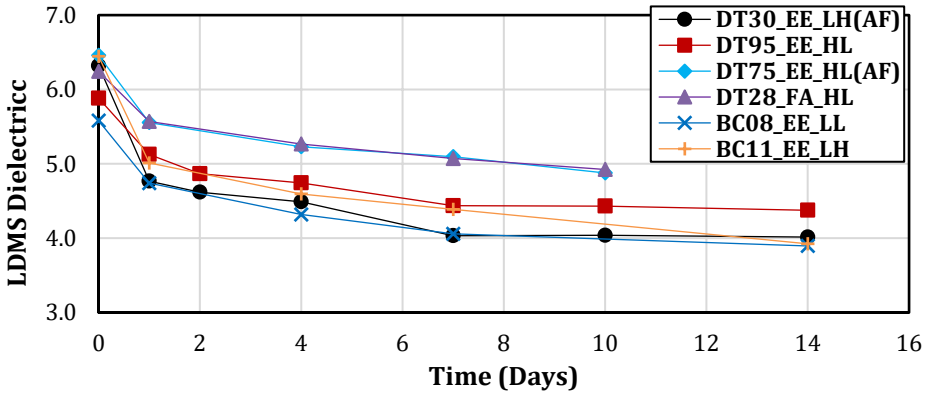

(b)

Figure 6.4 Dielectric Evolution: (a) DPS (b) LDMS

The measured dielectric values between the DPS and LDMS are inconsistent for the DT75_EE_HL(AF) project. This was expected as researchers were only able to sample RAP prior to crushing, and hence the material evaluated in the lab was not representative of the as-placed gradation. There are also less pronounced discrepancies in dielectric values measured in some of the other projects. However, these can be attributed to the differences in measurement methods. The trend in the DPS results confirm that all projects, except DT30_EE_LH(AF), may have attained an equilibrium moisture condition in the field by Day 3. This seems reasonable as among all the study projects, DT30_EE_LH(AF) had the highest IMC. The LDMS measurements follow similar trend with the gravimetric measurements. In the laboratory, most of the projects show relatively stable LDMS measured dielectric values by Day 7. However, it appears that DT75_EE_HL(AF), DT28_FA_HL and BC11_EE_LH had not entirely stabilized by their last day of testing. More diagnostic analysis may be required to ascertain if this observation is related to MC difference. Ultimately, the presented data suggests that equilibrium moisture condition may be achieved faster in the field compared to the controlled laboratory environmental curing conditions. The likelihood of this however decreases as the IMC increases.

6.1.3 Relationship between Moisture Content and Dielectric

It was established in the previous section that an increase in MC results in an increase in material dielectric. However, the resultant dielectric values are material dependent. Therefore, to holistically investigate a relationship between MC and dielectric, the subsequent values were normalized by computing the change from the IMC and dielectric measurements. Figure 6.5 shows that there exists a linear relationship between the change in MC and change in material dielectric, irrespective of the CIR material or project.

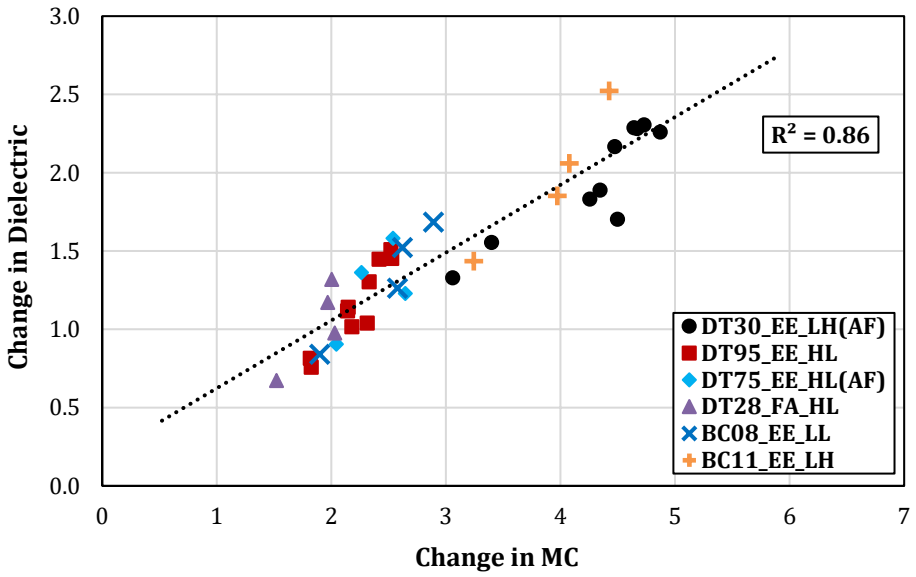

Figure 6.5 Relationship between Change in MC and Change in Dielectric

6.2 MECHANICAL PROPERTY EVOLUTION WITH CURING

6.2.1 Correlation between Field Measured Properties

The light weight deflectometer (LWD) and rapid compaction control device (RCCD) were employed to monitor the evolution of mechanical properties in the field. Both measurements were collected concurrently. The modulus of the of the CIR layers were estimated using the LWD. To account for temperature susceptibility of the CIR material, the modulus values were corrected to a reference temperature of 35°C (E_{35}). The RCCD measured the penetration depth of a penetrometer through the CIR layer. Currently, there is no established temperature correction for the RCCD measurements. Figure 6.6 shows that there is a fair logarithmic correlation between the uncorrected LWD modulus and RCCD penetration depth. The plotted values are an average of the measured points from each testing day. The RCCD detects a greater change in the mechanical property during early stages of curing as opposed to later stages while the LWD continues to detect pronounced changes at later stages.

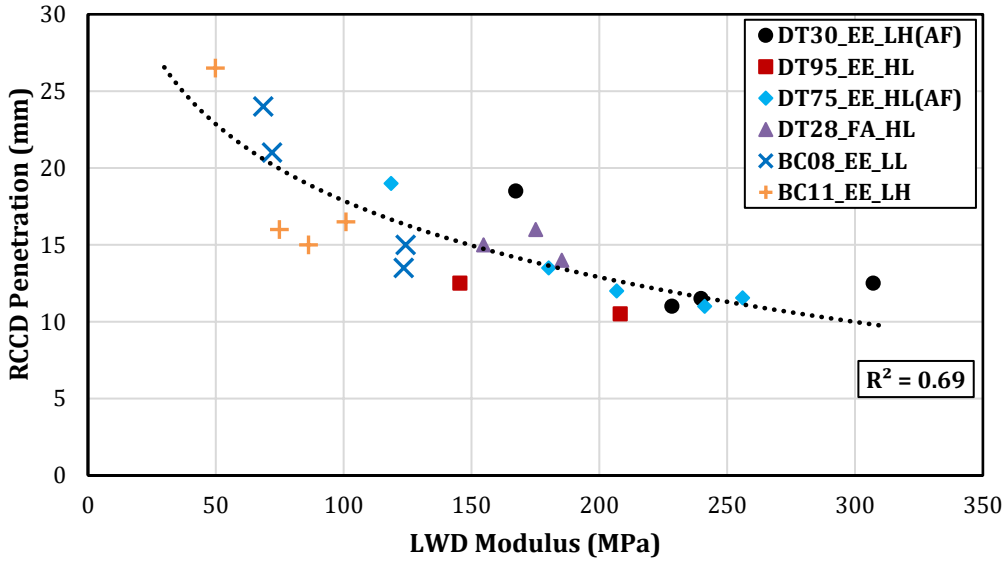

Figure 6.6 Correlation between LWD and RCCD Measurements

6.2.2 Correlation between Laboratory Measured Properties

Mechanical property evolution was monitored in the lab using resilient modulus (M_R) and indirect tensile strength (ITS) tests. Figure 6.7 also shows that there is a relatively strong linear relationship between the M_R and ITS results.

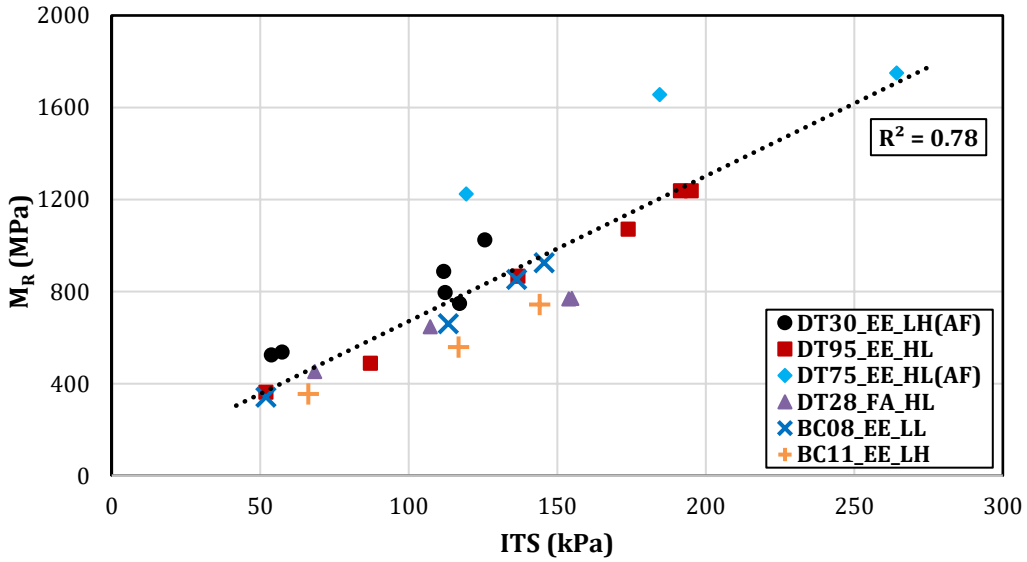

Figure 6.7 Correlation between M_R and ITS Results

6.2.3 Comparison of Field and Laboratory Mechanical Property Evolution

Following the findings from the previous subsections, only the LWD and ITS measurements are used to compare the mechanical property evolution with time. Past researchers have shown the applicability of the Michaelis-Menten (MM) model in representing the rate at which CIR mixtures properties evolve over time (Graziani et al., 2017; Graziani et al., 2018). Therefore, the MM model was fit to both the field and laboratory data. The MM model is a nonlinear model that describes an asymptotic evolution of the measured response as a function of time, through the evaluation of two parameters (y_A and K_C) as shown in equation 3.3:

$$y(t) = \frac{y_A \cdot t}{K_c + t} \tag{3.3}$$

Where:

y_A = Asymptotic value of mechanical property
K_C = Curing time required to achieve 50% of y_A
t = Curing time variable
$y(t)$ = Mechanical property variable being evaluated

Figure 6.8 and Figure 6.9 show examples of how the MM model fit both the field (LWD) and laboratory (ITS) measured data. Model fitting was done by transforming the model equations into a linear form using logarithmic transformation and method of least squares was used for optimization. The determined MM model parameters for each case are listed in Table 6.4. It is evident in the DT28_FA_HL project that there is a seemingly poor fit with the MM model. However, this is because the properties had almost stabilized prior to LWD testing and not an indication of inapplicability of the model.

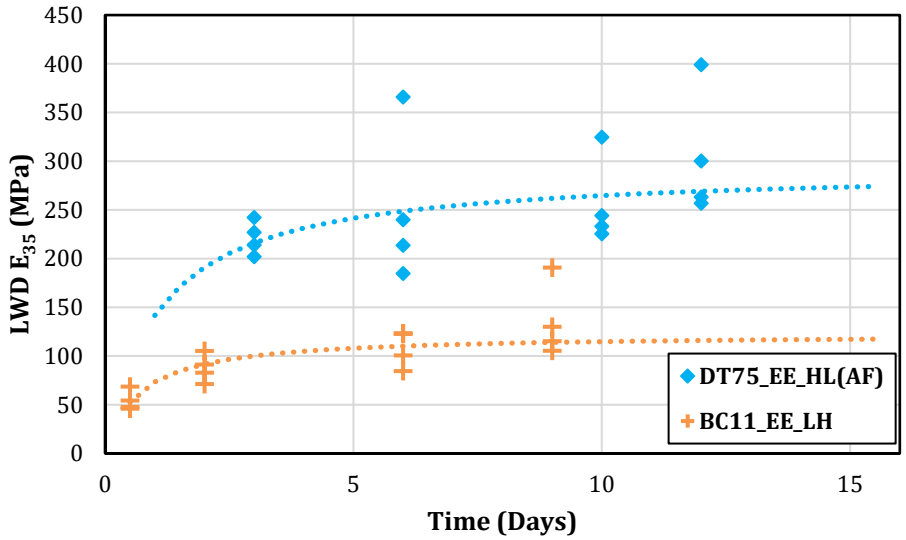

Figure 6.8 Select Example: Field Data MM Model Fitting

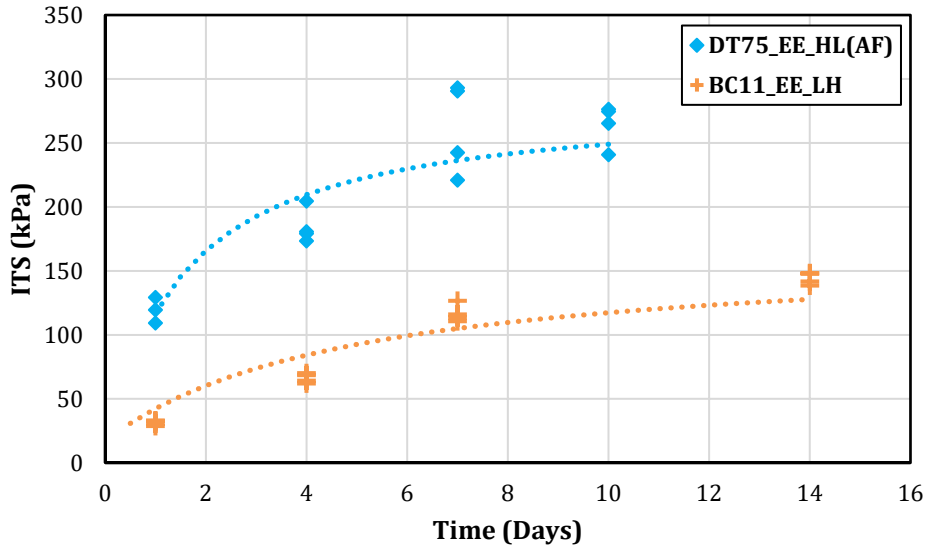

Figure 6.9 Select Example: Laboratory Data MM Model Fitting

Table 6.4 Fitted MM Model Parameters

Project ID	LWD Data			ITS Data		
	y_A	K_C	R^2	y_A	K_C	R^2
DT30_EE_LH(AF)	274	0.50	0.56	125	1.46	0.60
DT95_EE_HL	223	0.63	0.44	276	4.44	0.92
DT75_EE_HL(AF)	293	1.07	0.22	285	1.43	0.90
DT28_FA_HL	231	0.03	0.01	169	1.51	0.92
BC08_EE_LL	122	0.25	0.46	180	2.50	0.95
BC11_EE_LH	122	0.67	0.80	166	4.39	0.97

Figure 6.10 shows a comparison of the mechanical property evolution with respect to the LWD and ITS results. Only the MM model fit of the raw data are plotted for clearer depiction of the trend.

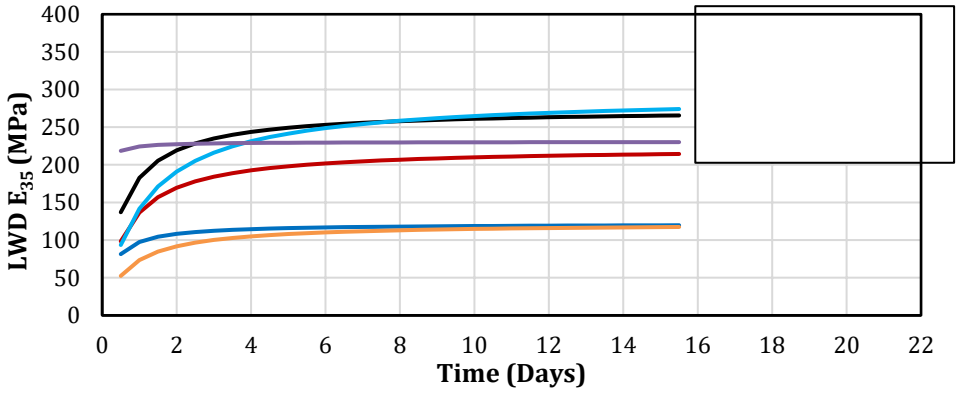

(a)

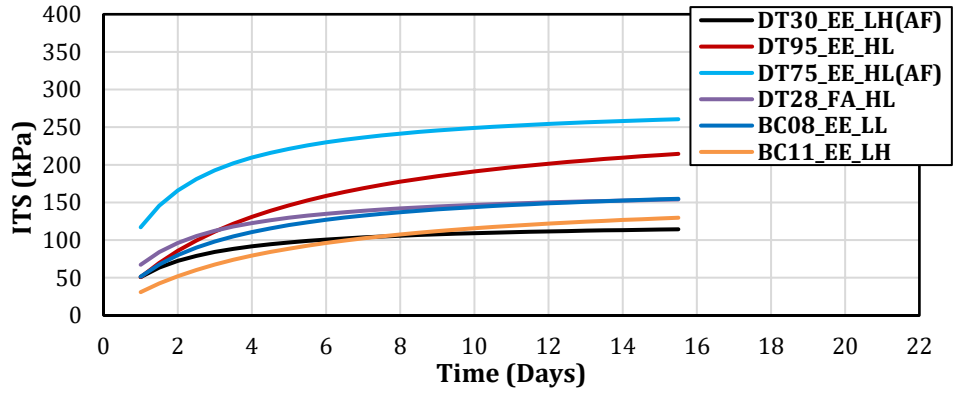

(b)

Figure 6.10 Mechanical Property Evolution: (a) Field LWD (b) Laboratory ITS

The ranking of the projects based on measured mechanical property significantly differ between the field and laboratory. Higher LWD E_{35} values were consistently measured on the DT30_EE_LH(AF) and DT75_EE_HL(AF) projects. It is likely that this is the effect of the presence of active filler; and with rainfall, there is continued hydration. On the other hand, the ITS values were relatively higher for projects with higher density (DT75_EE_HL(AF) and DT95_EE_HL). Irrespective of the inconsistencies in the actual measured values, the primary goal of this comparison to evaluate the evolution of the field and laboratory mechanical properties with time. The K_C parameter (referring to the curing time to achieve 50% of the final mechanical property) can be applicable in this regard for comparing the rate at which the properties evolve; the higher the K_C parameter, the slower the curing evolution. The K_C parameter is used as an example because it is readily obtainable from fitting the MM model. The information presented in Table 6.4 shows that the mechanical properties generally evolve faster in the field as opposed to the controlled laboratory environmental conditions. Therefore, researchers explored a possible correlation between the curing evolution in field and the laboratory using the K_C parameter. Figure 6.11 shows that excluding the points highlighted in red, there exists a very strong relationship between field- and laboratory-determined K_C parameter. These two points represent the projects that employed active filler. It is likely that these points do not correlate because of the influence of rain in further hydrating the active filler beyond the design target strength, as this is not captured in the laboratory. This relationship can be still applied to projects that employ active filler, but the results are expected to be conservative. The relevance of this

relationship is that it may be helpful to account for other factors that may impact the curing process and are not fully incorporated in the laboratory experimental design. Although this relationship is established using K_C parameter, it could also be extended to any desired reference curing time (with respect to any percentage of the final mechanical property). The regression line will always be the same in terms of the slope, but the intercept will be unique to the reference curing time.

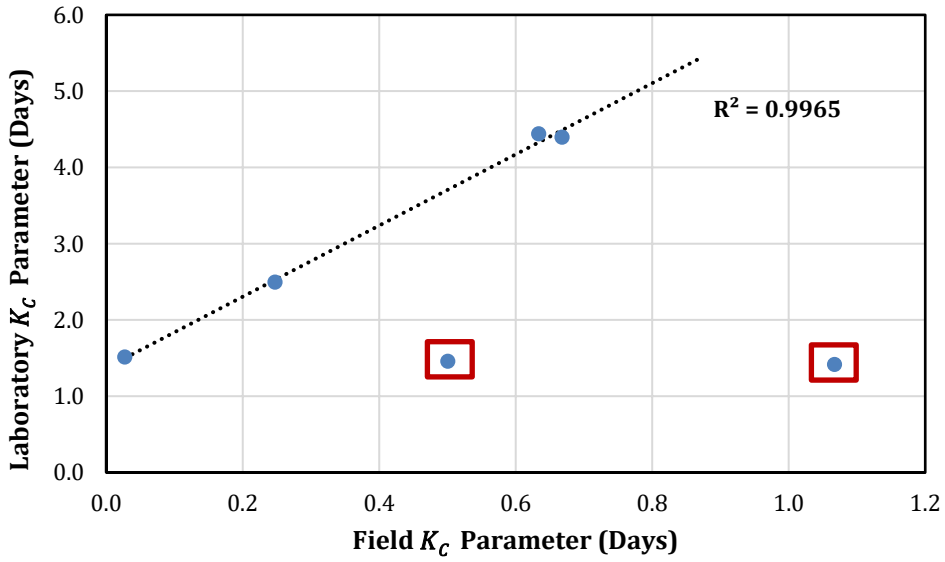

Figure 6.11 Correlation between Field- and Laboratory-determined K_C Parameter

6.3 SUMMARY OF FINDINGS FROM CORRELATION OF FIELD AND LABORATORY RESULTS

In order to facilitate the development of curing prediction model that can be translated into field conditions, it was paramount to develop a link between the laboratory and field curing conditions. Efforts made to develop this relationship relied on the as-built material and curing conditions of the six study projects that were replicated in the laboratory. Comparisons were done both in terms of the moisture content (MC) and mechanical property measurements. The significant findings from the investigation are as follows:

- NDMG tends to measure higher MC in the CIR layer in comparison to measurement obtained using the method of oven drying loose mixture. This highlights the need for MC correction of NDMG measurements if employed for CIR quality control. Irrespective of this, the trend in MC evolution with time seemed reasonable which confirms the applicability of NDMG for tracking in-situ curing.
- In general, the LDMS tend to measure higher dielectric values compared to the DPS. This can be attributed to the differences in measurement method, where the LDMS uses the time-of-flight method and the DPS uses surface reflectivity method. Regardless of the method used, it was observed that there is a strong linear relationship between changes in CIR material MC and dielectric which provides reliable results in tracking MC evolution in the laboratory and field.

- Results obtained using both NDMG and DPS suggest that equilibrium moisture condition may be achieved faster in the field compared to the controlled laboratory curing conditions employed in this study. The likelihood of this however decreases as the IMC increases.
- There is a good correlation between the LWD modulus and RCCD penetration depth measured on CIR layer. However, the RCCD has the propensity to detect more significant changes in mechanical property during early stages of curing while the LWD continues to detect pronounced changes at later stages.
- There is a relatively strong relationship between the M_R and ITS test results conducted on CIR materials. Given that the ITS test is simpler to conduct, the correlation can facilitate the estimation of material stiffness from ITS results.
- The Michaelis-Menten model provides a good fit to measured data in terms of modelling the mechanical property evolution of CIR materials as pertaining to curing.
- There is discrepancy in the ranking of the CIR study projects based on measured mechanical property in the field and laboratory. In the field, higher mechanical properties were consistently measured on projects that utilized active filler, which is an indication of continued hydration in presence of additional moisture from rainfall. In the laboratory, the mechanical property appears to be most significantly controlled by density.
- In agreement with the MC evolution, the mechanical property evolves faster in the field as opposed to the controlled laboratory environmental conditions. However, there is a very strong relationship between field and laboratory curing time which can facilitate the translation of the laboratory conditions to field conditions or vice versa. This relationship does not factor in the influence of rain, therefore conservative results are expected when active filler is used in the CIR mixture.

CHAPTER 7: CURING PREDICTION MODEL DEVELOPMENT

This chapter discusses all the analyses conducted to develop the curing prediction model. All statistical analyses are performed using the JMP Pro® statistical software. One of the significant findings from laboratory testing was that there is further gain in mechanical properties after the CIR mixtures have reached an equilibrium moisture condition. Additionally, from field results, the effect of rain was found to be negligible in increasing the MC of the CIR layer. Based on these findings, the prediction model focuses on curing as defined only in terms of mechanical property (ITS), as this is considered to be most critical.

7.1 DEFINITION OF VARIABLES

7.1.1 Predictor Variables

It was identified initially that there are several factors that may affect the evolution of curing of CIR materials. These may be grouped under the following categories:

- Climatic conditions – including variables such as temperature, humidity, wind speed, rainfall
- Component materials – including variables such as type and amount of stabilizing agent, type and amount of active filler, and initial moisture content
- Construction features – including variables such as compacted density, layer thickness, and condition of underlying layer

Ideally, to develop the prediction model, incorporating the effect of all the factors will require several field projects and/or laboratory trials with the capacity of simulating various conditions. However, due to feasibility, not all the above factors were investigated as part of this study. From a practical standpoint, only a subset of these factors was integrated in the experimental design. The factors included as model predictor variables and how they were incorporated are discussed as follows:

- **Stabilizer Type**: There are only two possible options of either engineered emulsion (EE) or foamed asphalt (FA). Fortunately, the sampled projects fully covered these options with one of the six field projects using FA while others used EE. Ideally, more projects incoporating FA would have been preferred to ensure full coverage of possible conditions. However, having at least one is adequate to incoporate the factor into the model. Since this variable is not numerical, to simplify the model, reference numbers were introduced as indicators (where EE is 0 and FA is 1).

- **Stabilizer Amount**: The six field projects contained varying stabilizer amount which were observed to be on the lower end of typical ranges used in stabilization. Therefore, a higher level within the range was specified in the lab to capture the contrast. Ultimately, the full range covered in the study was 1.5 – 3.5%.

- **Presence of Active Filler**: Among the field study projects, two included cement as active filler in the mix design while the remaining had no active filler. In addition to this, lime kiln dust (LKD) was sampled and included in the study. The initial intention was to have the active filler type and amout as variables, however, the data set is not robust enough for this. Therefore, the variable

was condensed to indicate either the absence or presence of active filler in each mixture. Similar to stabilizer type, reference numbers were introduced as indicators (where absence of active filler is 0 and presence of active filler is 1).

- **Initial Moisture Content:** The amount of added moisture per the mix design was similar for all projects using EE, while that of the project using FA was significantly higher. Whereas this information would have been simpler for use as variable, it is evident that weather conditions (especially rainfall) prior to construction can significantly alter the moisture conditions of the CIR layer. Therefore, to accurately characterize the moisture conditions, the initial moisture content (IMC) was determined following ASTM D2216. The IMC was used as the variable in the model to be more representative of the mixture characteristics. Overall, a range of 3.0 – 5.7% was covered.

- **Density**: In terms of CIR quality control, a target bulk density is typically specified. However, the specified bulk density is a function of the consitiuent materials and is unique to each project. Therefore, this variable was not treated as continuous. The variation in bulk density within each project was designated as either low or high. For instance, the as-built density for the DT30 project (1922kg/m^3 (120pcf)) was specified as low and the laboratory variation (2098kg/m^3 (131pcf)) was considered as high. The low variation is designated as -1 in the model, where as the high variation is designated as +1.

- **Curing Temperature**: Two different levels of this variable were considered. The target curing temperature for the controlled laboratory curing environment was set at either a low level of 15°C (59°F) or a high level of 25°C (77°F). Full details on why these two temperatures were chosen are provided in chapter 3. Ultimately, for better accuracy, sensors were installed to measure and record any possible deviations from the target temperature. Subsequently, the average of the recorded data through the curing period was determined and used as the model variable. This covered a range of 15 – 26°C.

- **Curing Relative Humidity**: This variable also relied on sensor measurements in the laboratory. Similar to the curing temperature, the average of the recorded data through the curing period was determined and used as the model variable. This ranged between 12 – 60%.

7.1.2 Response Variables

The goal of the prediction model is to calculate the time needed for necessary curing before allowing placement of the wear course. Having established the curing factors, it is important to define the response variable (variable being predicted) that characterizes the curing time. However, one challenge is how to define sufficient curing. It is acknowledged by the researchers that this may be subjective depending on the project. Therefore, three different alternatives were explored for the purpose of the study; sufficient curing was defined in terms of 70%, 80% and 90% of the final ITS. The final ITS values (y_A) were determined based on the MM model discussed in Chapter 6. Subsequently, the time it takes to achieve the target values (70%, 80% and 90% of y_A) were estimated based on the MM model equations and attributed as the response variables.

7.2 MULTIPLE LINEAR REGRESSION MODELLING

The aim of prediction model development is to identify the relationship between the predictor and response variables to be able to forecast future outcomes. Regression analysis provides a basis to determine the most suitable predictor variables for this purpose. In chapter 5, it was possible to isolate and graphically identify main effects of the curing factors. However, regression analysis provides a robust insight on not only main effects but also possible interaction between the various factors. Particularly, multiple linear regression analysis was chosen because of its computational efficiency. However, a limitation of this statistical technique is that it assumes the relationship between the predictor and response variables to be linear.

Polynomial models are the most commonly used models in regression to characterize a response. Past research has shown that low-degree polynomials are applicable over a limited-size region of interest (Cornell and Montgomery, 1996). Therefore, for this study, a full quadratic model (FQM) was explored. This is also referred to in JMP Pro® as a response surface. This model contains the main effects, all two-way interactions, and quadratic effects. A simplified version of this model with only two experimental factors is shown in equation 4.1:

$$Y = \beta_0 + \beta_1 X_1 + \beta_2 X_2 + \beta_{11} {X_1}^2 + \beta_{22} {X_2}^2 + \beta_{12} X_1 X_2 \quad (7.1)$$

Where:

Y	=	Response Variable
$X_1 \; and \; X_2$	=	Experimental factors
β	=	Model Coefficients

Given the amount of data points that are available, stepwise regression was identified to be applicable in determining the most significant factors that are to be included into the model, using the forward selection criteria. The forward selection criteria begin with the assumption that there are no predictor variables in the model, variables that cause the largest increase in R^2 (squared correlation between the observed response values and the predicted values by the model) for the model are then added sequentially . This continues until either all variables are in the model or variables not in the model would not significantly increase the R^2. Three different stopping rules that determine when to end the stepwise regression process were explored:

- P-value threshold: This rule specifies a minimum p-value that could be considered statistically significant. Therefore, only variables with p-value below the specified minimum are entered into the model. There is lack of consensus by statisticians as to what p-value to be specified in practice. However, p-value of 0.25 is commonly used and was employed for this analysis.
- Minimum AICc: AICc is the Akaike's Information Criteria which was corrected for smaller sample size. This is a metric that can be used for evaluating various models. It penalizes the inclusion of additional variables to a model by increasing the error. Generally, models with lower AICc are preferred. The minimum AICc rule therefore stops the stepwise regression when a model with the lowest AICc is obtained.

- Minimum BIC: BIC is the Bayesian information criteria. It is similar to the AICc but with a stronger penalty for the inclusion of additional variables. The rule also stops the stepwise regression process when the lowest BIC is obtained.

Table 7.1 shows details of the models developed using the three stopping rules. Time to achieve 70% of y_A is used as the baseline response variable (all other variations are included in Appendix E). The models are evaluated using three different metrics: number of variables, R^2 and root mean square (RMSE). Ideally, a model that generates the lowest number of predictor variables and least amount of error (higher R^2 and lower RMSE) is desirable. The model generated using the Minimum AICc rule has just two variables but a high prediction error. The model generated using the P-value stopping rule seemed to generate reasonable number of variables with satisfactory prediction error. However, the model generated using the Minimum BIC has only two additional variables which significantly improves the prediction error, and therefore is recommended.

Table 7.1 Stepwise Regression Model Comparison

Evaluation Metric	P-value	Minimum AICc	Minimum BIC
Number of Variables	8	2	11
R^2	0.73	0.42	0.84
RMSE	1.84	2.30	1.56

The selected model parameters are presented in Table 7.2. The second column presents estimated model coefficients, while the last column presents the overall effectiveness test for the selected predictor variables. The effectiveness test is done based on a significance level of 0.05; for each variable, a p-value less than 0.05 is considered statistically significant. The color coding is used to indicate the variables that are effective.

In terms of the main effects (experimental factors), the curing relative humidity (within the range considered in the experiment) was not originally included in the model as it did not seem to have a significant effect in prediction. Following the stepwise regression process, it can be observed that the effect of initial moisture content, density and curing temperature do not seem to be statistically significant on their own. However, there are significant two-way interactions with these factors which means that their effects are interdependent on other factors. These agree with some of the findings reported in chapter 5. In total, there are 5 two-way interactions and no quadratic effect included in the model.

Table 7.2 Selected Model (Time to achieve 70% of Final ITS) Parameters

Predictor Variables	Estimate	Std Error	t Ratio	Prob>|t|
Intercept	9.271	2.537	3.65	0.0029
Stabilizer Type	-4.809	1.224	-3.93	0.0017
Stabilizer Amount	-1.374	0.618	-2.22	0.0446
Active Filler	-3.534	0.697	-5.07	0.0002
Initial Moisture Content	0.065	0.427	0.15	0.8807
Density	0.080	0.388	0.21	0.8390
Curing Temp.	0.012	0.071	0.16	0.8716
(Stabilizer Type-0.16)*(Stabilizer Amount-2.528)	6.523	2.385	2.74	0.0170
(Stabilizer Type-0.16)*(Initial Moisture Content-4.06)	2.452	1.229	1.99	0.0675
(Stabilizer Amount-2.528)*(Initial Moisture Content-4.06)	-3.578	0.786	-4.55	0.0005
(Active Filler-0.52)*(Curing Temp.-20.823)	-0.579	0.151	-3.84	0.0021
(Density+0.04)*(Curing Temp.-20.823)	0.326	0.115	2.82	0.0143

Significance Level: Red color – p-value less than 0.05 but greater than 0.01; Orange color – p-value less than 0.01

7.3 MODEL EQUATIONS AND EXAMPLE CALCULATIONS

The stepwise regression analysis was used to identify the most effective predictor variables that contribute to the curing prediction model. The full model (with respect to time to achieve 70% of final ITS) with the determined coefficients is given in equation 7.2:

$$\begin{aligned} Y = 9.271 &+ (-4.809 \times X_1) + (-1.374 \times X_2) + (-3.534 \times X_3) + (0.065 \times X_4) + (0.080 \times X_5) \\ &+ (0.012 \times X_6) + \big(6.523 \times (X_1 - 0.16) \times (X_2 - 2.528)\big) \\ &+ \big(2.452 \times (X_1 - 0.16) \times (X_4 - 4.06)\big) + \big(-3.578 \times (X_2 - 2.528) \times (X_4 - 4.06)\big) \\ &+ \big(-0.579 \times (X_3 - 0.52) \times (X_6 - 20.823)\big) \\ &+ \big(0.326 \times (X_5 + 0.04) \times (X_6 - 20.823)\big) \end{aligned} \quad (7.2)$$

Where:

Y = Time to achieve 70% of final ITS (y_A)
X_1 = Stabilizer Type (EE = 0; FA = 1)
X_2 = Stabilizer Amount (%)
X_3 = Active Filler (No = 0; Yes = 1)
X_4 = Initial Moisture Content (%)
X_5 = Density (Low Density = -1; High Density = 1)
X_6 = Curing Temperature (°C)

Note that the equation 7.2 is used to estimate the time in terms of laboratory curing conditions. However, to translate the estimated time into field curing conditions, the linear relationship established in chapter 6 can be employed using equation 7.3:

$$A = (0.214 \times Y) - 0.680 \quad (7.3)$$

Where:

A = Field Curing Time to achieve 70% of final ITS

To demonstrate the use of the equation, two different cases (inputs and results shown in Table 7.3) are considered:

- an actual material and curing conditions used to develop the model (DT95 as-built)
- a hypothetical material and curing conditions within the range used for model development

Table 7.3 Example Calculations

Input Variables	DT95 As-built Conditions	Hypothetical Condition
Stabilizer Type	EE (0)	EE (0)
Stabilizer Amount	2.0 %	3.0 %
Active Filler Amount	0 %	0 %
Initial Moisture Content	3.0 %	4.5 %
Density	131pcf – High (1)	120pcf – Low (-1)
Average Curing Temperature (°C)	25.6	25
Results		
Estimated Time (Laboratory)	9 days	4 days
Estimated Time (Field)	2 days	1 day
Actual Timing of Overlay Placement	5 days	N/A

Table 7.3 also includes the actual timing for overlay placement in the DT95 project. In comparison, the model estimation shows that by the time the DT95 project was overlaid, it should have achieved at least 70% of the final mechanical property.

As indicated earlier, this model is based on the premise that the effect of rainfall event is negligible to the curing process. Going from laboratory and field observations, it is apparent that in an event of rainfall, the moisture does not infiltrate the CIR layer. Since the moisture is restricted to the surface, evaporation is quicker, and the moisture could dry up within a day. Therefore, it is recommended that in an event of rainfall within the estimated timeframe, the time should be increased by **1 day after the rain stops**.

7.4 SUMMARY OF CURING PREDICTION MODEL DEVELOPMENT

A dataset generated in the laboratory, consisting of 25 different CIR material and curing conditions, was used to develop a curing prediction model. The goal of the prediction model is to be able to calculate the time needed for necessary curing before allowing placement of the wear course. For this sufficient curing was defined using three different alternatives: time it takes to achieve 70%, 80% and 90% of final ITS. The factors incorporated include stabilizer type and amount, presence of active filler, initial MC, compacted density, curing temperature and RH. Multiple linear regression using a full quadratic model was employed because of its broad applicability. Stepwise regression analysis using forward selection criteria was conducted which facilitated the identification of the most significant predictor variables to be included into the model. Among the experimental factors explored, only the curing RH did not seem to have any effect and hence did not contribute to the final model equation. Ultimately, the model consists of 11 predictor variables (6 main effects, 5 two-way interactions and no quadratic effect). The model is of the

form of equation 7.4. A summary of the estimated model coefficients for each curing alternative is presented in Table 7.4.

$$Y = \beta_0 + \beta_1 X_1 + \beta_2 X_2 + \beta_3 X_3 + \beta_4 X_4 + \beta_5 X_5 + \beta_6 X_6 + \beta_{12} X_1 X_2 + \beta_{14} X_1 X_4 + \beta_{24} X_2 X_4 + \beta_{36} X_3 X_6 + \beta_{56} X_5 X_6 \quad (7.4)$$

Where:

Y = Time to achieve target value (70%, 80% or 90% of final ITS)
X_1 = Stabilizer Type (EE = 0; FA = 1)
X_2 = Stabilizer Amount (%)
X_3 = Active Filler (No = 0; Yes = 1)
X_4 = Initial Moisture Content (%)
X_5 = Density (Low Density = -1; High Density = 1)
X_6 = Curing Temperature (°C)
β = Model Coefficients

Table 7.4 Estimated Model Coefficients

Model Coefficients	% of Final ITS		
	70	80	90
β_0	9.271	15.894	35.761
β_1	-4.809	-8.244	-18.549
β_2	-1.374	-2.355	-5.299
β_3	-3.534	-6.058	-13.630
β_4	0.065	0.112	0.252
β_5	0.080	0.138	0.310
β_6	0.012	0.020	0.045
β_{12}	6.523	11.183	25.161
β_{14}	2.452	4.203	9.458
β_{24}	-3.578	-6.133	-13.800
β_{36}	-0.579	-0.992	-2.232
β_{56}	0.326	0.558	1.256

The model provides time estimate based on laboratory conditions and can be translated to field conditions using a linear regression relationship of the form shown in equation 7.5. The regression coefficients (m and c) for each curing alternative is shown in Table 7.5

$$Field\ Curing\ Time\ = (m \times Lab\ Curing\ Time)\ -\ c \quad (7.5)$$

Table 7.5 Laboratory to Field Regression Coefficients

Regression Coefficients	% of Final ITS		
	70	80	90
m	0.214	0.214	0.214
c	0.680	1.166	2.624

Subsequently, to accommodate for events of rainfall during the curing period, it was recommended that **1 day** be added the estimated time to ensure sufficient drying of surface moisture.

CHAPTER 8: CONCLUSIONS AND RECOMMENDATIONS

This chapter summarizes the effort from this research study and lists the key conclusions. Implementation steps for the research outcomes as well as recommendation for future extension are also included.

8.1 SUMMARY

A thorough literature review was conducted regarding the state of the art and state of the practice for quality control and acceptance tools to assess the curing extent and performance of CIR pavements. A survey was developed to collect information on current practices that are used in state and local agencies within Minnesota to control curing and determine timing of opening to traffic and application of overlay. Ultimately, the literature review was necessary to help to establish information such as factors affecting curing of CIR, laboratory curing methods and conditions, current practices for control of curing/allowing traffic on CIR, critical CIR performance characteristics and test methods used to measure them, and existing tools for in-situ determination of curing extent.

This study used a case-study based approach to evaluate curing, where six CIR pavement projects were selected for in-situ testing, constituent material sampling, and collection of field data. A series of in-situ tests were assessed based on their ability to detect changes in material properties as curing progress. The key findings from field evaluation have led to the recommendation that curing be evaluated in terms of mechanical property as opposed to relying on moisture content measurements.

Laboratory tests were conducted to generate experimental data, which were used in developing a curing prediction model. The model incorporated a limited number of variables including stabilizer type and amount, presence of active filler, IMC, compacted density, and curing temperature. It also provided some options of defining sufficient curing based on criticality of the project. Ultimately, this research provided a tool for pavement engineers and practitioners to reliably predict the recommended time (as a function of mechanical property) for placing an overlay on CIR layers.

8.2 CONCLUSIONS

Based on the technical tasks undertaken as part of this research study, key conclusions are highlighted as follows:

- The dielectric profiling system (DPS) can successfully be applied in tracking the early age moisture content evolution of CIR pavement during the curing period, with an additional benefit of providing a more extensive spatial coverage as opposed to spot measurements.
- The rapid compaction control device (RCCD) is the most promising tool for evaluating CIR mechanical response in curing duration, due to its better precision and simplicity. However, further research is recommended to better understand how the measurement could be influenced by temperature and develop threshold values.

- CIR continues to gain mechanical property even after equilibrium moisture condition has been reached. This finding suggests that moisture content measurement may not be a reliable method for determining extent of CIR curing.
- There is enough evidence that suggests that rainfall does not significantly alter the moisture content of CIR pavements and as such may not necessarily delay the curing process.
- The Michaelis-Menten model can adequately characterize the mechanical property evolution of CIR materials as pertaining to curing.
- Curing in CIR is mostly influenced by following factors: stabilizer type and amount, presence of active filler, initial MC, compacted density, and curing temperature.

8.3 RESEARCH IMPLEMENTATION

The performance prediction equations were programmed in a user-friendly computer tool (Excel spreadsheet). The tool is included in Appendix E together with a detailed user-guide. This tool automatically provided an estimate of when to place the wearing course. Based on the criticality of the project, there was an option for the user to choose timing based on a desired level of structural capacity. The required inputs include stabilizer type and amount, presence of active filler, initial moisture content, in-situ density and curing temperature.

The following steps are required to gather required input information for application of the prediction model:

- **Job Mix Formula**: Practically, mix design data will suffice for determining the material attributes. This would include information such as stabilizer type and amount, if active filler is used, and target density for the project. However, it is well known that during CIR construction, slight changes are typically made to the mix design. For better accuracy, these nuances could be accommodated in the inputs but are not required as they may not significantly change the estimated time.
- **Quality Control Data**: The project QC data will be very helpful in providing information regarding the initial MC of the CIR mixture. This prediction model relies on the gravimetric initial MC determined through oven drying the loose mixture. Therefore, it is recommended that the CIR mixture be sampled during construction and sealed for determination of MC in the QC laboratory. This is feasible since most CIR projects already require the sampling of RAP/CIR mixture for verification of gradation and binder content. Additionally, the NDMG is currently employed in verifying the as-placed density of the layer, but it also has the capacity to measure the volumetric MC of the layer. Alternatively, this information may be used as input, but note that it will require a conversion from volumetric to gravimetric MC. This conversion factor can be incorporated in the prediction model tool. It was highlighted in Chapter 4 that NDMG has the propensity to measure a higher MC. Hence, it may lead to conservative time estimates.
- **Weather Information**: The curing temperature input will require weather information from the closest weather station to the specific project. The time period of interest is subjective, thus the

daily temperature should be averaged over the time period and included as the input. Additionally, rain events during the period of interest should be noted.

- **Expert Judgement**: From a practical standpoint, some of the input variables could rely on expert judgement. Density is unique to each project and will require a guided decision by the user whether it should be considered as low or high. Furthermore, it is apparent that most CIR construction is done during the warmest period of the construction season. The expected average daily temperature during this period is typically close to 25°C (77°F). This could be left as a default value unless estimated otherwise. Ultimately, expert judgement is required on the definition of sufficient curing. Three alternative model equations are provided relating to sufficient curing as defined in terms of 70%, 80% and 90% of the final ITS.

This tool could be a stand-alone or coupled with in-situ testing for verification. A tiered approach as summarized in Table 8.1 may be employed to implement this tool. A higher tier relates to better reliability. Pavement engineers and practitioners are recommended to select an option based on project criticality. It is, however, noteworthy that the recommended companion in-situ tests may require an establishment of threshold/target values that may be used as reference. This is beyond the scope of this study and further research is recommended.

Table 8.1 Recommendation for Implementing Developed Tool (Prediction Model)

Tier	Recommendation	Comments
1	Spreadsheet	Overlay could be placed on the recommended day. This tier provides the lowest reliability. May be most applicable to local roads, which inherently experience low traffic.
2	Spreadsheet + RCCD	Upon the use of the spreadsheet to estimate curing time, supplementary RCCD testing could be done on the recommended day for verification. This approach is recommended for use in highways with intermediate traffic conditions, such as collector and minor arterial roadways.
3	Spreadsheet + RCCD + DPS	This tier may be most applicable in longer sections where the DPS may provide a more efficient way to evaluate the CIR pavements. RCCD testing could further be done in fewer locations that may be identified based on significant differences in dielectric values. This approach is recommended for use in roadways with high traffic volumes, such as, principal arterials and freeways.

8.4 RECOMMENDATIONS FOR FUTURE EXTENSION

Any developed model is only as good as the data used in its development. Therefore, there is potential to further enhance the precision of the developed prediction model. Ideally, doing this will require more field and laboratory experimental data. With the current dataset, there is also an alternative of exploring an innovative machine learning approach called self-validating ensemble modelling (SVEM). SVEM facilitates building and auto validating prediction models without having to split the limited dataset into

training and validation sets. Instead, SVEM incorporates a random weight re-sampling scheme into the experimental data. This procedure is an iterative process that fits several models to the data and model averaging is used to develop the final model. The intrinsic auto-validation component results in a more reliable model.

Due to feasibility, only factors that were possible to control in the laboratory were incorporated into the developed model in Chapter 7. This led to the correlation of laboratory and field curing conditions. However, for a higher reliability, the effect of these factors needs to be better understood either by incorporating more field projects and/or laboratory trials with the capacity of simulating such conditions. In addition, the range of the factors incorporated into the prediction model can be expanded beyond the current boundary conditions to obtain a more complete picture in terms of their effect.

Furthermore, since testing could only be done at a limited number of curing times, the developed model relied on the use of mathematical models from literature to define the full evolution of material properties with curing. The goodness of fit of the model to the experimental data varied based on conditions. Therefore, for better precision, additional validation and/or modification of these models may be required. This validation could be done by increasing the frequency of testing.

Lastly, the developed tool is currently set up such that there are only three choices for the final curing criterion used to determine the necessary time. Alternatively, a more holistic approach could be considered such that the model predicts the full curing evolution based on the provided inputs. This gives the user more variety of options to consider. From a pavement design perspective, the user could also specify a target mechanical property and assess the required curing time. Additionally, a lifecycle cost analysis could be incorporated that guides the decision-making process on the optimal mechanical property and time to achieve it.

The intended final product would provide a robust decision toolkit that can be easily implemented by state and local agencies across the U.S. to determine the optimal time to place an overlay on a CIR layer, both from a performance and lifecycle cost perspective.

REFERENCES

Apeagyei, A. K., & Diefenderfer, B. K. (2013). Evaluation of cold in-place and cold central-plant recycling methods using laboratory testing of field-cored specimens. *Journal of Materials in Civil Engineering, 25*(11), 1712-1720.

Arimilli, S., Jain, P. K., & Nagabhushana, M. N. (2016). Optimization of recycled asphalt pavement in cold emulsified mixtures by mechanistic characterization. *Journal of Materials in Civil Engineering, 28*(2), 04015132.

Asphalt Academy. (2019). *TG2 A guideline for the design and construction of bitumen emulsion and foamed bitumen stabilized materials*. Pretoria, South Africa: CSIR Built Environment.

Asphalt Institute & Asphalt Emulsion Manufacturers Association. (1979). *A basic asphalt emulsion manual.* Washington, DC: Department of Transportation, Federal Highway Administration.

Babagoli, R., Ameli, A., & Shahriari, H. (2016). Laboratory evaluation of rutting performance of cold recycling asphalt mixtures containing SBS modified asphalt emulsion. *Petroleum Science and Technology, 34*(4), 309-313.

Baghini, M. S., Ismail, A. B., Karim, M. R. B., Shokri, F., & Firoozi, A. A. (2017). Effects on engineering properties of cement-treated road base with slow setting bitumen emulsion. *International Journal of Pavement Engineering, 18*(3), 202-215.

Batista, F., Antunes, M., Mollenhauer, K., & McNally, C. (2012, June). Building blocks of best practice guide on cold in-place recycling. *Proceedings of 5th Eurasphalt & Eurobitume Congress,* Istanbul, Turkey.

Bessa, I. S., Almeida, L. R., Vasconcelos, K. L., & Bernucci, L. L. (2016). Design of cold recycled mixes with asphalt emulsion and Portland cement. *Canadian Journal of Civil Engineering, 43*(9), 773-782.

Betti, G., Airey, G., Jenkins, K., Marradi, A., & Tebaldi, G. (2017). Active fillers' effect on in situ performances of foam bitumen recycled mixtures. *Road Materials and Pavement Design, 18*(2), 281-296.

Bowering, R. H. (1970, April). Properties and behavior of foamed bitumen mixtures for road building. *Proceedings of the 5th Australian road research board conference* (pp. 38-57).

Bowering, R. H., & Martin, C. L. (1976). Performance of newly constructed full-depth foamed bitumen/crushed rock pavements. *Australian Road Research Board Conference Proc*eedings, *8.*

Budge, A. S., & Wilde, W. J. (2007). Monitoring curing of emulsion-stabilized roadways using the dynamic cone penetrometer. In *Soil and Material Inputs for Mechanistic-Empirical Pavement Design* (pp. 1-8).

Cardone, F., Grilli, A., Bocci, M., & Graziani, A. (2015). Curing and temperature sensitivity of cement–bitumen treated materials. *International Journal of Pavement Engineering, 16*(10), 868-880.

Chomicz-Kowalska, A., & Maciejewski, K. (2015). Multivariate optimization of recycled road base cold mixtures with foamed bitumen. *Procedia Engineering, 108,* 436-444.

Chou, C. P., Lin, Y. C., & Chen, A. C. (2017). Temperature adjustment for light weight deflectometer application of evaluating asphalt pavement structural bearing capacity. *Transportation Research Record*, *2641*(1), 75-82.

Čížková, Z., Šedina, J., Valentin, J., & d Engels, M. (2016). Laboratory experience with the application of monotonic triaxial test on the cold recycled asphalt mixes. *Proceedings of 6th Eurasphalt & Eurobitume Congress,* Prague, Czech Republic.

Cohen, E. H. U. D., Sidess, A. R. I. E. H., & Zoltan, G. A. B. R. I. E. L. (1989). Performance of a full-scale pavement using cold recycled asphalt mixture. *Transportation Research Record, 1228,* 88-93.

Cornell, J. A., & Montgomery, D. C. (1996). Interaction models as alternatives to low-order polynomials. *Journal of Quality Technology*, *28*(2), 163-176.

Covey, D. J. (2016). Evaluation of Oregon tack coat performance to reduce tracking and increase interlayer shear strength of asphalt pavements. (Master's Thesis, Oregon State University).

Cox, B. C., Howard, I. L., & Campbell, C. S. (2016). Cold in-place recycling moisture-related design and construction considerations for single or multiple component binder systems. *Transportation Research Record, 2575*(1), 27-38.

Cross, S. A. (1999). *Evaluation of cold in-place recycled mixtures on US-283* (KDOT Report No. KS-99-4). Topeka, KS: Kansas Dept. of Transportation, Research Branch.

Cross, S. A. (2003). Determination of Superpave® gyratory compactor design compactive effort for cold in-place recycled mixtures. *Transportation Research Record*, *1819*(1), 152-160.

Dal Ben, M., & Jenkins, K. J. (2014). Performance of cold recycling materials with foamed bitumen and increasing percentage of reclaimed asphalt pavement. *Road Materials and Pavement Design, 15*(2), 348-371.

Diefenderfer, B. K., Apeagyei, A. K., Gallo, A. A., Dougald, L. E., & Weaver, C. B. (2012). In-place pavement recycling on I-81 in Virginia. *Transportation Research Record, 2306*(1), 21-27.

Du, S. (2015). Performance characteristic of cold recycled mixture with asphalt emulsion and chemical additives. *Advances in Materials Science and Engineering, 2015,* 1-8.

Fu, P., Jones, D., Harvey, J. T., & Bukhari, S. A. (2009). Laboratory test methods for foamed asphalt mix resilient modulus. *Road Materials and Pavement Design, 10*(1), 188-212.

Fu, P., Jones, D., Harvey, J. T., & Halles, F. A. (2010). Investigation of the curing mechanism of foamed asphalt mixes based on micromechanics principles. *Journal of Materials in Civil Engineering, 22*(1), 29-38.

Galehouse, L., & Chehovits, J. (2010). Energy usage and greenhouse gas emissions of pavement preservation processes for asphalt concrete pavements. *Compendium of Papers from the First International Conference on Pavement Preservation*, (pp 27-42), Newport Beach, CA.

Gao, L., Ni, F., Charmot, S., & Luo, H. (2014). Influence on compaction of cold recycled mixes with emulsions using the superpave gyratory compaction. *Journal of Materials in Civil Engineering*, *26*(11), 04014081.

García, A., Lura, P., Partl, M. N., & Jerjen, I. (2013). Influence of cement content and environmental humidity on asphalt emulsion and cement composites performance. *Materials and Structures, 46*(8), 1275-1289.

Godenzoni, C., Cardone, F., Graziani, A., & Bocci, M. (2016). The effect of curing on the mechanical behavior of cement-bitumen treated materials. *8th RILEM International Symposium on Testing and Characterization of Sustainable and Innovative Bituminous Materials* (pp. 879-890). Dordrecht, Netherlands: Springer.

Godenzoni, C., Graziani, A., & Perraton, D. (2017). Complex modulus characterization of cold-recycled mixtures with foamed bitumen and different contents of reclaimed asphalt. *Road Materials and Pavement Design, 18*(1), 130-150.

Gonzalez, A., Cubrinovski, M., Pidwerbesky, B., & Alabaster, D. (2009). Performance strength and deformational characteristics of foamed bitumen pavements. *2009 AAPA Flexible Pavements Conference* (pp. 1-20).

Graziani, A., Godenzoni, C., Cardone, F., & Bocci, M. (2016). Effect of curing on the physical and mechanical properties of cold-recycled bituminous mixtures. *Materials & Design*, 95, 358-369.

Graziani, A., Iafelice, C., Raschia, S., Perraton, D., & Carter, A. (2018). A procedure for characterizing the curing process of cold recycled bitumen emulsion mixtures. *Construction and Building Materials, 173,* 754-762.

Grilli, A., Graziani, A., & Bocci, M. (2012). Compactability and thermal sensitivity of cement–bitumen-treated materials. *Road Materials and Pavement Design, 13*(4), 599-617.

Grilli, A., Graziani, A., Bocci, E., & Bocci, M. (2016). Volumetric properties and influence of water content on the compactability of cold recycled mixtures. *Materials and Structures, 49*(10), 4349-4362.

Grilli, A., Raschia, S., Perraton, D., Carter, A., Rahmanbeiki, A., Kara De Maeijer, P., Lo Presti, D., Airey, G., Ogbo, C., Dave E., & Tebaldi, G. (2020). Experimental Investigation on Water Loss and Stiffness of CBTM

Using Different RA Sources. *Proceedings of the RILEM International Symposium on Bituminous Materials*, ISBM Lyon 2020, Lyon, France.

Guatimosim, F. V., Vasconcelos, K. L., Bernucci, L. L., & Jenkins, K. J. (2018). Laboratory and field evaluation of cold recycling mixture with foamed asphalt. *Road Materials and Pavement Design, 19*(2), 385-399.

He, G. P., & Wong, W. G. (2008). Effects of moisture on strength and permanent deformation of foamed asphalt mix incorporating RAP materials. *Construction and Building Materials, 22*(1), 30-40.

Hodgkinson, A., & Visser, A. T. (2004, September). The role of fillers and cementitious binders when recycling with foamed bitumen or bitumen emulsion. *8th Conference on Asphalt Pavements for Southern Africa (CAPSA'04)* (pp. 12-16).

Hoegh, K., Roberts, R., Dai, S., & Zegeye-Teshale, E. (2019). Toward core-free pavement compaction evaluation: An innovative method relating asphalt permittivity to density. *Geosciences, 9*(7), 280.

Hoegh, K., Steiner, T., Zegeye-Teshale, E., & Dai, S. (2020). Minnesota Department of Transportation case studies for coreless asphalt pavement compaction assessment. *Transportation Research Record*, *2674*(2), 291-301.

Islam, M. R., Rivera, J. A., & Kalevela, S. A. (2018). *Dynamic modulus of cold-in-place recycling (CIR) material* (No. CDOT 2018-13). Denver, CO: Colorado Dept. of Transportation, Research Branch.

Isola, M., Betti, G., Marradi, A., & Tebaldi, G. (2013). Evaluation of cement treated mixtures with high percentage of reclaimed asphalt pavement. *Construction and Building Materials, 48*, 238-247.

Iwanski, M., & Chomicz-Kowalska, A. (2013). Laboratory study on mechanical parameters of foamed bitumen mixtures in the cold recycling technology. *Procedia Engineering, 57*, 433-442.

James, A. (2006). Overview of asphalt emulsion. *Transportation Research Circular E-C102: Asphalt Emulsion Technology*, 1-15.

Jenkins, K. J., & Van de Ven, M. F. C. (1999). Mix design considerations for foamed bitumen mixtures. *Proceedings of 7th Conference on Asphalt Pavements of Southern Africa, RSA*.

Jenkins, K. J., Long, F. M., & Ebels, L. J. (2007). Foamed bitumen mixes= shear performance? *International Journal of Pavement Engineering*, *8*(2), 85-98.

Jenkins, K. J., Twagira, M. E., Kelfkens, R. W., & Mulusa, W. K. (2012). New laboratory testing procedures for mix design and classification of bitumen-stabilized materials. *Road Materials and Pavement Design, 13*(4), 618-641.

Kavussi, A., & Modarres, A. (2010). A model for resilient modulus determination of recycled mixes with bitumen emulsion and cement from ITS testing results. *Construction and Building Materials*, *24*(11), 2252-2259.

Khosravifar, S., Schwartz, C. W., & Goulias, D. G. (2013). Foamed asphalt stabilized base: A case study. In *Airfield and Highway Pavement 2013: Sustainable and Efficient* Pavements (pp. 106-117).

Kim, Y., & Lee, H. D. (2006). Development of mix design procedure for cold in-place recycling with foamed asphalt. *Journal of Materials in Civil Engineering, 18*(1), 116-124.

Kim, Y., & Lee, H. D. (2012). Performance evaluation of cold in-place recycling mixtures using emulsified asphalt based on dynamic modulus, flow number, flow time, and raveling loss. *KSCE Journal of Civil Engineering, 16*(4), 586-593.

Kim, Y., Im, S., & Lee, H. D. (2011). Impacts of curing time and moisture content on engineering properties of cold in-place recycling mixtures using foamed or emulsified asphalt. *Journal of Materials in Civil Engineering*, *23*(5), 542-553.

Kim, Y., Lee, H. D., & Heitzman, M. (2009). Dynamic modulus and repeated load tests of cold in-place recycling mixtures using foamed asphalt. *Journal of Materials in Civil Engineering, 21*(6), 279-285.

Kuna, K., Airey, G., & Thom, N. (2016). Development of a tool to assess in-situ curing of foamed bitumen mixtures. *Construction and Building Materials*, *124*, 55-68.

Lane, B., & Kazmierowski, T. (2003). Expanded asphalt stabilization on the Trans-Canada Highway. *Proc. of Transportation Research Board (TRB) 82nd Annual Meeting (CD-ROM)*.

Lee, H. D., Woods, A., & Kim, Y. T. (2011). *Examination of curing criteria for cold in-place recycling* (Phase 3: Calibration of moisture loss indices and development of stiffness gain model) (No. TR-609). Ames, IA: Iowa Dept. of Transportation, Highway Research Board.

Lee, H., & Im, S. (2008). *Examination of curing criteria for cold in-place recycling* (No. IHRB Report TR-553). Ames, IA: Iowa Dept. of Transportation, Highway Research Board.

Lee, K. W. W., Brayton, T. E., & Huston, M. (2002). *Development of performance-based mix-design for cold in-place recycling (CIR) of bituminous pavements based on fundamental properties* (No. FHWA-CIR-02-01). Washington, DC: U.S. Federal Highway Administration Office of Pavement Technology.

Lee, K. W., Brayton, T. E., Mueller, M., & Singh, A. (2016). Rational mix-design procedure for cold in-place recycling asphalt mixtures and performance prediction. *Journal of Materials in Civil Engineering, 28*(6), 04016008.

Leech, D. (1994). Cold bituminous materials for use in the structural layers of roads, vol. 75. *Crowthorne (Berkshire, UK): Transport Research Laboratory, Project Report, UK. ISSN*, 0968-4093.

Li, Z., Hao, P., Liu, H., Xu, J., & Chen, Z. (2016). Investigation of early-stage strength for cold recycled asphalt mixture using foamed asphalt. *Construction and Building Materials, 127*, 410-417.

Lin, S., Ashlock, J. C., Kim, H., Nash, J., Lee, H., & Williams, R. C. (2015). *Assessment of non-destructive testing technologies for quality control/quality assurance of asphalt mixtures* (No. IHRB Project TR-653). Ames, IA: Iowa Dept. of Transportation, Highway Research Board.

Loizos, A., & Plati, C. (2007). Ground penetrating radar as an engineering diagnostic tool for foamed asphalt treated pavement layers. *International Journal of Pavement Engineering, 8*(2), 147-155.

Long, F. M., & Ventura, D. G. C. (2004). *Laboratory testing for the HVS Test on the N7* (Contract report CR-2003/56). Pretoria, South Africa: CSIR Transportek.

Long, F., & Theyse, H. (2004, September). Mechanistic-empirical structural design models for foamed and emulsified bitumen treated materials. *Proceedings of the 8th Conference on Asphalt Pavements for Southern Africa (CAPSA'04)*,

Ma, T., Wang, H., Zhao, Y., Huang, X., & Pi, Y. (2015). Strength mechanism and influence factors for cold recycled asphalt mixture. *Advances in Materials Science and Engineering*, *2015,* 1-10.

Maccarrone, S., Holleran, G., Leonard, D. J., & Hey, S. (1994). Pavement recycling using foamed bitumen. *Proceedings of the 17TH ARRB Conference, Gold Coast, Queensland, August 15-19, 17, Part 3*.

Marquis, B., Bradbury, R. L., Colson, S., Malick, R. B., Nanagiri, Y. V., Gould, J. S., ... & Marshall, M. (2003, January). Design, construction and early performance of foamed asphalt full depth reclaimed (FDR) pavement in Maine. *Proceedings of the TRB 82th Annual Meeting*, CD ROM.

Mehranfar, V., & Modarres, A. (2020). Evaluating the recycled pavement performance and layer moduli at variable temperature by nondestructive tests. *International Journal of Pavement Engineering*, *21*(7), 817-829.

MNDOT (Minnesota DOT). (2020). Standard specifications for construction. St. Paul, MN: MnDOT.

Modarres, A., & Ayar, P. (2014). Coal waste application in recycled asphalt mixtures with bitumen emulsion. *Journal of Cleaner Production, 83,* 263-272.

Modarres, A., & Ayar, P. (2016). Comparing the mechanical properties of cold recycled mixture containing coal waste additive and ordinary Portland cement. *International Journal of Pavement Engineering, 17*(3), 211-224.

Modarres, A., Rahimzadeh, M., & Zarrabi, M. (2014). Field investigation of pavement rehabilitation utilizing cold in-place recycling. *Resources, Conservation and Recycling, 83,* 112-120.

Mohammad, L. N., Abu-Farsakh, M. Y., Wu, Z., & Abadie, C. (2003). Louisiana experience with foamed recycled asphalt pavement base materials. *Transportation Research Record, 1832*(1), 17-24.

Muthen, K. M. (1998). *Foamed asphalt mixes-mix design procedure* (Contract report CR-98/077). Pretoria, South Africa: SABITA Ltd & CSIR Transportek.

Nassar, A. I., Thom, N., & Parry, T. (2016, October). Examining the effects of contributory factors on curing of cold bitumen emulsion mixtures. In *Functional Pavement Design–Proceedings of the 4th Chinese-European Workshop on Functional Pavement Design, CEW* (pp. 1037-1048).

Nataatmadja, A. (2001). Some characteristics of foamed bitumen mixes. *Transportation Research Record*, *1767*(1), 120-125.

Niazi, Y., & Jalili, M. (2009). Effect of Portland cement and lime additives on properties of cold in-place recycled mixtures with asphalt emulsion. *Construction and Building Materials, 23*(3), 1338-1343.

Ojum, C., Kuna, K., Thom, N. H., & Airey, G. (2014). An investigation into the effects of accelerated curing on cold recycled bituminous mixes. *Asphalt Pavements—Proceedings of the International Conference on Asphalt Pavements, ISAP, 1*, 1177-1188.

Omrani, M. A., & Modarres, A. (2018). Emulsified cold recycled mixtures using cement kiln dust and coal waste ash-mechanical-environmental impacts. *Journal of Cleaner Production, 199*, 101-111.

Oruc, S., Celik, F., & Akpinar, M. V. (2007). Effect of cement on emulsified asphalt mixtures. *Journal of Materials Engineering and Performance, 16*(5), 578-583.

Papavasiliou, V., Loizos, A., & Plati, C. (2010). Monitoring the performance of cold in-depth recycled pavements. Proceedings of the 11th Int. Conf. on Asphalt Pavements, International Society for Asphalt Pavements (ISAP).

Plati, C., Loizos, A., Papavasiliou, V., & Kaltsounis, A. (2010). Investigating in situ properties of recycled asphalt pavement with foamed asphalt as base stabilizer. *Advances in civil engineering*, *2010*, 1-10.

Quick, T., & Guthrie, W. S. (2011). Early-age structural properties of base material treated with asphalt emulsion. *Transportation Research Record, 2253*(1), 40-50.

Roberts, F. L., Engelbrecht, J. C., & Kennedy, T. W. (1984). Evaluation of recycled mixtures using foamed asphalt. *Transportation Research Record, 968,* 78-85

Ruckel, P. J., Acott, S. M., & Bowering, R. H. (1983). Foamed-asphalt paving mixtures: Preparation of design mixes and treatment of test specimens. *Transportation Research Record*, *911*, 88-95.

Saleh, M. F. (2004). New Zealand experience with foam bitumen stabilization. *Transportation Research Record*, *1868*(1), 40-49.

Sangiorgi, C., Tataranni, P., Simone, A., Vignali, V., Lantieri, C., & Dondi, G. (2017). A laboratory and filed evaluation of cold recycled mixture for base layer entirely made with reclaimed asphalt pavement. *Construction and Building Materials, 138,* 232-239.

Santagata, E., Chiappinelli, G., Riviera, P. P., & Baglieri, O. (2010). Triaxial testing for the short-term evaluation of cold-recycled bituminous mixtures. *Road Materials and Pavement Design, 11*(1), 123-147.

Scholz, T., Rogge, D. F., Hicks, R. G., & Allen, D. (1991). Evaluation of mix properties of cold in-place recycled mixes. *Transportation Research Record, 1317*, 77-89.

Schwartz, C. W., Diefenderfer, B. K., & Bowers, B. F. (2017). Material properties of cold in-place recycled and full-depth reclamation asphalt concrete (No. Project 09-51). Transportation Research Board, Washington, D.C.

Sebaaly, P. E., Bazi, G., Hitti, E., Weitzel, D., & Bemanian, S. (2004). Performance of cold in-place recycling in Nevada. *Transportation Research Record*, *1896*(1), 162-169.

Sebaaly, P. E., Ortiz, J. A., Hand, A. J., & Hajj, E. Y. (2019). Practical method for in-place density measurement of cold in-place recycling mixtures. *Construction and Building Materials, 227*, 116731.

Serfass, J. P. (2002). Studies and research-emulsion coatings: For a new study method. *Revue Générale des Routes et des Aerodromes*, *808,* 85.

Serfass, J. P., Poirier, J. E., Henrat, J. P., & Carbonneau, X. (2004). Influence of curing on cold mix mechanical performance. *Materials and Structures, 37*(5), 365-368.

Steiner, T., Hoegh, K., Zegeye-Teshale, E., & Dai, S. (2020). Method for assessment of modeling quality for asphalt dielectric constant to density calibration. *Journal of Transportation Engineering, Part B: Pavements*, *146*(3), 04020054.

Stimilli, A., Ferrotti, G., Graziani, A., & Canestrari, F. (2013). Performance evaluation of a cold-recycled mixture containing high percentage of reclaimed asphalt. *Road Materials and Pavement Design, 14*(sup1), 149-161.

Sultan, T., Kamal, M. A., & Latif, A. (2016). Performance evaluation of cold recycled asphalt mixes at different temperatures and loading rates. *Pakistan Journal of Engineering and Applied Sciences, 18,* 21-30.

Tebaldi, G., Dave, E. V., Marsac, P., Muraya, P., Hugener, M., Pasetto, M., ... & Wendling, L. (2014). Synthesis of standards and procedures for specimen preparation and in-field evaluation of cold-recycled asphalt mixtures. *Road Materials and Pavement Design*, *15*(2), 272-299.

Terrell, R. L., & Wang, C. K. (1971). Early curing behavior of cement modified asphalt emulsion mixtures. *Association of Asphalt Paving Technologists Proceedings, 40*.

Teshale, E. Z., Hoegh, K., Dai, S., Giessel, R., & Turgeon, C. (2020). Ground penetrating radar sensitivity to marginal changes in asphalt mixture composition. *Journal of Testing and Evaluation*, *48*(3), 2295-2310.

Thanaya, I. N. A., Zoorob, S. E., & Forth, J. P. (2009, February). A laboratory study on cold-mix, cold-lay emulsion mixtures. *Proceedings of the Institution of Civil Engineers-Transport, 162*(1), 47-55.

Thomas, T., & Kadrmas, A. (2002). Performance-related tests and specifications for cold in-place recycling: Laboratory and field experience. *Proceedings Transportation Research Board 81st Annual Meeting,* (pp. 2-5).

Tia, M., & Wood, L. E. (1983). Use of asphalt emulsion and foamed asphalt in cold-recycled asphalt paving mixtures. *Transportation Research Record, 898,* 315-321.

Wirtgen. (2012). Wirtgen cold recycling technology. *Wirtgen GmBH*, Windhagen, Germany.

Woods, A. M. (2011). *Evaluation of curing criteria for cold in-place recycling of asphalt* (Doctoral dissertation, The University of Iowa).

Woods, A., Kim, Y., & Lee, H. (2012). Determining timing of overlay on cold in-place recycling layer: Development of new tool based on moisture loss index and in situ stiffness. *Transportation Research Record, 2306*(1), 52-61.

Xiao, J., & Yu, Y. (2011). Research on moisture susceptibility of emulsion treated cold reclaimed asphalt mixture. In *Pavements and Materials: Recent Advances in Design, Testing and Construction* (pp. 45-52).

Yan, J., Leng, Z., Li, F., Zhu, H., & Bao, S. (2017). Early-age strength and long-term performance of asphalt emulsion cold recycled mixes with various cement contents. *Construction and Building Materials, 137,* 153-159.

Yan, J., Ni, F., Yang, M., & Li, J. (2010). An experimental study on fatigue properties of emulsion and foam cold recycled mixes. *Construction and Building Materials, 24*(11), 2151-2156.

Zhu, C., Zhang, H., Huang, L., & Wei, C. (2019). Long-term performance and microstructure of asphalt emulsion cold recycled mixture with different gradations. *Journal of Cleaner Production, 215*, 944-995.

APPENDIX A
MINNESOTA LOCAL AGENCY SURVEY REPORT

Task 2 Survey Report

MnDOT_LRRB_CIR_Curing_Project_Task 2 Survey
June 16, 2020 7:42 AM MDT

1 - To start, please enter your name, title, affiliation, email address and phone number

Name	Title	Affiliation	Email Address	Phone Number
Adam Nafstad	City Engineer	Albertville	Anafstad@ci.albertville.mn.us	7634973384
Anthony Schrempp	Project Manager	Ramsey County	anthony.schrempp@co.ramsey.mn.us	6512667192
Guy Kohlnhofer	Transportation Czar	Dodge County	guy.kohlnhofer@co.dodge.mn.us	(507) 951-2526
Chris DeDene	Materials Engineer	City of Minneapolis	chris.dedene@minneapolismn.gov	612-673-2823
Dillon Dombrovski	Deputy Public Works Director/City Engineer	City of Rochester	ddombrovski@rochestermn.gov	507-328-2421
Nick Klisch	County Engineer	Cottonwood COunty	nick.klisch@co.cottonwood.mn.us	507-832-8811
Sam Muntean	County Highway Engineer	Lac qui Parle	sam.muntean@lqpco.com	3205987252
Wayne Stevens	County Engineer	Brown County	wayne.stevens@co.brown.mn.us	507-233-5700
Joe Wilson	Engineer	Lincoln Co.	jwilson@co.lincoln.mn.us	507-694-1124
David Overbo	County Eng	Clay Co	david.overbo@co.clay.mn.us	2182995099
Nick Bergman	County Engineer	Pipestone County	nick.bergman@co.pipestone.mn.us	507-825-1245
Jed Nordin	County Engineer	Hubbard County	jed.nordin@co.hubbard.mn.us	2182555169
Tim Stahl	County Engineer	Jackson County	tim.stahl@co.jackson.mn.us	5078472525
Ryan Sutherland	Assistant County Engineer	Itasca County	ryan.sutherland@co.itasca.mn.us	2183272833
Ryan Thilges	County Engineer	Blue Earth County	ryan.thilges@blueearthcountymn.gov	507-304-4025
Stephen Schnieder	Public Works Director	Nobles County	sschnieder@co.nobles.mn.us	507-295-5322
Cory Slagle	Assistant County Engineer	Washington County	cory.slagle@co.washington.mn.us	651-430-4337
Andrew Engel	Engineering Supervisor	Carver County	aengel@co.carver.mn.us	9524665212

Name	Title	Affiliation	Email Address	Phone Number
CHAD HAUSMANN	Asst. Co. Engineer	Wright County	chad.hausmann@co.wright.mn.us	3202933656

2 - Has your County/Town/City/District undertaken any cold in-place recycling projects in the recent past (10 years or less)?

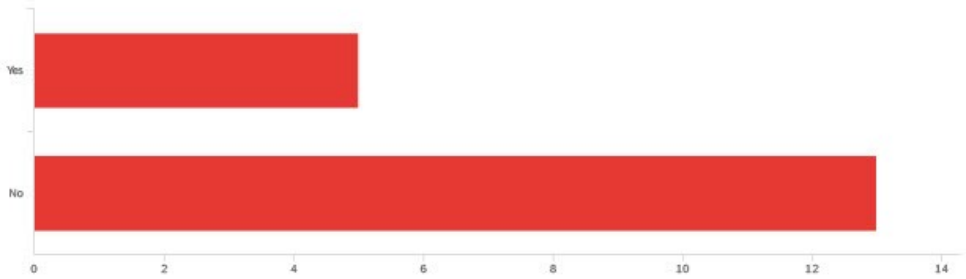

#	Field		Choice Count
1	Yes	27.78%	5
2	No	72.22%	13
			18

Showing rows 1 - 3 of 3

2a - How many CIR projects?

How many CIR projects?
38
3
4
2
1

2b - What specifications do you utilize for quality control and acceptance for your CIR projects?

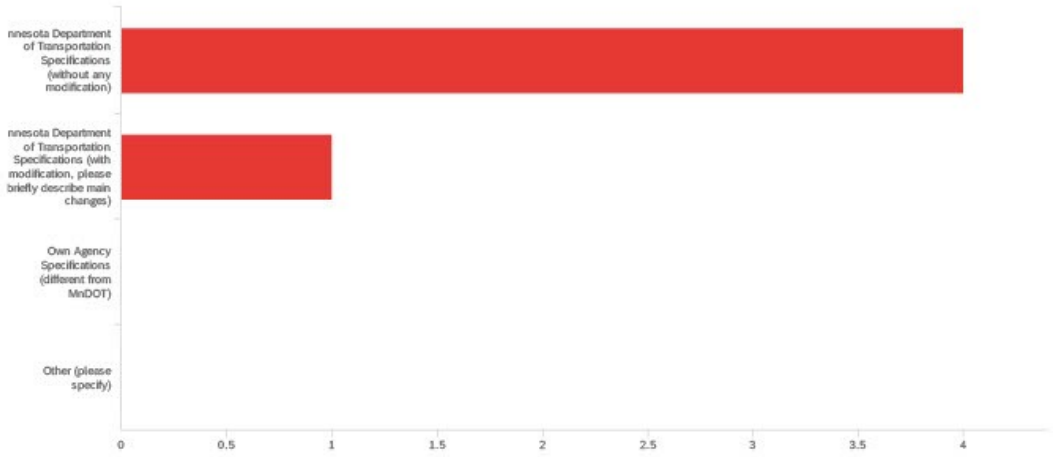

#	Field		Choice Count
4	Minnesota Department of Transportation Specifications (without any modification)	80.00%	4
5	Minnesota Department of Transportation Specifications (with modification, please briefly describe main changes)	20.00%	1
6	Own Agency Specifications (different from MnDOT)	0.00%	0
7	Other (please specify)	0.00%	0
			5

Showing rows 1 - 5 of 5

2b_5_TEXT - Minnesota Department of Transportation Specifications (with modification, p...

Minnesota Department of Transportation Specifications (with modification, p...
February 6, 2015 Edition

2b_7_TEXT - Other (please specify)

Other (please specify)

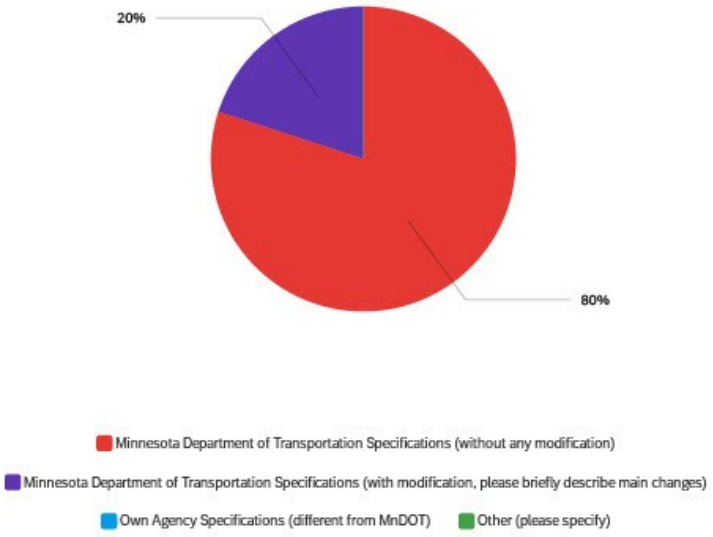
20%
80%
Minnesota Department of Transportation Specifications (without any modification)
Minnesota Department of Transportation Specifications (with modification, please briefly describe main changes)
Own Agency Specifications (different from MnDOT)
Other (please specify)

2b - Please attach specification you utilize

2b_Id - Id

Thumbnail	Name	Size	Type
Proposal (2-2020).pdf	Proposal (2-2020).pdf	1.38MB	application/pdf

2c - For CIR projects in your agency, typically who determines the degree of CIR curing (for decisions such as allowance of traffic or application of wear course)? (select all that apply)

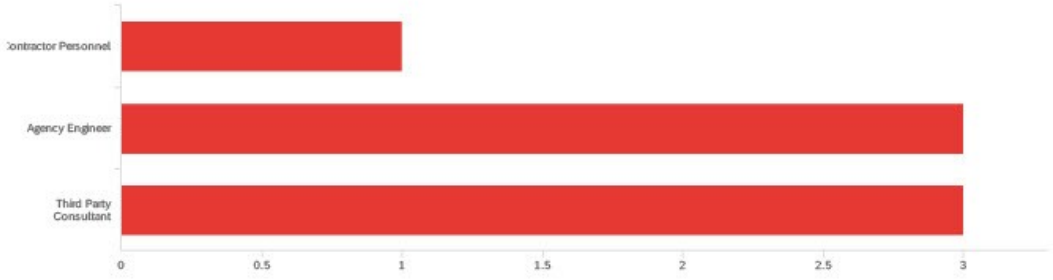

#	Field		Choice Count
1	Contractor Personnel	14.29%	1
2	Agency Engineer	42.86%	3
3	Third Party Consultant	42.86%	3
			7

Showing rows 1 - 4 of 4

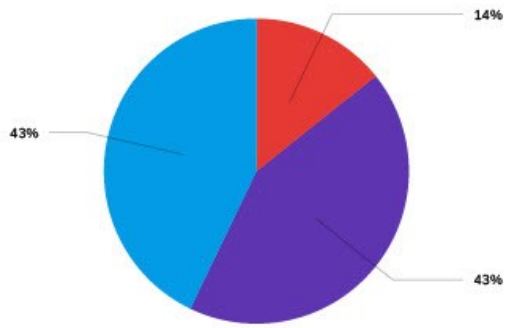


Contractor Personnel
Agency Engineer
Third Party Consultant

2d - During curing, how do you determine the timing for allowing traffic on the CIR layer or placing of overlay? (select all that apply)

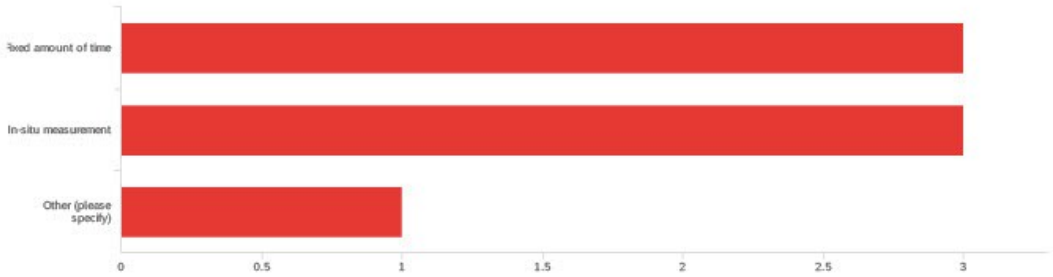

#	Field		Choice Count
4	Fixed amount of time	42.86%	3
5	In-situ measurement	42.86%	3
7	Other (please specify)	14.29%	1
			7

Showing rows 1 - 4 of 4

2d_7_TEXT - Other (please specify)

Other (please specify)
We determine when to place the overlay based on a minimum amount of time combined with air temperature, humidity, precipitation and review of the CIR surface. We have closed the road to thru traffic. Our paving contractors have not planned to mobilize the paving crew until 14 days after the CIR was complete.

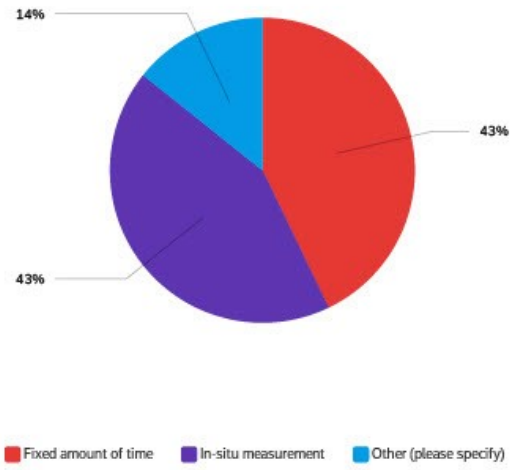
14%
43%
43%
Fixed amount of time
In-situ measurement
Other (please specify)

2e - What in-situ testing or measurement do you use to determine CIR degree of curing (conducted in-house or contracted out)?

What in-situ testing or measurement do you use to determine CIR degree of c...
% moisture
Moisture in material must be 2.0 percent or less - tests are contracted out

2a - Is there any reason why your agency has not recently used CIR for rehabilitation of asphalt pavements? Please explain

Is there any reason why your agency has not recently used CIR for rehabilit...
We have previously, but not recent. I am not certain for the reasonsing as newer employee.
We typically need more structure so do FDR and SFDR. Also don't like reflective cracking.
The void content of a CIR pavement is somewehre around 12%, compared to a typical pavement of 8%, so employing CIR means our pavement will "fluff" aobut 4% - which means I can't match in to existing infrastructure, like gutters, manholes, and driveways.
In the past we typincally did FDR or SFDR. We are about to try our first CIR Project this year with Brown County.
All projects have been mill and overlay or complete reconstruction
We continue to try to add strength to the roads using overlays. The CIR is an added cost that would not help build much strength.
have not found the correct location and need to learn more about it - maybe some guidance on which roads we have that would be a perfect candidate, then we'd maybe try one
No particular reason, we may try it some day.
Existing pavements are too thin
Success with SFDR
Have not needed to due to pavement quality of bituminous projects selected.
No roads in a condition to warrant this treatment.

3 - From your experience with CIR, are there any challenging areas you have identified that need to be addressed by research studies?

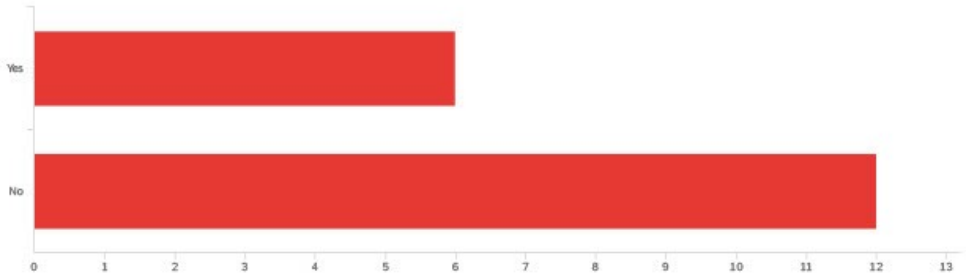

#	Field		Choice Count
5	Yes	33.33%	6
6	No	66.67%	12
			18

Showing rows 1 - 3 of 3

3a - Please explain the challenging areas

Please explain the challenging areas
The void content of a CIR pavement is somewehre around 12%, compared to a typical pavement of 8%, so employing CIR means our pavement will "fluff" aobut 4% - which means I can't match in to existing infrastructure, like gutters, manholes, and driveways. The CIR paving train is almost a quarter of a mile long, including the rollers, which means I have close several intersections at once in order to get a continuous product. It will create a massive detour route for my city. Maybe we could look at CCPR - but that still has the matching issues. And how long does a project have to be before it's economical? Maybe on a parkway...
We have never used it, so I would be interested in learning how it's worked along an urban cross-section with curb and gutter
CIRs often raise the profile which in turn narrows the road shoulders. This is an issue on roads that already have narrow shoulders. Because of this, milling prior to a CIR may be required. When having to mill, CIR becomes less competitive with a traditional mill and overlay or SFDR. CIRs are also susceptible to rutting in my experience. When doing say a 4" CIR with a 3" Bit overlay, what is the best oil to use for the overlay? Because CIRs are susceptible to rutting, should a 58-28 binder be used? Or should a 58-34 binder be used to resist thermal cracking? Are there other practices that could be used to prevent rutting?
Problems with subgrade - How to address with CIR paving train.
We used to have issues with the CIR material not setting up quickly enough and not holding up under traffic, while the material cured. We switched to using a polymer-modified emulsion and it works much better. CIR projects need to be designed. We used to run into the mindset that the amount of oil injected could be determined in the field, which is not always the case. We recommend always having a mix design prepared before letting the project.
1. A curing curve (similar to concrete strength curve) to allow traffic on the CIR.

4 - Are there any additional information about the current state of practice of CIR you could provide that will be helpful?

Are there any additional information about the current state of practice of...
For my city, it's feasibility. The economics are there - just waiting for a good project to make the pitch.
I tried CIR and sealcoat on four projects. That did not work out as I would have liked. A CIR and two inch overlay is working well. Most of our projects we did a CIR and three or four inch overlay.
not sure
Answered no to previous questions on problems since I haven't done any CIR projects.

2d_7_TEXT - Topics

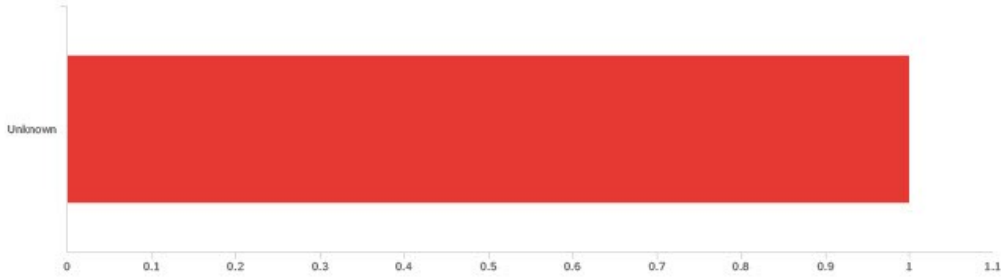

#	Field		Choice Count	
Unknown	Unknown		100.00%	1

Showing rows 1 - 1 of 1

2d_7_TEXT - Parent Topics

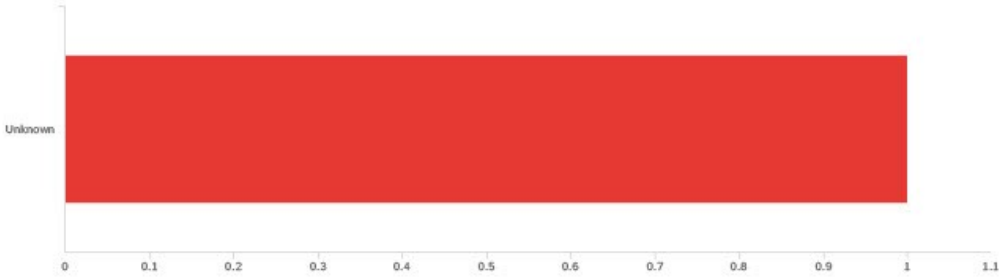

#	Field		Choice Count
Unknown	Unknown	100.00%	1

Showing rows 1 - 1 of 1

End of Report

APPENDIX B
FIELD PROJECT PLANS

Link web repository of project plans:
https://unh.box.com/s/ph5oa2qozqnh06n8f2kr1j5po6w0bh89

APPENDIX C
IN-SITU TEST DATA

Link to web repository of in-situ test data:
https://unh.box.com/s/q2s2qmnao3pmrz6aydvowlk3cj65pm3f

APPENDIX D
LABORATORY TEST DATA

Link to web repository of laboratory test data:
https://unh.box.com/s/z9eyz8e0lak6q03fqegj4d4yxh2dgd88

APPENDIX E
CURING PREDICTION MODEL USER GUIDE

OVERVIEW

This prediction model is developed to calculate the time needed for necessary curing before allowing placement of the wear course on CIR layers.

Download Link:

SOFTWARE NEEDED

Microsoft Excel®: The workbook runs on most available versions of the Microsoft Excel. Check that Excel is installed on computer. Once file is downloaded, double click to open workbook.

WORKBOOK LAYOUT

The workbook is divided into 2 sheets named: **Info** and **Curing Prediction**.

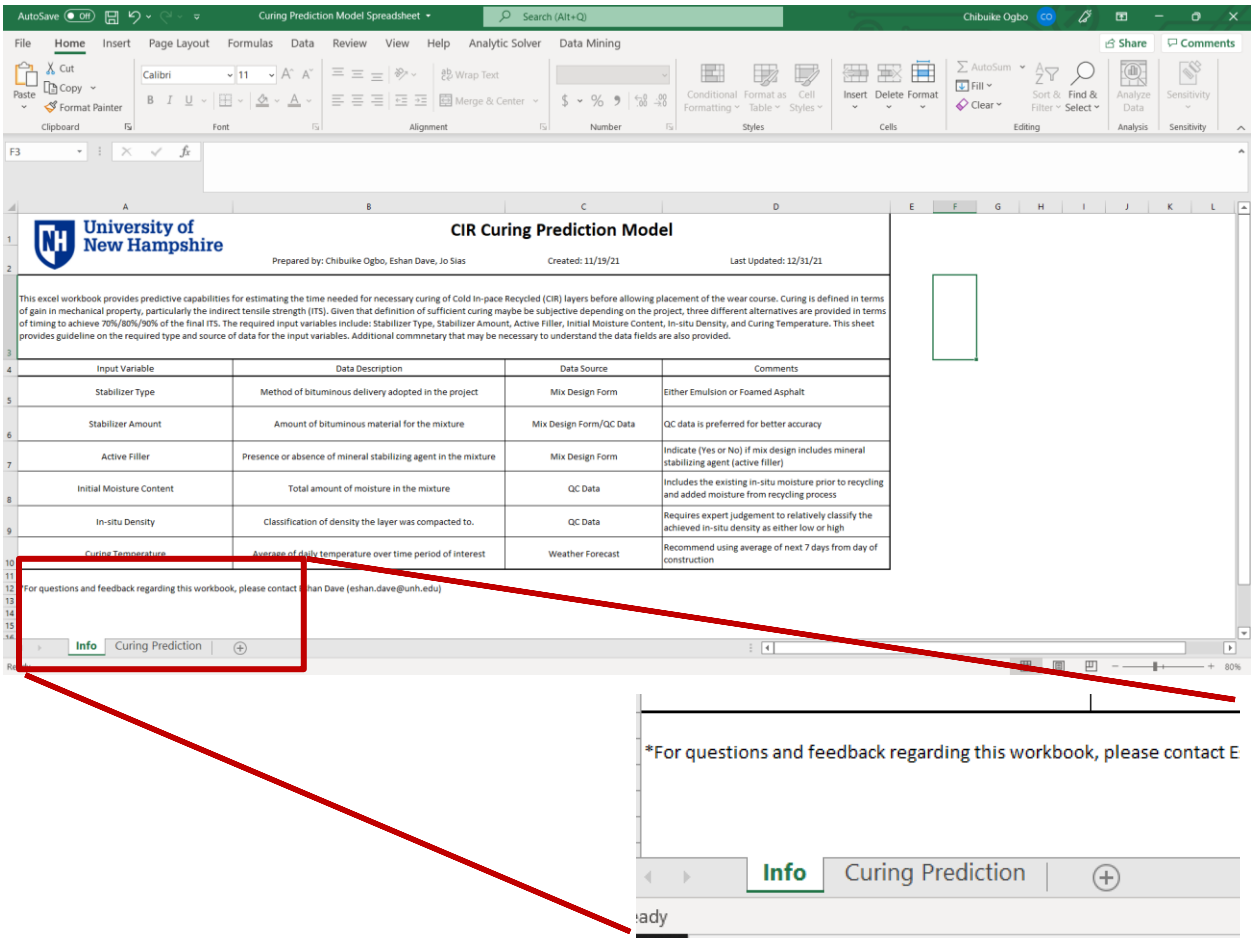

The **Info sheet** presents background information regarding capabilities of the prediction model, as well as an extensive description of the variables incorporated into the model. It is recommended to read through the provided information prior to navigating to the **Curing Prediction**.

The **Curing Prediction sheet** contain the programmed prediction model equation. It is divided into 2 parts: **Input** and **Output.**

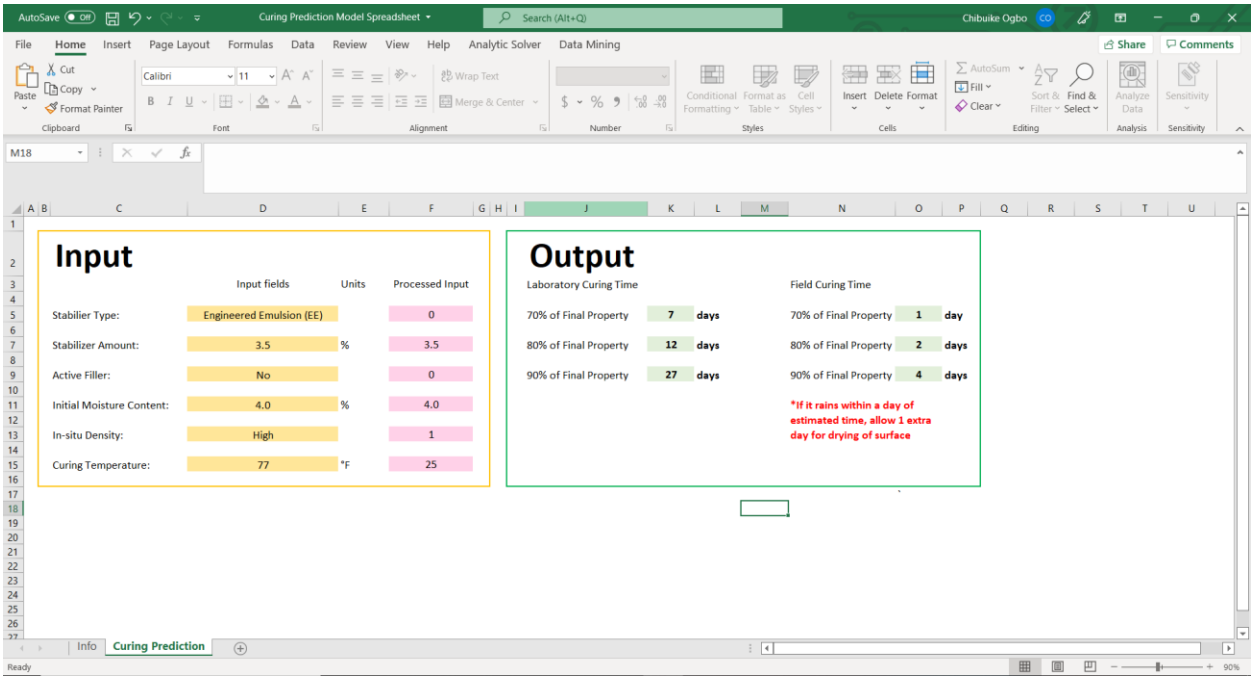

INPUT

The **Input** part (highlighted in yellow) consists of the model input variables. For each input variable listed, there is an **Input Field** adjacent to it. This is the only user-interactive part of the workbook.

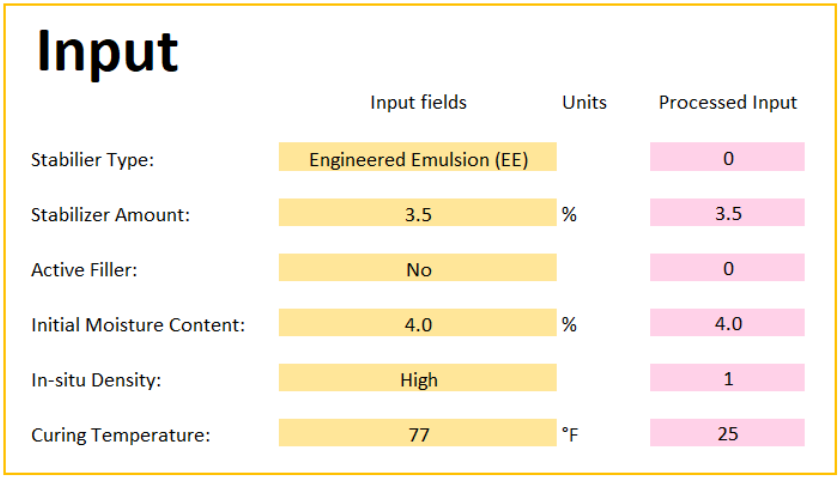

When you click on each **Input Field**, a message pops up with information regarding the format of the **Input Field**. It is either a dropdown menu or a numeric value field. All that is required from the user is to select options from the dropdown menu or provide the required numeric input value.

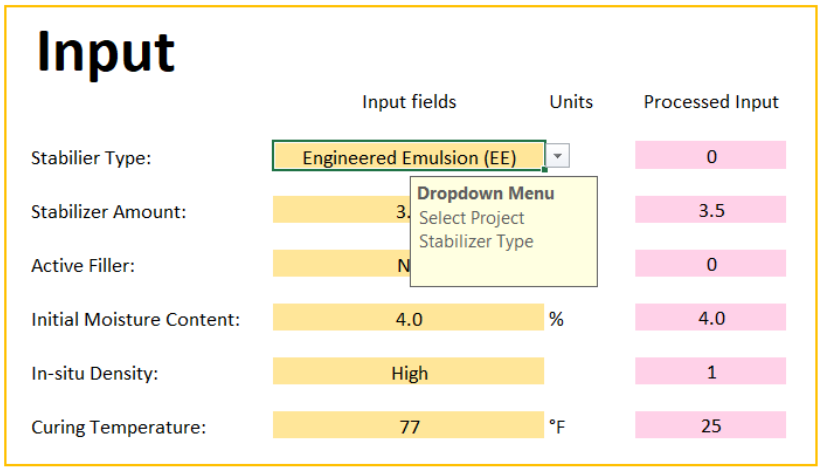

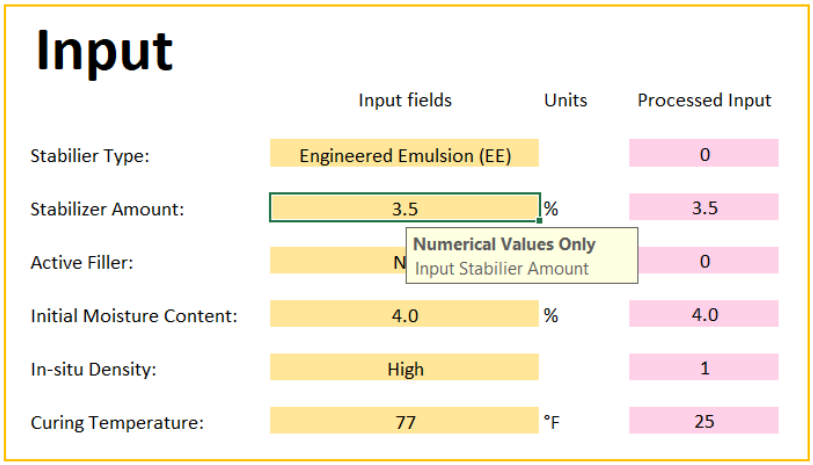

The **Processed Input** column automatically updates based on information provided in the **Input Fields**. The **Processed Input** is what goes into the computation.

OUTPUT

The result of the computation is given in the **Output** part (highlighted in green). The calculation based on alternatives for defining sufficient curing (in terms of timing to achieve 70%/80%/90% of final ITS) is provided. There is corresponding **Field Curing Time** for each determined **Laboratory Curing Time**. A recommendation for when it rains is also highlighted in red text.

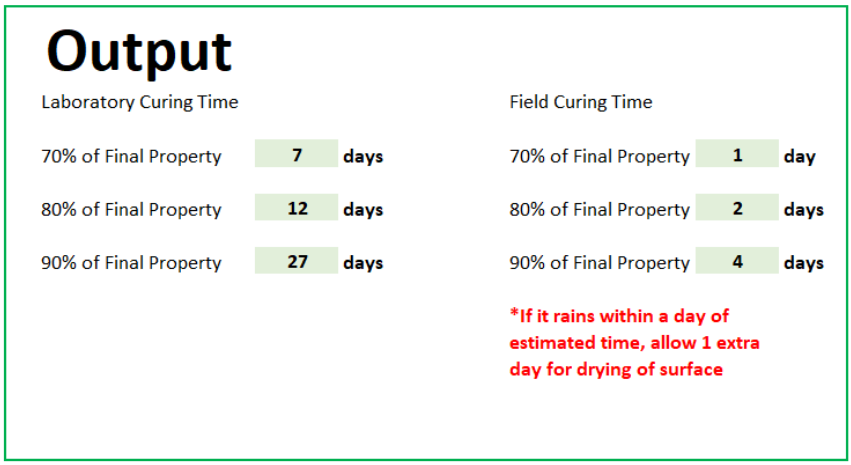

43

DISCLAIMER

At this time, the researchers do not recommend extrapolation of the models beyond the range of numeric variables used in the development as listed below:

- Stabilizer Amount: Engineered Emulsion (1.5 – 3.0%), Foamed Asphalt (2.5 – 3.5%)
- Initial Moisture Content: 3.0 – 6.0%
- Curing Temperature: 60 – 80 °F

Any attempt to extrapolate may result in a warning/error message.